DIPARTIMENTO DI MEDICINA VETERINARIA

CORSO DI DOTTORATO IN SCIENZE VETERINARIE

INDIRIZZO: RIPRODUZIONE, PATOLOGIA, ALLEVAMENTO E BENESSERE

CICLO: XXXII

Coordinatore del Corso Prof.ssa Fiammetta Berlinguer

Infectious agents of Pacific oysters (*Crassostrea gigas*) farmed in Sardinia: isolation, molecular characterization, tissue localization and inflammatory reaction

Tutor
Prof.ssa Elisabetta Antuofermo

Co-Tutor
Prof. Fulvio Salati

Dottorando
Dott.ssa Daniela Mandas

Anno accademico 2018-2019

INDEX

Abstract **1**

Chapter 1 ..... **3**

Introduction **3**

1.1 Global aquaculture production **4**

1.1.1 Global aquaculture production of bivalve molluscs **7**

1.1.1.1 Aquaculture production of bivalve molluscs in Italy **9**

1.1.1.2 Aquaculture production of bivalve molluscs in Sardinia **11**

1.1.1.3 Classification of production areas **13**

1.2 Origin of oysters culture **16**

1.2.1 Culture techniques **18**

1.2.1.1 Off-bottom culture **21**

1.2.1.2 Bottom culture **22**

1.2.1.3 Suspended culture **23**

1.2.1.4 Rope systems culture **24**

1.2.2 Anatomy of bivalve molluscs **25**

1.2.2.1 The shell **26**

1.2.2.2 Mantle **27**

1.2.2.3 Gills **28**

1.2.2.4 The foot **29**

1.2.2.5 Gonads **30**

1.2.2.6 Labial palps, alimentary canal and digestive gland **30**

1.2.2.7 Excretory organs **33**

1.2.2.8 Heart and hemolymph vessels **33**

1.2.2.9 Bivalve defense system **34**

1.2.2.10 Nerves and sensory receptors **36**

1.2.3 Oyster life cycle **37**

1.3 Oyster pathogens **40**

1.3.1 Oyster viruses **40**

1.3.1.1 Ostreid herpesvirus-1 (OsHV-1) and its variants **41**

1.3.2 Oyster bacteria **48**

1.3.2.1 Vibrio genus **48**

1.3.3 Oyster parasites **52**

1.3.4 Oyster mortality and diagnostic methods of diseases **56**

1.4 References 58

Chapter 2 **..... 73**

Sampling site and processing techniques of sampled oysters 73

2.1 Study area 74

2.2 Sampling sites 76

2.2.1 The San Teodoro lagoon 76

2.2.2 The Tortolì lagoon 77

2.2.3 The Marceddì lagoon 77

2.2.4 The Calich lagoon 78

2.3 Material and methods 79

2.3.1 Necropsy 80

2.3.2 Microbiological analysis 82

2.3.3 Biomolecular analysis 85

2.3.3.1 DNA extraction 85

2.3.3.2 PCR 85

2.3.3.3 Real-time PCR 87

2.3.4 Histopathology 91

2.3.4.1 Digestive gland atrophy evaluation 95

2.3.5 Statistical analysis 96

2.4 Results 97

2.4.1 San Teodoro lagoon 98

2.4.2 Tortolì lagoon 99

2.4.3 Marceddì lagoon 100

2.4.4 Calich lagoon 100

2.5 References 101

Chapter 3 **..... 103**

Vibrio **bacteria and related tissue lesions in oysters (*C. gigas*) from Sardinia 103**

3.1 Introduction 104

3.2 Material and methods 106

3.2.1 Study area 106

3.2.2 Sampling 106

3.2.3 Gross pathology evaluation 106

3.2.4 Microbiological analysis 106

3.2.5 Biomolecular analysis 107

3.2.6 Histopathology 110
3.2.7 Digestive diverticula atrophy evaluation 110
3.2.8 Statistical analysis 110
3.3 Results 111
3.3.1 Microbiology 111
3.3.2 Molecular biology 112
3.3.3 Histopathology 117
3.3.4 PCR and histopathology correlation 120
3.3.4.1 San Teodoro lagoon 125
3.3.4.2 Tortolì lagoon 128
3.3.4.3 Marceddì lagoon 130
3.3.4.4 Calich lagoon 132
3.3.5 Digestive gland atrophy 134
3.4 Discussion 136
3.5 References 141
***Chapter 4* 148**
Ostreid herpesvirus-1 and parasites in oysters (*C. gigas*) from Sardinia 148
4.1 Introduction of OsHV-1 149
4.2 Materials and methods 150
4.2.1 Sampling areas 150
4.2.2 PCR 150
4.2.3 Histopathology 152
4.2.4 Statistical analysis 152
4.3 Results 152
4.4 Discussion 155
4.5 Introduction of parasites 156
4.6 Results 158
4.7 Discussion 160
4.8 References 162
Conclusions 168
Acknowledgements 171

Abstract

Massive mortality outbreaks in oysters have been globally reported with heavy economic and social impact on Pacific oyster production.

Several studies highlighted the multifactorial triggers of mortality including environmental and physiological factors (i.e water temperature and oyster genetics) and pathogens as Ostreid Herpesvirus-1 (OsHV-1) and *Vibrio* species.

OsHV-1 has been associated with significant mortality in Pacific oyster and was often co-detected with *V. aestuarianus*. Moreover, the potential role of *V. aestuarianus* in mass mortality events has been only marginally evaluated. In Sardinia, oyster farming represents a developing business and recently mortality episodes caused important economic losses.

The aim of this study was to evaluate the occurrence and related lesions in target organs of OsHV-1, *V. aestuarianus* and *V. splendidus* in Pacific oysters (*Crassostrea gigas*) farmed in Sardinia by a microbiological, biomolecular and histopathological approach.

Four hundred and forty oyster samples were collected from Sardinian lagoons (358 specimens from San Teodoro, 59 from Tortolì, 10 from Marceddì, and 13 from Calich), during 2016, 2017 and 2018 years. In particular, oysters affected by *V. aestuarianus* were sampled in the San Teodoro (85%) and in the Tortoli (12%) lagoons. Mantle was the most affected organ and the highest bacterial load was associated with a moderate to severe hemocytes infiltration (46%), mostly with a multifocal distribution, in connective tissue and hemolympahic vessels.

OsHV-1 was not detected in oyster from San Teodoro but only in Tortolì lagoon (47%). However, no histopathological lesions were associated with OsHV-1.

V. splendidus was detected mostly in oysters from Marceddì lagoon (90%) without tissue lesions.

Overall, a relationship between *V. aestuarianus* bacterial load, degree of hemocytes infiltration in the mantle tissue and mortality episodes in oysters was demonstrated.

To the best of our knowledge, differently from what have been reported by reference studies, that do not support a primary effect of *V. aestuarianus* in oyster mortality events, we suggest a potential role of *V. aestuarianus* in oysters mortality in one of the most devoted lagoon to extensive aquaculture in Sardinia.

Chapter 1

Introduction

1.1 Global aquaculture production

The global financial crisis of 2007-2009 and the Eurozone debt crisis since the end of 2009 produced major consequences in several European countries, causing a strong economic recession between 2008 and 2013.

This deleterious economic situation has led to the Eurozone debt crisis: since 2009 some countries have not been able to fulfill the agreements concerning the repayment of national debt and as a consequence there was the need for economic support from other Eurozone countries or from the European Central Bank. Large economic and employment losses were inevitable consequences for all branches of retail trade, including fish products and its production chain, leading to imbalances in aquaculture production and in total volume of sales.

Greece and Spain represent the main European aquaculture producers who received economic support after this period of crisis. Specially in Greece, the Eurozone debt crisis contributed on restructuring of the sea bass and sea bream industry (FAO, 2017).

Fig. 1.1 Aquaculture main species production in Europe, 2014 (FAO, 2017).

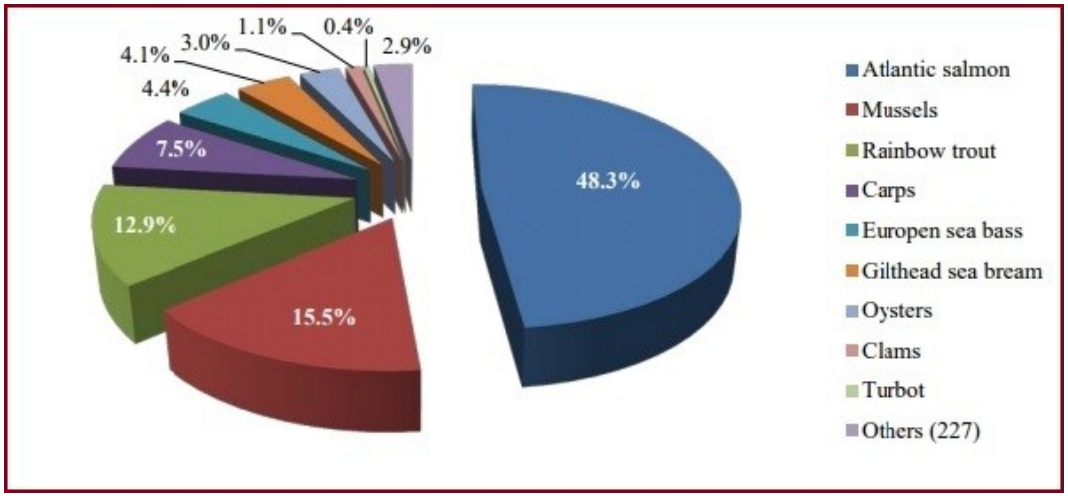

Global aquaculture production in 2016 represented 46.8% of the total fish products originating from fishing and aquaculture activities: this value increased compared to previous

years, in 2014 it was 44.1%, 42.1% in the 2012 and 31.1% in 2004 (FAO, 2016; FAO, 2018). As shown in Fig. 1.2, global aquaculture production amounted to 80 million tons in 2016, and it comprised 54.1 million tons of finfish, 17.1 million tons of molluscs, 7.9 million tons of crustaceans, 938,500 tons of other aquatic species and 30.1 million tons of aquatic plants (seaweeds and microalgae are included) (FAO, 2018).

Over the years it was observed a worldwide increment of aquaculture production, and Asia represents major producer country, with a total amount of 71.5 million tons of fish products, followed by Americas (3.3 million tons), Europe (3 million tons), Africa (2 million tons) and Oceania (210,000 tons), as shown in Fig. 1.3.

Fig. 1.2 Species global aquaculture production from 1990 to 2016 (FAO, 2018).

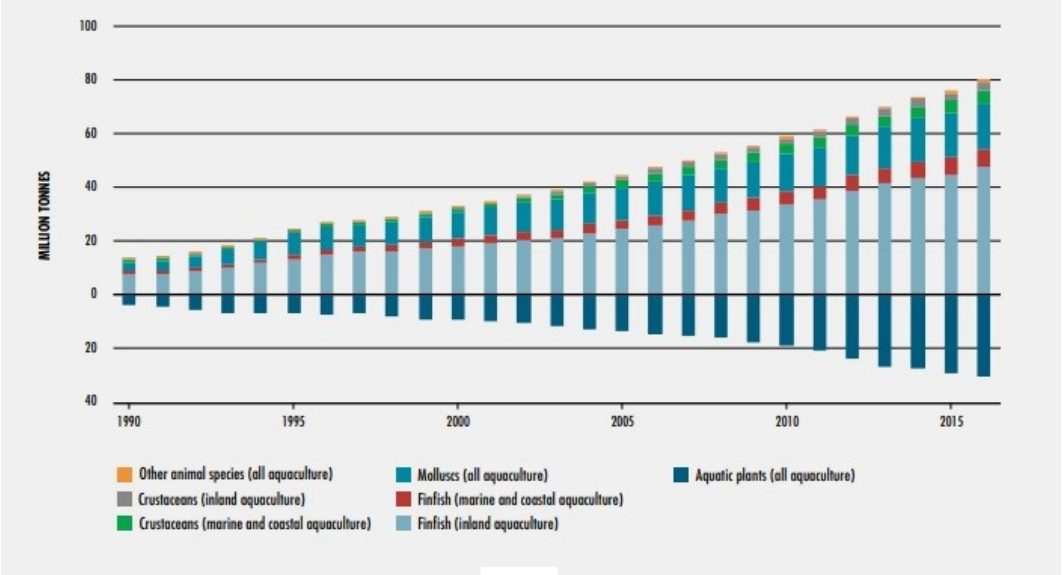

Fig. 1.3 Global aquaculture production (FAO, 2018).

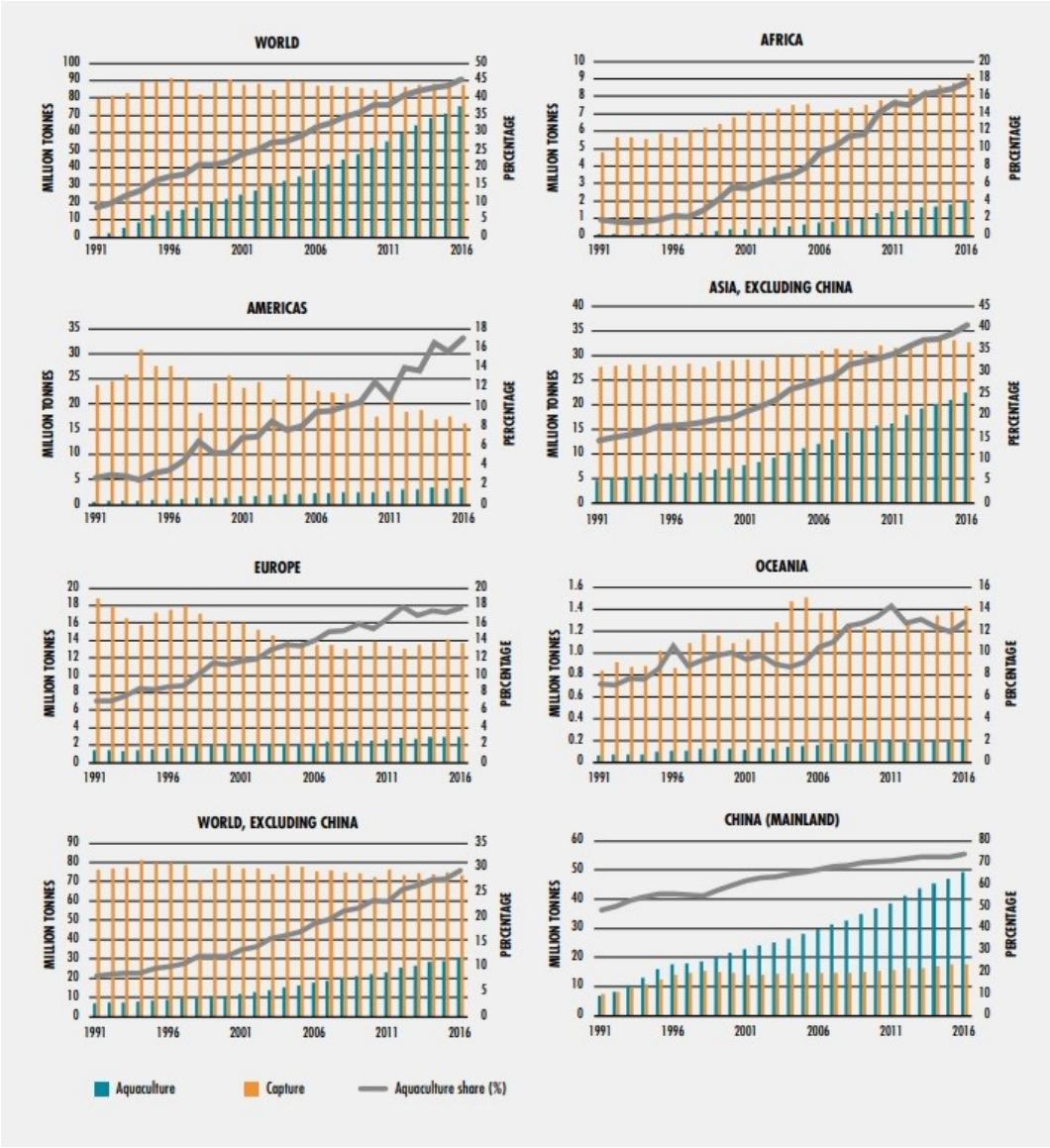

Main breeding species in the world are finfish (369 species), molluscs (109 species), crustaceans (64 species), frogs and reptiles (7 species) and aquatic invertebrates (9 species); moreover, there are 40 several aquatic plants. Total number of commercially farmed species increased by 26,7%, from 472 in 2006 to 598 in 2016 (FAO, 2018).

In the last decade, aquaculture production has grown by 5.8% per year, with a decrease in average growth compared to the previous decade. Finfish production is the main activity on a global level, which recorded a 65% increase in fish production in the 2005-2014 decade.

1.1.1 Global aquaculture production of bivalve molluscs

Production of non-fed species represents an important sector of aquaculture, which includes algae, microalgae and filtering organisms. This type of breeding counted a production of 24.4 million tons in 2016 and aquatic invertebrates were 15.6 million tons (mostly bivalve molluscs).

Bivalve molluscs market plays an extremely important role worldwide: it represents about 15% of total aquaculture production. China is the world's leading producer country (12 million tons), followed by Japan (377,000 tons), the Republic of Korea (347,000 tons) and Thailand (210,000 tons) (FAO, 2016).

In Europe, instead, this activity represents about 60% of total production: in 2016 it amounted to 842,512 tons, with Spain (230,870 tons), France (160,870 tons) and Italy 119,166 tons) as the major producing countries. This sector recorded a slight improvement in productions compared to 2014 data, in which they were 223,000 tons in Spain, 155,000 tons in France and 111,000 tons in Italy (FAO, 2016; FAO, 2019). Among bivalve molluscs main bred species are mussels (548,147 tons), oysters (83,244 tons) and clams (41,511 tons) (Table 1.1).

Table 1.1 European production (tons) of clams, mussels and oysters in 2016 (FAO, 2019).

Countries	**Clams**	**Mussels**	**Oysters**
Denmark	-	45,130	145
France	725	57,960	64,969
Germany	-	44,506	-
Greece	-	23,360	50
Ireland	2	15,121	8,192
Italy	36,500	63,700	145
Netherlands	-	54,000	3,288
Portugal	2,536	832	633
Spain	1,695	215,948	1,448
UK	3	16,302	2,253
Others EU	50	11,288	2,121
Total	41,511	548,147	83,244

The Ostreidae family has about 50 species resulting from capture or reproduction activities, which makes this mollusc one of the most bred in the world (in 2010 the annual production was over 4.8 million tons). China is the first producer country in the world, with a production of about 4.2 million tons (China, Korea, Japan, United States and France production is 95% of global production). About 30 species of oysters are farmed in China, but *Crassostrea angulata*, *C. hongkongiensis* e *C. gigas* are the main produced species (production of *C. gigas* represents about 98% of the production in the world) (ISMEA, 2013).

Fig. 1.4 Global aquaculture production of *C. gigas* until 2014 (tons).

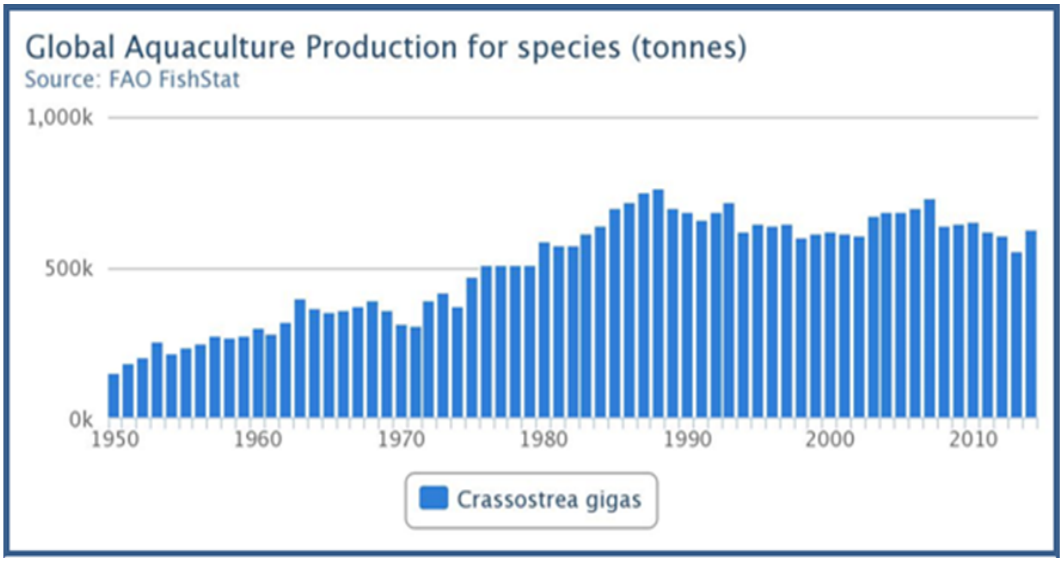

Aquaculture farming is currently the main production technique of *C. gigas*: in 2010 the production amounted to around 103,000 tons in Europe, 88% from France followed by Ireland, Spain, Portugal, Germany and Italy (FAO; ISMEA, 2013).

Fig. 1.5 EU production and trade of oysters in 2009 (Eurostat).

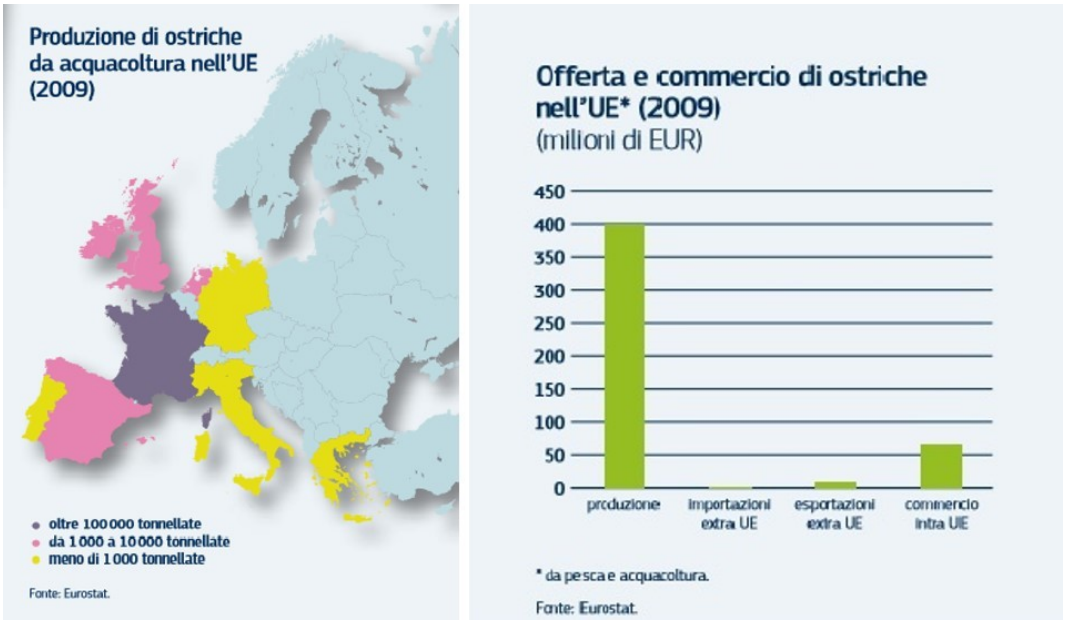

European production of oysters is a self-contained production, with an estimated market of about 400 million Euros (Fig. 1.5). France represents the country with the largest production in Europe, and, therefore, it's able to support product requests from other EU countries.

Latest FAO reports refer about an increase of global exports by France, which gives to this country a prestige position in international trade (in 2017 there was a 20% increase in exports compared to the previous year). Currently, France is the fifth country in global production but it appears to be the most active country in international trade (Globefish FAO, 2018).

1.1.1.1 Aquaculture production of bivalve molluscs in Italy

Bivalve aquaculture in Italy was initially backward because of restricted production areas, which were strictly confined to lagoon or coastal environments. A great improvement was observed as a consequence of the expansion of the production in open sea zone, and this action reduced previous recurrent environmental and sanitary issues.

As consequence of these measures, bivalve molluscs farming became the main productive activity of aquaculture in Italy (about 50% of the total aquaculture production), that in 2016

counted 139,707 tons, with a prevalent production of mussels (*Mytilus galloprovincialis*), clams (*Tapes philippinarum*, *Tapes decussatus*) and oysters (*C. gigas* and *Ostrea edulis*) (Prioli, 2001; Prioli, 2008; FAO, 2019).

Despite recent improvements, oyster farming in Italy still remains a marginal activity, counting low production generally associated with other bivalve products such as mussels and clams (*M. galloprovincialis, T. philippinarum, T. decussatus*).

The production is about 150 tons per year but the product request amounts from 5,000 to 10,000 tons per year: to fill this gap oysters are mainly imported from France, Spain and Holland (Table 1.2; Fig. 1.6) (FAO, 2019). The main Italian farms are located in Sardinia, Puglia, Veneto, Emilia-Romagna, Marche, Liguria.

Table 1.2 Main *C. gigas* producer countries in EU and marine/brackish water production (tons) in 2017 (FAO, 2019).

Country	*C. gigas*
France	64,200
Germany	80
Ireland	9,822
Italy	**145**
Norway	-
Portugal	600
Romania	-
Spain	806
UK	2,294
Total	77,947

Fig. 1.6 Oysters trade imports from France to Italy (1992-2009).

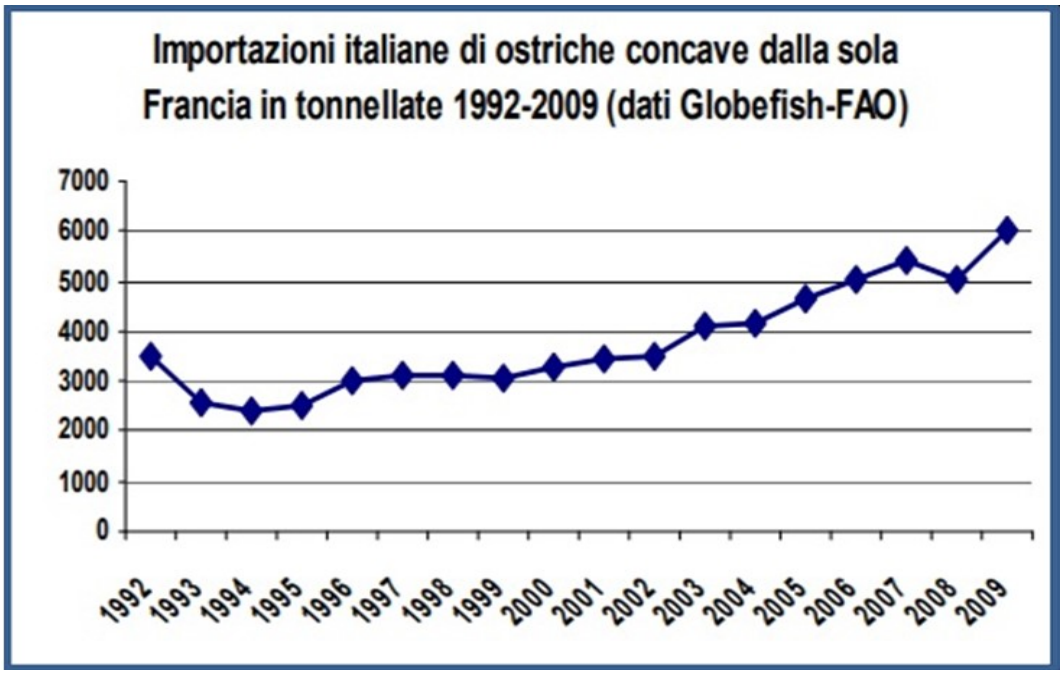

1.1.1.2 Aquaculture production of bivalve molluscs in Sardinia

Aquaculture in Sardinia is an activity rooted in the territory; it was extensively developed first in ponds and brackish lagoons and subsequently it has spread along coasts of this island. Sardinia have an optimal geographic position, with about 1850 km of coast and about 60 ponds/lagoons, covering approximately a surface of 15,000 hectares (Fig. 1.7).

Fig. 1.7 Aquaculture in Sardinia: blue-green markers are fish farms, red markers are molluscs farms.

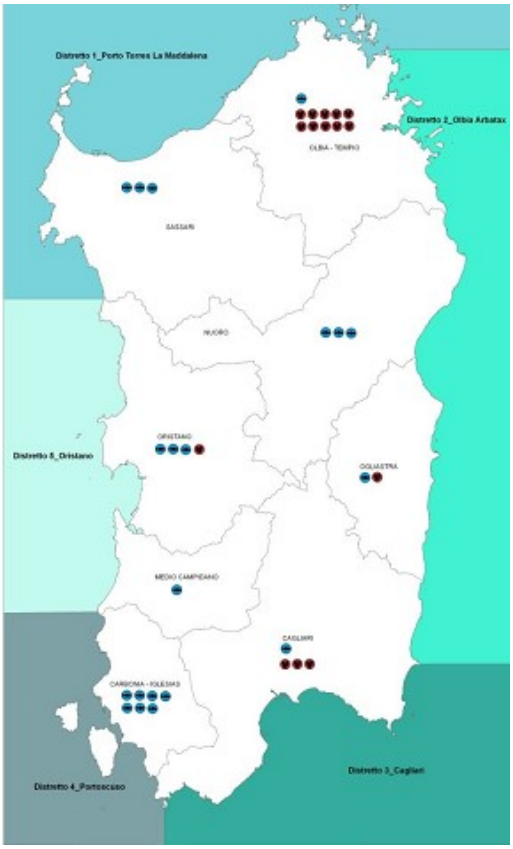

In the production of bivalve molluscs, in particular, mussel farming plays a predominant role in the Sardinian economy, thanks to the labor supply and the economic value it represents. This aquaculture activity is practiced in sea (mainly in the Gulf of Oristano and Olbia) and in lagoon's areas (Tortolì, the lagoon complex of Sarràbus, Santa Gilla, Cirdu, and the lagoon of Porto Pozzo) and sometimes it's associated with oyster farming structures (mainly *C. gigas* species) (Viale *et al*., 2016).

The most important Sardinian oyster producer is located in San Teodoro lagoon (North eastern Sardinia).

Shellfish production in lagoon showed an increase in 2007/2010 three-year period (34% of the total lagoon production in Sardinia) compared to the previous decade (13% of the total lagoon production in Sardinia). In fact, in 1992 total production of lagoon and marine shellfish was 4,000 tons of mussels and 3 tons of oysters; in 2008, the production increased with 10,700

tons of mussels and 6 tons of oysters; finally, in 2013 the production amounted to 13,200 tons of mussels and 31 tons of oysters (Cataudella & Spagnolo, 2011; Viale *et al*., 2016).

1.1.1.3 Classification of production areas

Italian legislation regulates the classification of farming areas, based on the detection of microbiological pollution indicators in molluscs. Marketable molluscs must satisfy the sanitary requirements of Reg. (CE) 853/2004 and 854/2004; it has been applied by Regione Sardegna with council resolution n. 26/9 del 3.6.2009 (Table 1.3; Table 1.4 A, B, C, D).

The competent authority allows bivalve molluscs collection on the basis of the level of faecal contamination detected by the Most Probable Number method, MPN, according to ISO/TS 16649-3. The production areas are thus divided in three classes (A, B or C):

- Class A area: bivalve molluscs reared in this area can be marketed without any purification or housing process. Contamination with *E. coli* must be ≤ 230/100 g of flesh and intravalvular liquid in the 80% of collected bivalve molluscs from these areas (samples from a single period collection), whereas the remaining 20% of molluscs must have a load of *E. coli* ≤ 700/100 g of flesh and intravalvular liquid.

- Class B area: bivalve molluscs need purification treatment or a short housing process before sale and consumption. 90% of collected bivalve molluscs must present a contamination of *E. coli* ≤ 4600/100 g of flesh and intravalvular liquid, whereas 10% remaining molluscs must have a load of *E. coli* ≤ 46000/100 g of flesh and intravalvular liquid.

- Class C area: bivalve molluscs need a long housing process, at least two-month process. Molluscs collected in these areas must have a load of *E. coli* ≤ 46000/100 g of flesh and intravalvular liquid.

- Prohibited area: bivalve molluscs with a contamination with *E. coli* > 46000/100 g of flesh and intravalvular liquid cannot be collected, marketed and aren't suitable for human consumption.

Table 1.3 Table from regional guidelines (council resolution n. 26/9 del 3.6.2009).

CLASSE	STANDARD MICROBIOLOGICO	TRATTAMENTO RICHIESTO
A	***Escherichia coli***: ≤ 230 per 100 g di polpa e liquido intervalvare (metodo ISO TS 16649-3). ***Salmonella spp.***: assente	Nessuno
B	***Escherichia coli:*** ≤ 4.600 per 100 g di polpa e liquido intravalvare (metodo ISO TS 16649-3)	1) Depurazione in stabilimenti riconosciuti; 2) Depurazione naturale in zone classificate ai fini della stabulazione 3) Trasformazione in stabilimenti riconosciuti.
C	***Escherichia coli***: ≤ 46.000 per 100 g di polpa e liquido intravalvare (metodo ISO TS 16649-3)	Stabulazione di lunga durata (≥2 mesi) oppure trasformazione in stabilimenti riconosciuti . L'Autorita' competente può stabilire un tempo di depurazione inferiore ai 2 mesi sulla base di un'analisi del rischio effettuata dall'operatore stesso.
Proibita	Qualora i valori riscontrati siano maggiori di 46.000 ***Escherichia coli*** per 100 g di polpa e liquido intravalvare (metodo ISO TS 16649-3)	Divieto di raccolta

Table 1.4 (A, B, C, D) Classification of Sardinian waters for shellfish production (https://www.regione.sardegna.it/).

A

ZONA CLASSIFICATA	CLASSE	TIPO	STAGIONALE/ ANNUALE	PERIODO	DATA ATTO DI CLASSIFICAZIONE (giorno.mese)	ANNO DET.	NUMERO DET.	SUPERFICIE	SPECIE
ASSL CAGLIARI									
Santa Gilla mitili zona nord	B	produzione	annuale	gennaio-dicembre	16.01	2014	748/Det/13	circa 28 ettari	*cozza o mitilo (Mytilus galloprovincialis)*
Santa Gilla ostriche zona nord	B	produzione	annuale	gennaio-dicembre	25.09	2017	17835/Det/510	2,5 ettari	*ostrica concava (Crassostrea gigas) e ostrica piatta (Ostrea edulis)*
Santa Gilla molluschi zona sud	B	produzione	annuale	gennaio-dicembre	16.01	2014	748/Det/13	circa 31 ettari	*cozza o mitilo (Mytilus galloprovincialis), ostrica concava (Crassostrea gigas) e ostrica piatta (Ostrea edulis)*
	B	produzione	annuale	gennaio-dicembre	20.03	2015	5018/Det/560		
Santa Gilla veneroidi	B	produzione	annuale	gennaio-dicembre	16.01	2014	748/Det/13	circa 70 ettari	*specie di molluschi dell'ordine Veneroida*
Stagno di Feraxi	A	produzione	annuale	gennaio-dicembre	26.11	2015	19934/Det/1188	circa 4 ettari	*Mytilus galloprovincialis (cozza o mitilo) Ruditapes spp. (vongole)*
					10.08	2017	15581/Det/481	circa 0,8 ettari	*Crassostrea gigas (ostrica concava), Ostrea edulis (ostrica piatta)*
Stagno di San Giovanni	A	produzione	annuale	gennaio-dicembre	05.02	2016	1607/Det/41	3 ettari	*molluschi dell'ordine Veneroida (vongole Ruditapes spp., cuori Cardium spp.)*
	B								*Mytilus galloprovincialis (cozza o mitilo), Crassostrea gigas (ostrica concava)*

B

ASSL OLBIA									
Prestagno di San Teodoro – Pescaia	C	produzione	annuale	gennaio-dicembre	07.03	2019	3837/Det/117	circa 24 ettari	*Crassostrea gigas (ostrica concava), Ostrea edulis (ostrica o ostrica piatta)*
	B				04.06	2019	9458/Det/290		*Ruditapes decussatus (riapertura con determinazione 9458/Det/290 del 04/06/2019)*
Golfo di Olbia (Seno Cocciani)	B	produzione	annuale	gennaio-dicembre	07.03	2019	3830/Det/113	circa 19 ettari	*cozza o mitilo (Mytilus galloprovincialis) - ostrica concava (Crassostrea gigas)*
Golfo di Olbia (Isola Cavallo-Scoglio di Mezzocammino-Foci del Padrongianus)	B	produzione	annuale	gennaio-dicembre	07.03	2019	3834/Det/115	circa 95 ettari	*cozza o mitilo (Mytilus galloprovincialis) - ostrica concava (Crassostrea gigas)*
Golfo di Olbia (Cala Saccaia)	B	produzione	annuale	gennaio-dicembre	07.03	2019	3831/Det/114	circa 60 ettari	*cozza o mitilo (Mytilus galloprovincialis)*
Laguna di Porto Pozzo	A	produzione	annuale	gennaio-dicembre	19.03	2019	4570/Det/142	circa 3 ettari	*ostrica concava (Crassostrea gigas)*
Lido del Sole – Punta delle Saline	B	produzione	annuale	gennaio-dicembre	07.03	2019	3836/Det/116	17 ettari	*mitilo (Mytilus galloprovincialis) - ostrica concava (Crassostrea gigas)*
Golfo di Cugnana	B	produzione	annuale	gennaio-dicembre	18.05	2017	10215/Det/248	circa 1 ettaro	*cozza o mitilo (Mytilus galloprovincialis)*
"Golfo di Olbia - Foci del Padrongianus - cannolicchi"	B	produzione	annuale	gennaio-dicembre	05.11	2018	17051/Det/529		*cannolicchi (Solen spp.)*
"Golfo di Olbia – Cala Saccaia - tartufo"	B	produzione	annuale	gennaio-dicembre	19.03	2019	4569/Det/141	4,2 ettari	*tartufo (Venus verrucosa)*
"Golfo di Olbia - Foci del Padrongianus – vongola"	B	produzione	annuale	gennaio-dicembre	19.03	2019	4569/Det/141	52 ettari	*vongola (Ruditapes decussatus)*
"Golfo di Olbia - Foci del Padrongianus - tartufo"	B	produzione	annuale	gennaio-dicembre	19.03	2019	4569/Det/141	57 ettari	*tartufo (Venus verrucosa)*

C

ASSL NUORO									
Stagno Avalè Su Petrosu	B	produzione	annuale	gennaio-dicembre	25.02	2015	3456/Det/479	circa 20 ha	*specie dell'ordine Veneroida*
	B	produzione	annuale	gennaio-dicembre	16.12	2015	21304/Det/1320	circa 20 ha	*cozza o mitilo (Mytilus galloprovincialis)*
ASSL LANUSEI									
Stagno di Tortoli mitili e ostriche	B	produzione	annuale	gennaio-dicembre	25.09	2017	17825/Det/509	80 ha	*specie cozza o mitilo (Mytilus galloprovincialis), ostrica concava (Crassostrea gigas), ostrica piatta (Ostrea edulis)*
Stagno di Tortoli vongole	B	produzione	annuale	gennaio-dicembre	25.09	2017	17825/Det/509	84 ha	*Ruditapes decussatus (vongola verace)*

ASSL CARBONIA									
Stagno di Cirdu	A	produzione	annuale	gennaio-dicembre	11.01	2013	437/Det/3	23 ha	*mitili (Mytilus galloprovincialis), ostriche (Ostrea edulis – Crassostrea angolata) e vongole (Ruditapes decussatus)*
"Bugasu – mitili e ostriche"	A	produzione	annuale	gennaio-dicembre	30.11	2016	19139/Det/682	30 ha	*ostrica concava (Crassostrea gigas), Ostrica piatta (Ostrea edulis), mitilo (Mytilus galloprovincialis)*
"Bugasu – Veneroidi"	A	produzione	annuale	gennaio-dicembre	30.11	2016	19139/Det/682	30 ha	*vongola verace (Ruditapes decussatus e Ruditapes phillippinarum), cuore edule (Cerastoderma glaucum), tartufo (Venus verrucosa).*
ASSL ORISTANO									
Marceddì-Torrevecchia	B	produzione	stagionale	maggio-agosto	15.05	2017	9888/Det/231	71 ettari	*Ruditapes decussatus (vongola verace), Cardium spp. (cuori)*
Marceddì-Terzapeschiera	B	produzione	stagionale	maggio-agosto	22.06	2015	10676/Det/799	115 ettari	*molluschi dell'ordine Veneroida.*
	B	produzione	stagionale	maggio-settembre	22.06	2015	10676/Det/799	115 ettari	*cozza o mitilo (Mytilus galloprovincialis)*
Stagno di Corru S'Ittiri	B	produzione	stagionale	maggio-agosto	15.05	2017	9893/Det/232	160 ettari	*Ruditapes decussatus (vongola verace) e Cardium spp. (cuore)*
Stagno di S'Ena Arrubia	B	produzione	stagionale	maggio-agosto	15.05	2017	9895/Det/233	248.000 m2	*Ruditapes decussatus (vongola verace)*
Stagno di Corru Mannu	B	produzione	annuale	gennaio-dicembre	12.11	2015	19043/Det/1126	77.000 m2,	*specie Mytilus galloprovincialis (cozza o mitilo), allevata in sistemi sospesi nella colonna d'acqua, e vongole veraci (Tapes spp.), allevate nelle medesime condizioni dei mitili (sistemi sospesi nella colonna d'acqua)*
	B	produzione	annuale	gennaio-dicembre	14.12	2017	22822/Det/823	77.000 m2,	*Cerastoderma glaucum e Ruditapes decussatus*
Torre Grande	B	produzione	annuale	gennaio-dicembre	01.06	2017	11238/Det/286	320.000 m2	*cozza o mitilo (Mytilus galloprovincialis)*
Capo San Marco	stabulazione		annuale	gennaio-dicembre	04.05	2017	9189/Det/186	320.000 m2	*cozza o mitilo (Mytilus galloprovincialis)*

D

1.2 Origin of oysters culture

Oysters farming is an activity with ancient origin; they were indeed already known and appreciated in Neolithic period, as evidenced by several fossil finds. The Chinese probably were the pioneers of this activity. In Italy, a Roman engineer realized the first "table" breeding system between 140 and 91 B.C., in which oysters were collected in bags fixed on some tables which could be positioned in the intertidal water (in which they suffered tidal effect during the day, this is typical in Atlantic coasts of France) or totally immersed. In some countries this method is still used.

In Europe, oysters farming developed in late Renaissance, first by the exploitation of oyster natural beds (*O. edulis*), subsequently by the realization of more complex breeding systems. In the second half of the 19th century, Napoleon III, to avoid the risk of extinction of the oyster *O. edulis*, introduced laws for the regulation of fishing on the French coast. In those

years French government strongly encouraged imports to stimulate the growth of breeding activities.

Fig. 1.8 *Natura morta con ostriche* - Edouard Manet (1862).

In the early 1900s, oyster farming in Italy underwent an increase in production thanks to the introduction of several techniques. However, this growth was abruptly interrupted by the First World War and, due to several factors, such as difficulties in commercial connections and the typhus epidemics of those years, the decline continued in the following years. Currently the production is still marginal but it is a growing activity, and it is often associated with the production of mussels (Cataudella & Spagnolo, 2011).

In the second half of the 20th century this activity gained importance in Europe as a consequence of the increase of its economic size. It firstly started with the farming of flat oyster, followed by the Portuguese oyster, whose farming failed because of mortalities caused by gill disease, and finally the Japanese oyster, *C. gigas*, that was imported in 1970s, mainly in France (Andrews, 1980). In Sardinia, oyster farming in lagoon firstly developed in 1984, exploiting brackish environments. Initially it was considered a challenge with *O. edulis* and *C. gigas* species associated with mussel farms, but gradually real oyster farms developed, first in

Tortolì and in San Teodoro lagoon. Currently, *C. gigas* still represents one of the most important bred and marketed species worldwide.

1.2.1 Culture techniques

Design of an oyster breeding system needs a careful study and selection of the optimal area, as oysters are strongly affected by the environment. They are indeed filtering organisms, dysplaying a filter capability up to 150-200 liters of water every day. An essential factor for oysters growth is the presence of optimal values of dissolved oxygen, salinity and constant availability of phytoplankton, as commonly found in basins with marine currents that guarantee frequent water exchanges.

However, filtering activity can lead to negative aspects as oysters, as well as all bivalve molluscs, can accumulate any biological and chemical contaminant by filtering water of farming site (bacteria, viruses, heavy metals, hydrocarbons, etc.) (Seguin *et al*., 2016; Olalemi *et al*., 2016). Scientific studies widely showed acute and chronic toxic effects of chemical contaminants on oysters. They can in fact interfere on endocrine functions (fertility and reproduction) and act like immunosuppressant thus altering susceptibility to pathogens (De Vico and Carella, 2016).

Fig. 1.9 "Manuale di buona prassi igienica per la produzione primaria." Attività di molluschicoltura, 2011.

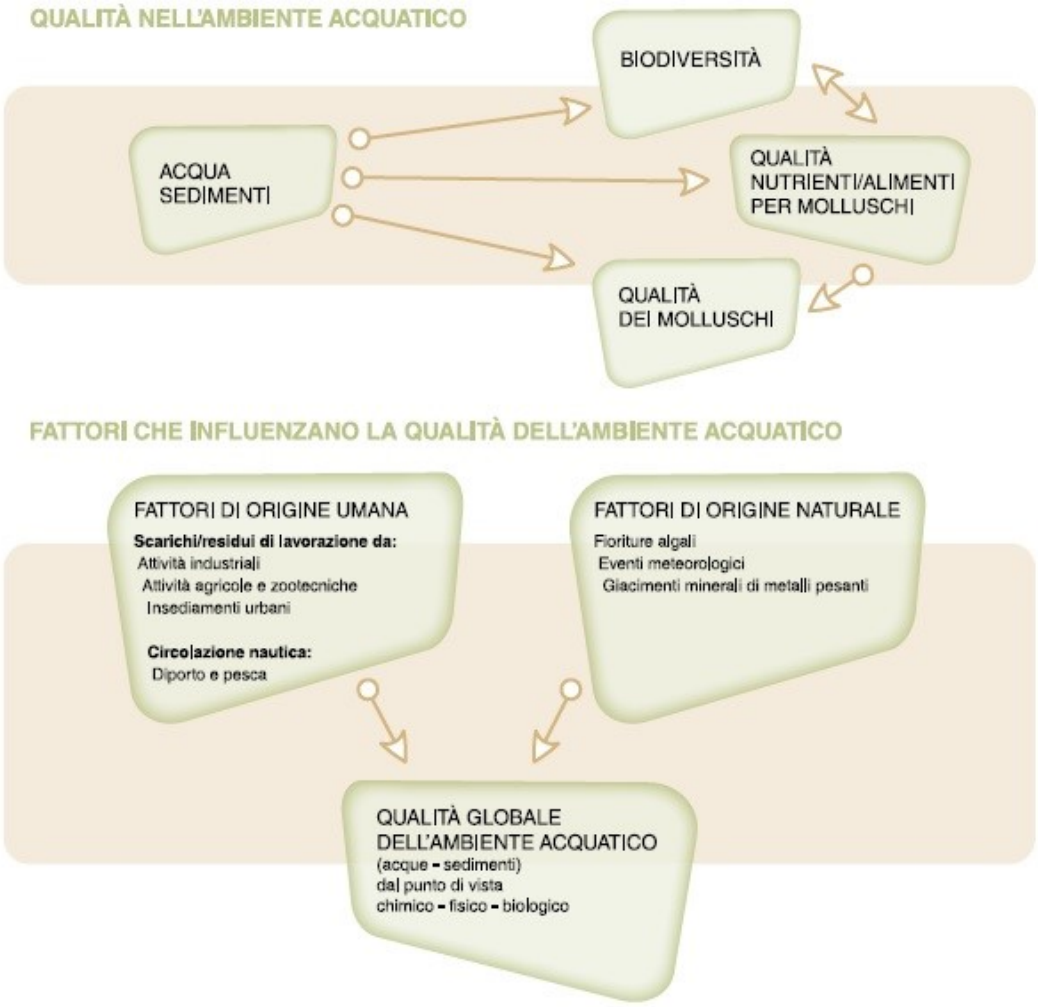

Seed supply represents the first stage of oyster culture. Traditionally, in southern Europe it was obtained by wild seeds capture with traditional techniques such as "lentisco" branches bundles placed on the bottom and then recovered some week later: at the end of the process young oysters were found fixed on the "lentisco" branches. Sometimes, other structures were placed on the bottom as attach material, such as tiles.

These capturing techniques are currently used in farms, together with modern methods. Most farms take seeds by hatcheries (mainly French hatcheries) whose core business is production of uniform size product, sometimes by reproduction or capture/detachment.

Generally, hatcheries provide triploid oysters, obtained through diploid and tetraploid crosses. Results are hypofertile oysters, which use most of their energies in their growth, instead of

development of reproductive system, as diploid ones do. Scientific studies showed in fact that triploid larvae growth was 280-300 microns, whereas diploid ones grew 250-260 microns in the same period. This difference in growth was maintained up to adult stage. Diploid oysters produce “milky fluid” during sexual maturation process; lack of this fluid make triploid oysters more marketable. Finally, these oysters have farming advantageous characteristics and better trade quality (FAO; Yang *et al*., 2018).

Every farmer places seed in specific breeding structures that vary according to the environmental conditions of the area (temperature, tidal range, water depth, food availability).

- Off-bottom culture
- Bottom culture
- Suspended culture
- Rope systems culture

1.2.1.1 Off-bottom culture

Off-bottom culture method provides the use of *poches* (polyethylene bags) or perforated plastic trays. These structures are tied to poles with rope or rubber bands, which are fixed on the bottom in the intertidal zone where they suffer tidal effect. This culture technique can be used both in nursery for the intermediate growth phase and in ongrowing process up to the reaching of the commercial size. This method needs regular maintenance to clean poches or trays and oysters must be transferred on new bags as they grow (Fig. 1.10) (Quayle, 1980; FAO).

Fig. 1.10 Off-bottom culture.

1.2.1.2 Bottom culture

In bottom culture seed can be placed directly on the bottom in the intertidal zone or in deep water, provided that this bottom is enough firm and compact, and there are no other species' breeded.

Generally, the sowing density is low as not require any maintenance until harvesting, when oysters have reached commercial size. Sometimes it is necessary a protection against predators (enclosure or covers) and defense against wave action (Fig. 1.11) (Quayle, 1980; FAO).

Fig. 1.11 Bottom culture.

1.2.1.3 Suspended culture

Suspended culture is the most widespread technique, which is organized in long-lines or rafts. This method can be arranged with many ropes or cables of shells, which are hard substrate that allow oysters adhesion. Another technique used in the suspended culture, particularly in deep waters, is the employment of grid or plastic containers (lanterns) tied together and vertically suspended by rafts or horizontal *lines*. Farmer must regard arrangement of the strings that carry the specimens, to avoid them touching the bottom and minimize fouling formation.

Routine maintenance is required to manage oysters density and to clean containers (Fig. 1.12) (Quayle, 1980; FAO).

Fig. 1.12 Suspended culture.

1.2.1.4 Rope systems culture

First phase of this technique involves the use of suspension lanterns from which oysters are transferred when they have reached a suitable size. Oysters are individually attached on strings with a cementing substance, maintaining an appropriate distance from each other. Strings are then hung from a vertical and horizontal poles structure and fixed on the bottom.

When oyster have reached the commercial size, they are “hardened” for about four months: this practice consists of alternating periods of air exposure and immersion daily, as simulation of tidal effect. Sometimes they are transferred to different basins.

These practices have an optimal effect on quality and external aspect of the final commercial product (Fig. 1.13) (FAO).

Fig. 1.13 Rope systems culture.

1.2.2 Anatomy of bivalve molluscs

The Pacific cupped oyster, *C. gigas* (Thunberg, 1793), is a marine invertebrate and it is classified as follow:

Phylum	*Mollusca*
Class	Bivalvia
Subclass	Pteriomorphia
Order	Ostreida
Superfamily	Ostreoidea
Family	Ostreidae
Subfamily	Crassostreinae
Genus	*Crassostrea*
Specie	*Crassostrea gigas*

C. gigas origins from Japan, where it has been cultivated for a long time. It then was introduced in America in 1920 and it has finally spread in Europe in 1960. In several European countries *C. gigas* found favorable environmental conditions, such as temperature, that favoured his adaptation until it has colonized European coasts (Cognie *et al*., 2006; FAO). Morphologically, *C. gigas* is characterized by cupped shell, inside which the mollusc is surrounded by mantle and it is connected to the valves by adductor muscle.

Fig. 1.14 Oyster anatomy.

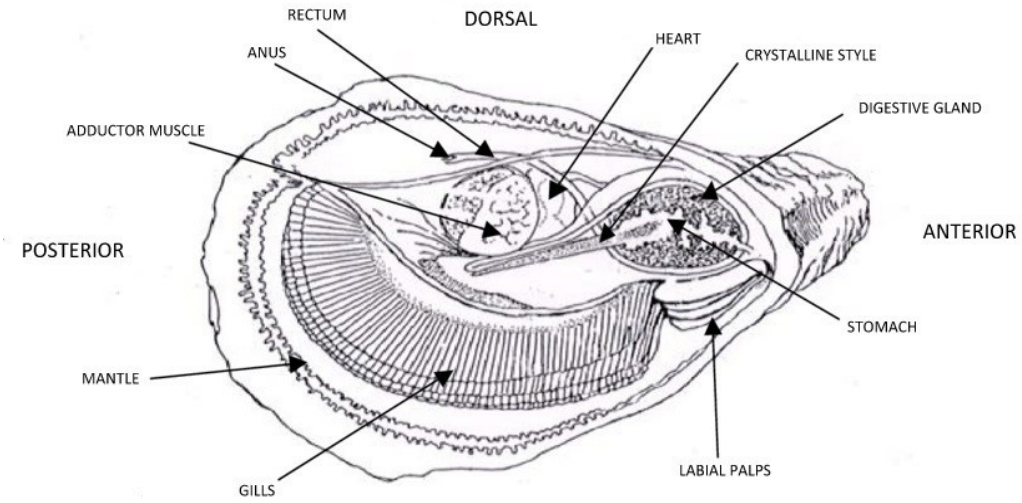

1.2.2.1 The shell

Bivalve molluscs shell provides the skeleton structure to which adductor muscle attaches, offers protection against predators and finally prevents debris, mud and sand to entry inside mantle cavity (Gosling, 2003; De Vico and Carella, 2016). Shell component is mainly represented by calcium carbonate and secondarily from another protein, conchiolin. These constituents are organized in three layers:

- Externally there is a thin conchiolin layer; sometimes it could be reduced because of mechanical actions, fouling, organisms, parasites or diseases;
- Intermediate layer of aragonite or calcite (crystalline forms of calcium carbonate);
- Inner layer of nacre, it appears with an opaque or iridescent aspect.

External mantle produces the first and the second layers, whereas third layer is produced by the entire mantle surface; this tissue is also responsible for shell growth and thickening.

Oyster shell formation begins during larval stage with mantle first secretions; subsequently these secretions increase and promote shell growth. Definitive shell of adult oyster is strongly calcified and shows different pigmentations.

Calcium used to shell growth comes from diet and sea water, whereas carbonate derives from CO_2/bicarbonate reserves in shellfish tissues. All the shell formation process requires a large amount of energy.

Cultured oysters, belonging to different species, show different types of shell. *O. edulis* has circular valves shell with one flat valve, whereas *C. gigas* has cup-shaped valve. In these species shell growth can reach 100 mm. Finally, *C. virginica* has elongated shell, with one valve more cup-shaped than the other, and with a growth that can arrive up to 350 mm (Gosling, 2003).

1.2.2.2 Mantle

Two lobes of connective tissue form mantle structure, which wraps the mollusc inside the shell. Mantle is a thin and transparent structure, with thick and black margins (maybe it has a protective function against solar radiations). In contains many hemolymph vessels, nerves and muscles, mainly located close to the margins. On the inner surface of mantle there are cilia, whose functions are to direct particles towards gills and to remove larger particles towards expulsion area. Waste materials are frequently “blown out” from mantle cavity by valves strong closing movements.

Margins of mantle consist of three layers: the external layer that secretes substances for shell formation; the intermediate layer, a highly innervated part with a sensory function, in which there are chemoreceptor and tactile cells, and the inner layer, called *velum*, composed of muscular tissue, whose function is to control water flow in mantle cavity.

Little space with pallial fluid separates mantle from the inner side of the shell; the only connection between the mollusc and the shell is the adductor muscle.

Mantle has an exhalant opening and a smaller inhalant opening, to permit outflow and inflow of water, respectively.

Sensory cells and ocelli in mantle are involved in predator's detection: sudden closure of valves is a self-defense modality as a result of any sensorial stimulation (Gosling, 2003; De Vico and Carella, 2016).

1.2.2.3 Gills

Oysters, also called lamellibranches, are "filter feeding" organisms thet feed on sea or lagoon water.

Gills are two large suspended structures, connected to the dorsal margin of the mantle by the ctenidial axis. There are also branchial nerves, afferent and efferent vessels of branchial hemolymph. Gills appear spread on the entire surface exposed to water flow, tracing shell shape, to maximise the inhalation of water.

Each gill is constituted by numerous filaments disposed to form W shape. These filaments have a collagen skeleton, to reinforce their structure. The half of the filament, the demibranch, is a V-shaped structure formed by many arms called lamellae. Therefore, every demibranch is make by an inner descending lamella and an external ascending lamella: in the space between these two structures there is an exhalant chamber that is connected to exhalant opening in mantle margins; also, there is an inhalant chamber ventrally to filaments, that is connected to inhalant opening in mantle margins. Neighboring filaments are attached by interfilament junctions, with narrow spaces between them.

Oysters gills have some folds to increase filtering surface, probably an adaptation to life in difficult conditions, such as coarse surfaces. Folded area filters largest particles and cilia of filaments filters thinner particles.

Based on their position, cilia of filaments accomplish specific roles. In fact, lateral cilia filter the water which flows through gills filaments and heads towards exhalant opening, whereas retained particles move to the external surface of gills, the frontal cilia, that carry particles to

ventral side of each lamella. Cilia movements are controlled by nerves: in every branchial axis there is a branchial nerve which innervates filament groups.

Gills have the double function of alimentation and respiration. Their extended surface and the great hemolymph supply promote gas exchanges. Afferent vein carries deoxygenated hemolymph from kidneys to gills; this vein has small ramifications which go into each filament where gas exchanges take place, thanks to vein thin walls. Oxygenated hemolymph goes from gills to kidneys and heart by efferent vein.

Gills are also involved in bioaccumulation of harmful substances, such as pesticides, hydrocarbons, heavy metals. These substances could cause tissues damage, such as the loss of gills cilia or cells degeneration. In gills and digestive gland there are proteins specialized in binding of heavy metals to counteract harmful activity of this substances (Gosling, 2003; De Vico and Carella, 2016).

1.2.2.4 The foot

The foot appears at the pediveliger stage of oyster life cycle, when their length is about 200 µm. It has an important role in first movements and attachment. At the beginning of the settlement, pediveliger larvae length is about 250-300 µm, and they go down towards sea bottom.

The foot is constituted by several longitudinal and circular muscular layers that surround a little chamber with hemolymph. There are nine different types of glands that allow movements and attachment.

Attachment phase is accomplished by the secretion of cementing substance by byssal gland of the larva, that adheres to this cement by left valve. The attached larva is ready for metamorphosis, the morphological change that determine the shift from pelagic phase (free in water environment) to sessile phase (anchored to a substrate). Once attached to cement, oyster

detachment is not possible. In *Ostrea* and *Crassostrea* genera the complete loss of the foot occurs during the metamorphosis (Gosling, 2003).

1.2.2.5 Gonads

Oysters reproductive system covers the external surface of the digestive gland. Gonads are constituted by branches of tubules covered by an internal epithelium in which gametes are formed. Tubules combine each other to form ducts, which lead to larger ducts, and end in short gonadal ducts. Sometimes, these gonadal ducts end into mantle cavity through pores. Generally, fertilization is an external process, but in few cases it occurs within the mantle cavity. This happens in *O. edulis*, whose eggs are fertilized inside the mantle cavity where they develop up to floating larva stage until they are released in the environment. Because of this, *O. edulis* oysters are called *larvipare*. Conversely, *Crassostrea* oysters are called *ovipare*, because they spawn and release sperm in external environment, where fertilization occurs.

Both oyster species are protandric hermaphrodites.

In *Ostrea* genus at the beginning of sexual maturity gonad develops in testicle, maintaining some female cells, that will develop later causing reversible sex change. In *Crassostrea* genus, environmental conditions, water temperature and food availability influence sex determination (Gosling, 2003; De Vico and Carella, 2016).

1.2.2.6 Labial palps, alimentary canal and digestive gland

Bivalve molluscs are filtering organisms, that feed on plankton and food particles from water. Gills and mantle's cilia and labial palps transport these particles towards the mouth.

Labial palps are four triangular structures located on the sides of the mouth in which gills terminate. Their inner surface is folded to form crests provided with few cilia, whereas the

external surface is smooth. The space between these two surfaces is filled with muscular connective tissue.

These structures preserve gills from filtered particles to prevent their saturation. Some particles are removed as pseudo-feces towards the excretory tract of mantle, and thus eliminated, whereas the remaining filtered particles are conveyed towards the mouth for ingestion. Ciliated mouth is a small opening connected to the stomach by ciliated esophagus; cilia are in fact located in the entire alimentary canal to propel material up to stomach.

The stomach contains a crystalline style, a semi-transparent structure that communicates with the intestine. Its function is to secrete digestive enzymes in the stomach thus allowing extracellular digestion.

The stomach is a large oval structure within digestive gland (also named hepatopancreas). These two structures are connected by some ducts, divided in ciliated primary ducts and their small ramifications, and secondary ducts without cilia that terminate with blind tubules. Inside these ducts, there is a constant material flow, which enters digestive gland for intracellular digestion and absorption, and then it returns to stomach and intestine.

Two different types of cells, digestive cells and basophil (secretory) cells, characterize the tubules: both producing a high number of enzymes. Digestive cells, responsible for intracellular digestion, are more abundant, with rich lysosomal system and a variable size depending on the reproductive cycle phase. Basophil cells are fewer and they play a fundamental role in the synthesis and secretion of digestive enzymes (Fig. 1.15).

Histological changes are based on physiological status (digestive and reproductive cycles) and environmental stresses (i.e. tidal rhythm).

Life cycle phases of tubules epithelial cells are:

I. Normal or holding;

II. Absorptive and digestive;

III. Disintegrating;

IV. Reconstituting.

Epithelial cells change in disintegrating phase has been sometimes studied in order to detect histopathological alterations due to environmental factors (pollutants or pathogen agents) (De Vico and Carella, 2016; Usheva *et al*., 2006; Carella *et al*., 2015).

Fig. 1.15 Transverse section of digestive tubules: digestive cells (A), basophil cells (B), phagocytes (P), connective tissue (CT), food vacuoles (FV), lumen (L) (modified from Yonge 1926).

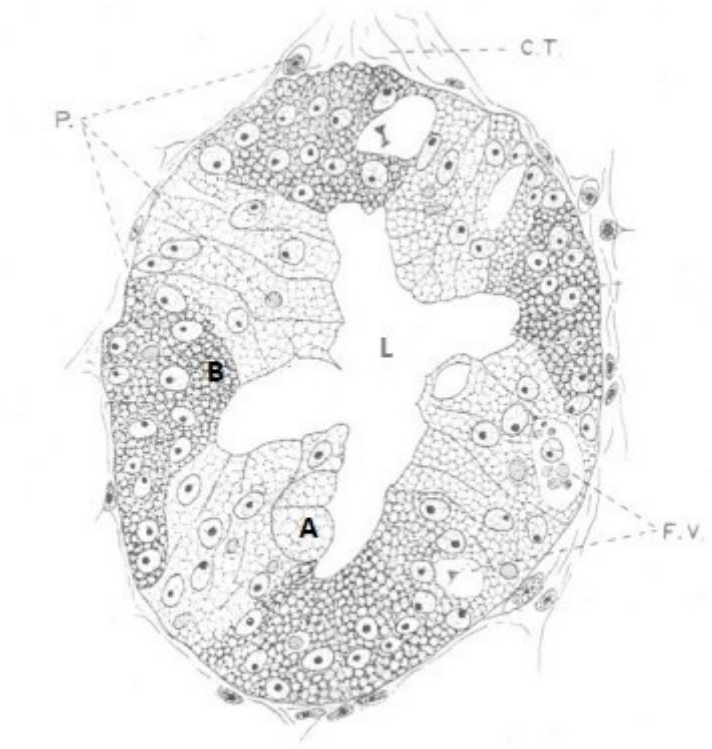

Digestive gland is involved in defense mechanisms, substances absorption, synthesis of digestive enzymes and detoxification processes. Another fundamental role is the storage of metabolic reserves, that could be useful during gametogenesis and periods of physiological stress (Gosling, 2003; De Vico and Carella, 2016).

1.2.2.7 Excretory organs

Excretory organs in oysters are kidneys and pericardial glands. Waste are accumulated in cells of pericardial glands, released inside pericardial cavity and subsequently eliminated through kidneys. Kidneys have a granular portion connected with pericardium and a bladder-like portion with thin walls, that ends inside mantle cavity.

Pericardial glands have hemolymph filtering cells that filtrate flows into granular portion of the kidney where ions are secreted and reabsorbed. The resulting product is urine, with high concentration of ammonia and lower amounts of amino acids and creatine.

Ammonia, released as final product of protein metabolism is toxic but water-soluble that it's rapidly spread away from the animal (Gosling, 2003).

1.2.2.8 Heart and hemolymph vessels

The heart, enveloped by the pericardium, is located in the mid-dorsal area of the oyster's body, near the valves closing line. It consists of a single muscular ventricle and two small chambers, the auricles. Hemolymph flows from auricles towards the ventricle and enters inside the anterior aorta. This vessel then branches into pallial arteries, which supply the mantle with hemolymph, and into visceral arteries, which supply stomach, intestine, adductor muscle and foot with hemolymph.

Arterial ramifications carry hemolymph in all tissues, where it is drained towards the venous sinuses up to mid-ventral sinus, located above kidney-pericardium complex. Finally, the hemolymph reaches the kidney for purification, then it goes to gills and returns to the heart ventricle.

Hemolymph has many important functions in bivalve physiology, such as gas exchanges, osmoregulation, nutrients distribution, elimination of waste substances and immune defense. In addition, it is responsible of tissues turgor mainteinance, necessary for their support, in

mantle margins, in the foot and in the labial palps. In hemolymph there are some cells named hemocytes, that can move outside the sinus freely, in the connective tissue and in cavities, where they perform some functions, such as digestion, transport and excretion, tissues repair and internal defense (Gosling, 2003; De Vico and Carella, 2016).

1.2.2.9 Bivalve defense system

Immune system of bivalves consists of a physical and a biological barrier. The first physical barrier is the shell, which mainly plays a protective function for soft tissues against biological and chemical-physical traumas. Other physical barriers are skin and mucosa, that trap foreign agents and eliminate them with ciliary activity.

Hemocytes, innate immunity cells that flow in the circulatory system, in cavities and in tissues, ensure internal immune defense. Circulating hemocytes and humoral factors work together to neutralize foreign organisms (Allam *et al*., 2015).

Hemocytes can be divided in two morpho-functional categories: *granulocytes* and *agranulocytes* (or *hyalinocytes*) (Fig. 1.16). Granulocytes are large cells (about 10-20 μm) with phagocytic activity, that often display an eccentric nucleus and numerous cytoplasmic granules. They can be sub-classified in *eosinophils*, *basophils* and *mixed forms* based on staining properties (May-Grunwald Giemsa) (Chang *et al*., 2005; Allam *et al*., 2015; Pila *et al*., 2016; De Vico and Carella, 2016).

Fig. 1.16 H.E. staining of hemocytes (150X): hyalinocytes (small arrowhead), granulocytes (big arrowhead). (Photo from De Vico and Carella, 2012).

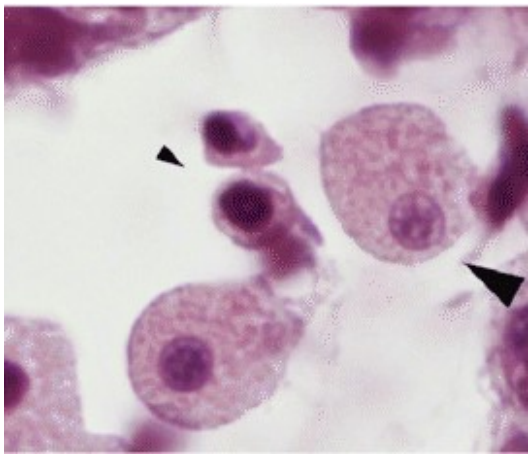

Agranulocytes are small cells, that lack cytoplasmic granules and present low aptitude for phagocytosis.

The first phase of phagocytosis is *chemotaxis*, that is represented by the hemocytes migration towards non-self components. The attachment to the surface of invading organisms is the subsequent phase and then there is the real phagocytosis. During this event some microbicidal processes take place and the production of hydrolytic and antimicrobial substances facilitate the neutralization of foreign agents.

There are numerous hemocytes in extra-pallial cavity, able to phagocytize biotic and abiotic particles, secrete several hydrolytic compounds (lysozyme and peptidase) and antimicrobials (agglutinins) in the extra-pallial fluid.

Another important role in defense against pathogens is accomplished by epithelial cells of mucosal surfaces that contribute to the regulation of microorganisms entrance by secreting several bioactive molecules into the mucus.

All bivalve mucosal epithelia, mantle epithelial cells (extrapallial and pallial surface), gills and digestive gland can perform endocytosis of biotic and abiotic molecules. This process has a double function, defensive and nutritional, because it enhances food particles absorption and it reduces infections by the capture of pathogens and their neutralization.

Some pathogens can bypass this barrier and establish an infection process in epithelial cells. In the infection sites, recruited hemocytes can interact with pathogens directly (through binding to membrane receptors) or indirectly (through plasma recognition factors).

The direct interaction is accomplished by pattern-recognition receptors (PRRs). These molecules are membrane receptors able to recognize bacterial surface molecules, such as *lectins*, carbohydrates binding proteins (they are implicated in host-pathogen interaction in different taxa), *peptidoglycan recognition proteins* (*PGRPs*) and *Toll-like receptors* (*TLRs*). TLRs are distributed mainly in bivalve pallial organs (e.g. the mantle) and can recognize different microbial genera.

Hemocytes and pathogens indirect interaction is mediated by plasma factors such as *agglutinins* that recognize and bind microbial cells, thus facilitating absorption by hemocytes (Allam *et al*., 2015; De Vico and Carella, 2016).

1.2.2.10 Nerves and sensory receptors

Bivalves molluscs nervous system is very simple, formed by three pairs of ganglia and several nerves bundles. Two bundles of nerves extend from *cerebral ganglion*, the first of which continues into the *visceral ganglion* (in the surface of upper adductor muscle) whereas the second one extends posteriorly and ventrally to *pedal ganglion*.

The cerebral ganglion innervates labial palps, anterior adductor muscle and a portion of the mantle; pedal ganglion controls the foot and, finally, visceral ganglion controls the largest area which includes gills, heart, pericardium, kidneys, digestive tract, gonads, posterior adductor muscle, mantle and pallial sensory organs.

Ganglia are constituted by different types of neurosecretory cells, the *neurons*; that produce some peptides which are released inside the circulatory system, thus regulating growth and gametogenesis.

The mantle of bivalve molluscs harbors several sense organs, both in margins and in the middle of the mantle. There are sensory epithelial cells, which contain many pallial tentacles, extremely sensitive to tactile stimulus. Due to this ability any small stimulus can cause musculature contraction as reflex action. A strong stimulus can cause retraction of the entire mollusc within the shell. This is an adaptive action mechanism and it's under visceral ganglion control (Gosling, 2003).

1.2.3 Oyster life cycle

Pacific oyster (*C. gigas*) is the most widely bred oyster species because of its rapid growth and its good adaptability to different environments. Oysters prefer static bottoms with rocks or another suitable substrate on which they can attach in the intertidal zone. They can also be found in muddy bottoms. Their optimal growth occurs at a temperature range between 9°C and 30°C and a salinity range between 20‰ and 30‰.

Oyster species are protandric hermaphrodites, as they can change their sex during the life, by the influence of environmental conditions. Although the maturation process usually leads firstly to the male gender, an environment richness of nutrients can promote female differentiation (FAO; Collin R., 2013; Henshaw J.M., 2018).

Oyster life cycle begins with the emission of male and female gametes in the water column, when oysters are about one year old and sexually mature. In this phase reproductive organs are about 50% of the total body volume of the mollusc. Presence of abundant phytoplankton in the environment is a crucial factor in this step because it is required a large amount of energy for the sexual maturation process.

Furthermore, the reproductive process needs optimal environmental conditions, such as salinity in the optimal range between 15‰ and 32‰ and water temperature of 20°C.

Generally, gametes of one sex are released and this stimulates the release of opposite sex gametes.

When released eggs and sperm are together in water column, the fertilization process begins. Fertilized eggs undergo cellular divisions and develop through several larval stages. They first become *trochophore* and subsequently larvae with a greater motility, the *veliger*. In this phase they feed on small algae suspended in water. Veliger larvae consist of a plate of protein matrix and a large ciliated lobe, the *velum* (Fig. 1.17). This plate folds medially and calcifies on both sides to form two valves of the larval shell. Velum and pre-oral cirri allow the larvae to float and feed.

Fig. 1.17 Oyster *veliger* larvae. (bo) mouth; (pi) foot; (st) stomach; (cu) heart; (a.b.) branchial sketch; (a.p.) posterior adductor muscle; (an) anus; (a.a.) anterior adductor muscle; (ve) velum; (g.d.) digestive gland; (in) intestine; (r.v.) *velum* retractor muscles (Cataudella e Bronzi, 2001).

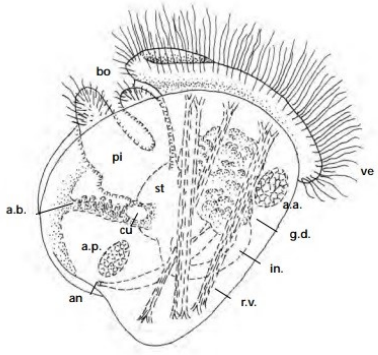

In this stage larvae stay in water column for few weeks, while marine currents support their dispersion and feeding. The emission process of each oyster counts more than one million of eggs, most which are destinated to become food for other marine organisms, without affecting the survival of the species.

About two weeks later larvae develop a “foot” and they became *pediveliger*. In this stage they concentrate on the bottom and the foot will permit them to search for a hard substrate on which they can attach (often these substrates are shells of other oysters).

Once the optimal substrate is found, larvae release a cementing substance from glands located in the foot that helps them to attach on this substrate. Pelagic life becomes now benthic life. Subsequently, larvae lose the foot and they become *spat* (Fig. 1.18).

Fig. 1.18 Oyster life cycle.

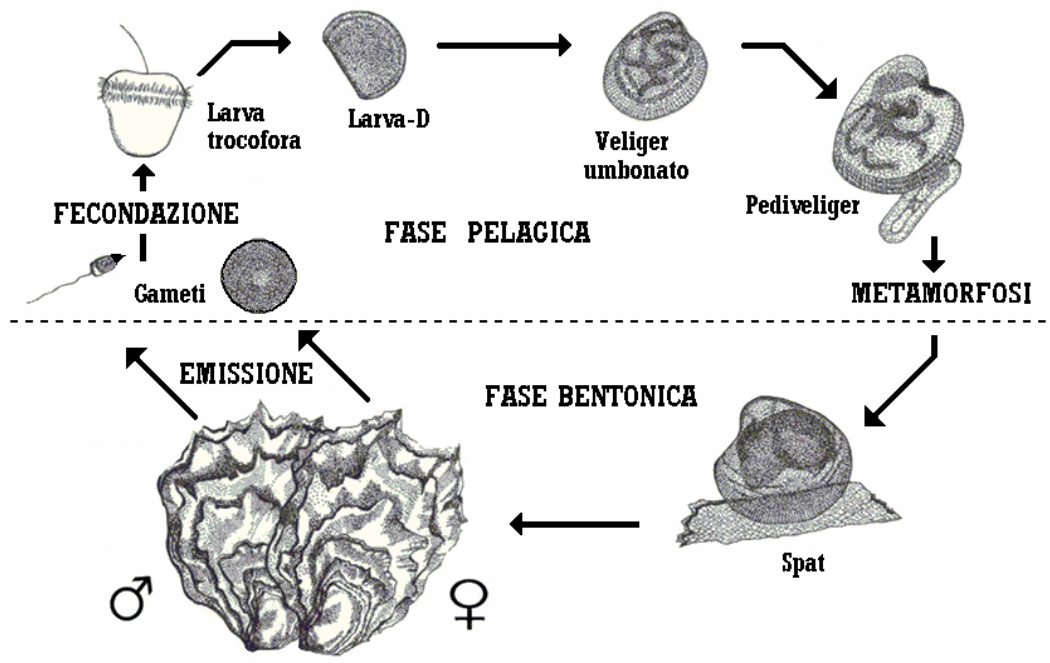

At this stage, oysters begin to feed on microalgae by filtering the water through gills and labial palps, structures located frontally to the mouth (Wallace *et al*., 2008).

Spat oysters use most of their energy reserves to the shell development and growth, which main component is calcium carbonate that derives from diet and water.

One-year old oysters become *juvenile* and then *adults* oysters at three years of age (Cataudella e Bronzi, 2001; Gosling, 2003; De Vico and Carella, 2016).

1.3 Oyster pathogens

1.3.1 Oyster viruses

Urban and industrial global development led to an increase in the exploitation of shellfish natural beds, causing an uncontrolled harvest and the local resources depletion. Because of great demand of product, management techniques and intensive farming were developed.

At the same time, the impact of infectious disease has been observed, strongly affecting productivity and product quality. Many countries in fact have registered great mortality episodes worldwide.

Viruses have been identified as one of the main causes of these pathological episodes. Different species have been isolated during mortality episodes in several molluscs, mainly belonging to *Iridoviridae*, *Herpesviridae*, *Papovaviridae*, *Reoviridae*, *Birnaviridae*, *Picornaviridae* families (Renault, 2008).

Viral infections affected oyster farms globally for over five decades, because of their easy transmissibility and their highly infectious potential.

In the 60s, a member of *Iridovirus* family was isolated in oyster farms of Atlantic coasts of France and USA. It firstly affected Portuguese oysters, *C. angulata*, and subsequently it was isolated from Pacific oysters, *C. gigas.* The latter oyster's species was introduced to replace the total loss of *C. angulata* stocks (Comps *et al*., 1977). After *Iridovirus* infection the oyster can develop necrotic lesions in gills and labial palps and, eventually, the destruction of gill filaments. Histologically, great atypical hemocytes infiltration has been observed. *Iridovirus* is considered the cause of *C. angulata* extinction in 1973.

In *C. gigas*, apparently resistant to *Iridovirus* a similar virus was identified, causing histological lesions in connective tissues in association with atypical cells.

Moreover, they suffered the infection by another virus, an irido-like virus (Oyster Velar Virus, OVV), which caused great mortality in oyster larvae in USA between 1976 and 1984.

The induced lesions, the loss of velar epithelium cilia and the detachment of velum, impeded larvae's correct movement (Renault, 2008).

1.3.1.1 Ostreid herpesvirus-1 (OsHV-1) and its variants

Another virus, a herpes-like virus, was identified in several countries, such as USA, Mexico, France, Spain, UK, New Zealand, Australia, and then all over the world, known because of high infectivity and damages caused in oyster farms (Farley *et al*., 1972; Hine *et al*., 1992; Comps and Cochennec, 1993; Renault *et al*., 1994a).

In the 70s there was the first description of a herpes-like virus, in oysters *C. virginica* from USA (Farley *et al*., 1972), subsequently identified also in *C. gigas* and *O. edulis* (Renault *et al*., 2000; Renault, 2008).

Mainly, herpes-like virus has been found in hatcheries, in larval and juvenile oysters, but also adults can be affected even if they rarely show damages.

Lesions in larvae are localised in the mantle and the velum, causing difficulty in swimming and floating, and thus reducing food activity, leading to the death of the oyster (Hine *et al*., 1992; Renault *et al*., 2000).

In juvenile oysters, sudden death episodes have been observed, often occurring during summer. Histological lesions can be observed in connective tissues, with an infiltration of abnormal cells.

Gills erosion in adult oysters has been observed with histological lesions located also in the mantle, gills, labial palps and digestive gland, associated with diapedesis but not with inflammatory reaction. Peculiar features of the disease are cellular changes, hypertrophy, nuclear margination and pyknosis (Renault *et al*., 2000; Friedman *et al*., 2005; Arzul *et al.,* 2017).

The virus can persist for a long time in the infected hosts without manifesting disease; sometimes DNA and proteins of herpes-like virus have been detected in asymptomatic organisms (Arzul *et al*., 2002; EFSA, 2015).

This herpes-like virus was firstly purified and classified by the transmission electron microscopy and it was named Ostreid herpesvirus-1, OsHV-1 (Le Deuff and Renault, 1999; Davison *et al*., 2005). It belongs to the order of *Herpesvirales*, family of *Malacoherpesviridae*, the only member of *Ostreavirus* genus. Nowadays, it is extensively studied because it still causes several mortality episodes in oyster farms (Davidson *et al*., 2009).

As all the Herpesvirus family members, it consists of a double-strand DNA genome (207 kbp), contained into an icosahedral capsid, and surrounded by a tegument layer and a lipid envelope layer, to which membrane proteins adhere (Fig. 1.19).

DNA replication, protein synthesis and procapsid formation take place in the nucleus. Subsequently, partially formed structure of the virus comes out from the nucleus obtaining the final components by nuclear membrane and trans-Golgi network.

Fig. 1.19 Herpes-like virus general structure.

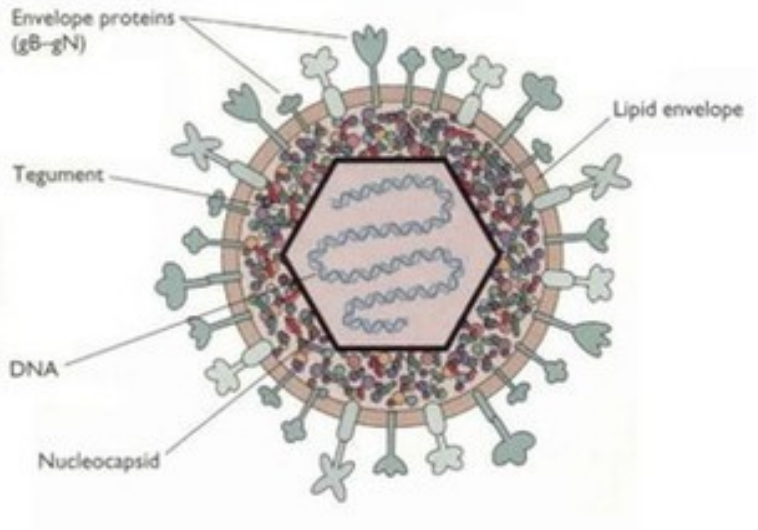

Genome structure consists of two regions U_L (167,843 bp) and U_S (3370 bp), each region is flanked by inverted repeat TR_L/IR_L (7584 bp) and TR_S/IR_S (9774 bp), they are separated by single X region of 1510 bp (Davison *et al*., 2005).

The most affected European country was France, where mortality episodes with the worst consequences were recorded since 1991 (Nicolas *et al*., 1992; Renault *et al*., 1994b), and then in 2008 and 2009 (Martenot *et al*., 2011). Since 2010 mortality also extended to Ireland, Great Britain, Jersey and Italy (Dundon *et al*., 2011).

Mortality episodes in oysters started with symptoms such as reduced feeding and difficulty in swimming, leading to a reported mortality up to 90-100%.

Several studies have been carried out about these episodes in order to better characterize the etiological agent. Total OsHV-1 genome was sequenced by Davison *et al*. (2005) (AY509253), and later some variants of this virus were identified.

Ostreid Herpesvirus-1 var (Arzul *et al*., 2001) variant was characterized by the loss of nucleotide of 2,8 kbp in one of the two TR/IR regions. In addition, it had a 200 bp deletion and 27 bp insertion in C region. Probably these mutations had fundamental role in virus infectious ability, indeed it was detected in *C. gigas* as well as in *T. philippinarum* (Arzul *et al*. 2001; Martenot *et al*., 2011).

Mortality event that occurred in 2008 caused serious consequences in French coasts. A new genotypic variant of OsHV-1 was isolated in most of affected oysters, as it was detected in 40% of 2008 samples and in 100% of 2009 samples.

This variant, named Ostreid Herpesvirus-1 µVar, is characterized by different mutations, such as deletions, substitutions and insertions in C region (ORF 4), which encodes an unknown function protein (Segarra *et al.,* 2010). Main deletion concerns 12 consecutive nucleotides in a microsatellite area characterized by "CTA" nucleotides repetition, followed by an adenine deletion (HQ842610-1) (Fig. 1.20) (Segarra *et al.,* 2010; Martenot *et al*., 2011; Martenot *et al*., 2012; Barbosa Solomieu *et al*., 2015; Mandas and Salati, 2017).

The same nucleotide deletion of C region has been detected in two different new variants of virus, with a difference only in the size of deletion: OsHV-1 µVar Δ9 (9 consecutive nucleotides deletion) and OsHV-1 µVar Δ15 (15 consecutive nucleotides deletion). These two variants have lower incidence than the OsHV-1 µVar variant (Martenot *et al*., 2011; Martenot *et al*., 2012; Barbosa Solomieu *et al*., 2015).

First virus identifications in infected oysters was accomplished by a transmission electron microscopy and the histopathological analysis of infected tissues (Renault *et al*., 1994 a, b). After that, new advanced biomolecular techniques for detection were soon identified, such as *in situ* hybridization (ISH), PCR and real time PCR (Renault *et al*., 2004; Batista *et al*., 2005; Batista *et al*., 2007; Oden *et al*., 2011; Mandas and Salati, 2017).

Fig. 1.20 Distinctive mutations between OsHV-1 and OsHV-1 µVar sequences (Segarra *et al.*, 2010).

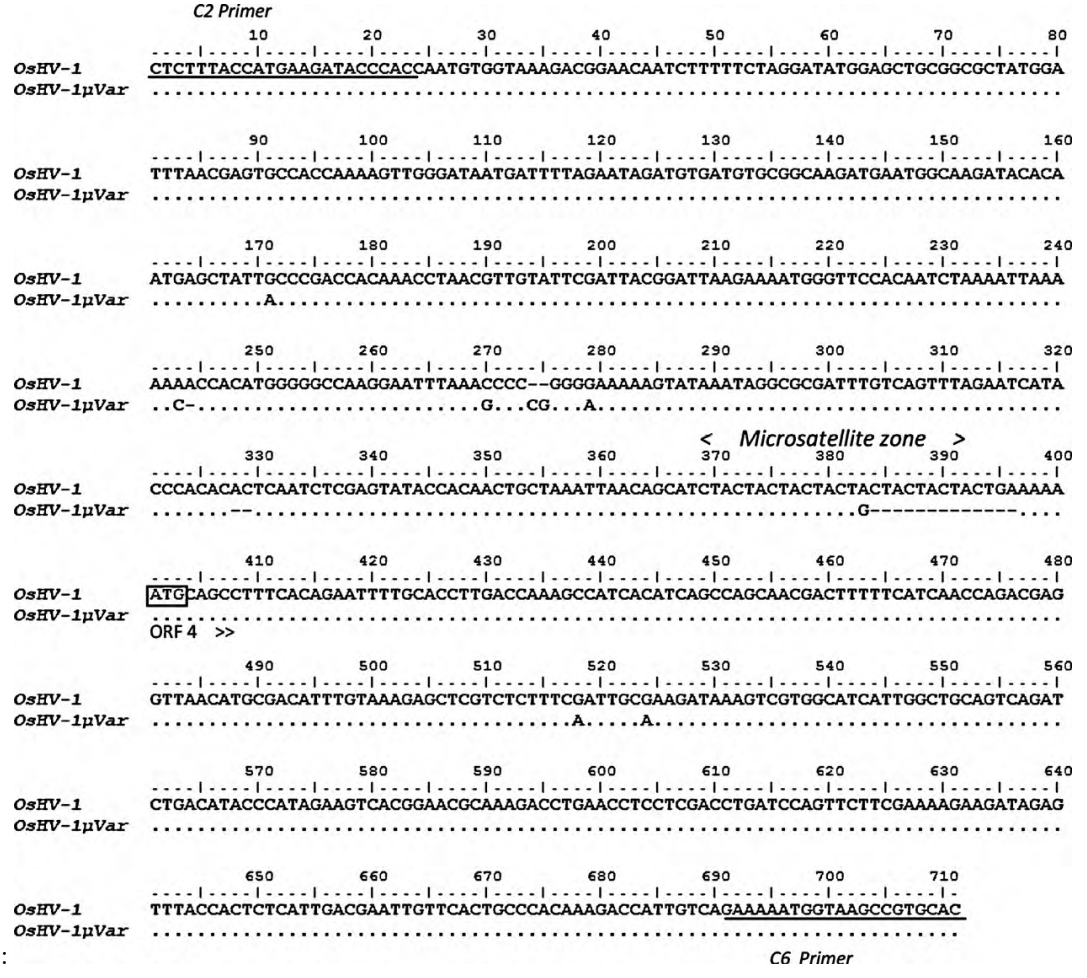

Currently, the most sensitive method for detection of OsHV-1 and its variants is polymerase chain reaction (PCR and real time PCR). Real time PCR is very sensitive method and it's able to detect low amounts of virus DNA in apparently healthy samples (EFSA, 2010; Oden *et al*., 2011).

Some available primers are C6 forward primer and C2 reverse primer, highly specific primers that amplify 709 bp fragment in C region (178181-178889), the main genetic mutations to distinguish OsHV-1 from OsHV-1 µVar, can be found (Fig. 1.20) (Renault and Arzul, 2001).

Nested-PCR represents another method to detect OsHV-1, that consists of two subsequent amplification reactions with different oligonucleotide sets. The first set of primer amplify a specific fragment, whereas the other set amplify smaller fragment within the previous one. Some primer set used in nested-PCR are C2/C4, C2/C6 (Batista *et al*., 2007) and C2/C6, CF/CR. This technique increases specificity of amplification reaction by reducing non-specific amplification of DNA. Different primers have been studied to amplify other fragments in C region, in A region, in B region or in Gp region, as shown in Fig. 1.21 (Renault and Arzul, 2001; Segarra *et al.,* 2010; Batista *et al*., 2007).

Fig. 1.21 OsHV-1 genome. (a) Position of A, B, C and Gp regions. (b) Position of each primer in the region (arrows). (Modified from Batista *et al.*, 2007).

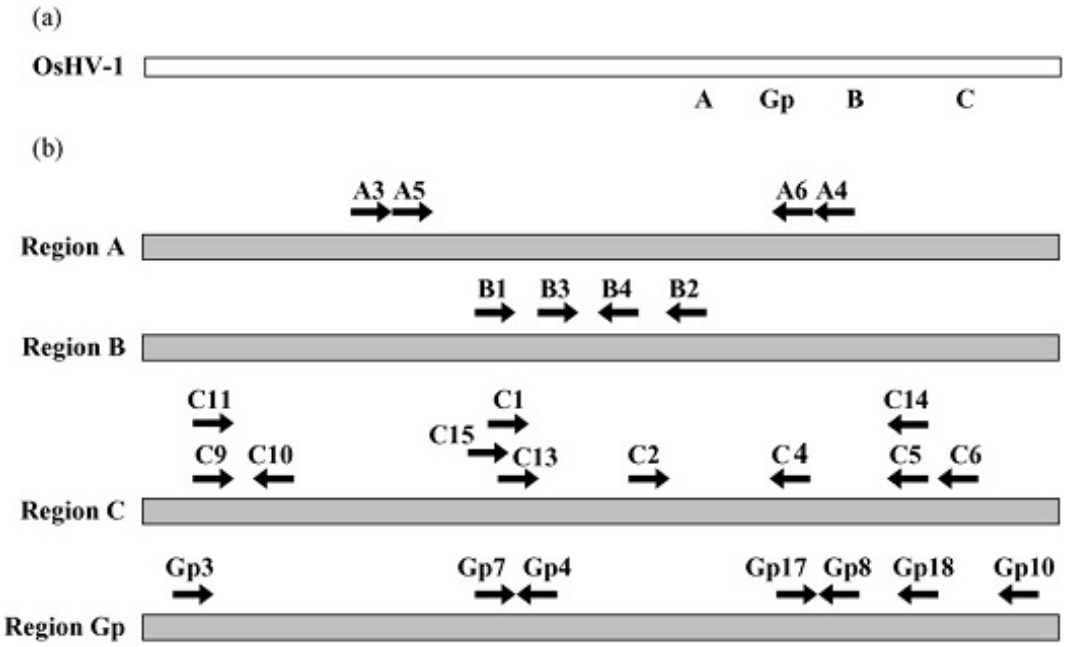

Sequencing analysis of PCR products represents the best method to distinguish viral variants of OsHV-1 (Mandas and Salati, 2017).

The crucial role of water in virus transmission has been assessed; because virus was detected by real time PCR in water in which infected oysters resided. This is then considered the main natural transmission route, even if it is still unknown the amount of virus that can cause the infection (Sauvage *et al*., 2009).

Experimental study of Schikorski *et al*. (2011) evaluated OsHV-1 µVar transmissibility in experimental challenges, performed using an extract of naturally-infected oysters by intramuscular injection and also by cohabiting injected oysters with healthy ones. Cohabitation of injected specimens with healthy oysters showed minor infectivity with a mortality rate of 50% against 90% of the infection obtained by intramuscular injection. It also emerged that the virus begins its infection in digestive gland, then it spreads to the hemolymphatic system and towards the other organs.

In the last 15 years several authors identified some cellular and tissues alterations probably associated with OsHV-1 infections. Friedman *et al*. (2005) observed few abnormal hemocytes with nuclear alterations (pycnosis or nuclear fragmentation) in some tissues, necrotic cells in mantle epithelium, probably involved in diapedesis process. Histological analysis on experimentally infected oysters showed pycnotic nuclei in gonad, adductor muscle, digestive gland, heart, mantle and gills tissues whereas digestive gland also showed hemocyte infiltrations (Lopez-Sanmartin *et al*., 2016). Moreover, OsHV-1 detection by IHC method on experimentally infected oysters performed by Martenot *et al*. (2016) showed a positive reaction in several connective tissue cells (mantle, gills, digestive gland, labial palps, heart, adductor muscle, female gonad), by the use antibodies against putative apoptosis inhibitor. Bueno *et al*. (2016) reported some non-specific histological alterations during an OsHV-1 associated to mortality episode in *C. gigas*, such as focally or diffuse hemocytosis, mainly in stromal connective tissues of digestive gland and mantle, some atrophy signs in digestive gland diverticula, cellular degeneration, and necrosis in mantle and gills connective tissues. More recently, Burioli *et al*. (2018) described hemocytosis in connective tissues of mantle and gills, necrotic areas in adductor muscle, hemocytic infiltration in muscular fibers, atrophy of digestive diverticula, abnormal hemocytes widespread in connective tissues and marked hemocyte proliferation.

However, it is not still clear if these alterations are OsHV-dependent: further and more depth studies are needed to clarify these aspects.

1.3.2 Oyster bacteria

1.3.2.1 Vibrio genus

Vibrio are gram-negative bacteria, facultative anaerobes, curved rod shaped, no spores forming, with a unique flagellum which allows mobility. They are ubiquitous in aquatic environments, both marine and freshwater, and their optimal growth occurs in environments rich of sodium. This bacterial population is strongly influenced by environmental conditions, such as temperature, salinity, pH and nutrients (Thompson *et al.*, 2004).

Several *Vibrio* species have been identified as pathogens for aquatic organisms such as fish, corals and molluscs, with the latter able to accumulate large amounts of bacteria because of their filtering attitude.

These microorganisms were detected in waters and in molluscs hemolymph in the 1970s. This was the starting point for more detailed investigations about these *Vibrio* species and molluscs diseases (Lipp *et al*., 1976; Tison and Seidler, 1983).

One of the isolated *Vibrio* species is *Vibrio splendidus*, detected in moribund oysters during several episodes of mortality in farms and associated with these mortality events (Sugumar *et al*., 1998; Lacoste *et al*., 2001; Waechter *et al*., 2002). Its role about pathogenicity/opportunism has been widely debated, because of the lack of specific techniques for assessing the real pathogenetic activity (Gay *et al*., 2004a; Gay *et al*., 2004b).

Epidemiological studies have been conducted in this direction showing a great genetic diversity among several *V. splendidus* strains and their polyphyletic nature. This didn't allow the identification of genetic markers of pathogenicity. Therefore, the only valid method to distinguish virulent from non-virulent strains is to perform experimental challenge, a valid method to understand the action mechanism of *V. splendidus*, precise tissue localization and cellular/tissue damages (Gay *et al*., 2004b).

Gay *et al.* (2004a) conducted an epidemiological study with the aim to identify virulent strains of *Vibrio* in *C. gigas*. Several *Vibrio* strains were isolated from moribund oysters and healthy

oysters and a collection of potentially pathogenic strains was created. These strains were subsequently characterized by gene sequencing and their pathogenicity was verified by experimental challenge, accomplished by intramuscular injection. This work allowed to highlight the great genetic diversity among *V. splendidus* strains isolated and their polyphyletic nature, as demonstrated by the experimental challenge that showed several virulence levels in strains, between low and medium level.

Moreover, no correlation was found between taxonomic affiliation and potential virulence. Therefore, bacterial identification cannot represent a method to identify the cause of mortality episodes, but the only certain method to define it is the experimental challenge (Gay *et al*., 2004a).

Another Vibrionaceae family member is *V. aestuarianus*, described for the first time in 80s. It was isolated during mortality episodes of *C. gigas* oysters and it was detected in molluscs as well as in sediments and waters (Tison and Seidler, 1983).

Vibrio aestuarianus and *V. splendidus* were both detected in several samples during mortality episodes that affected French coasts in 2009, but they were also identified in coasts without mortality events. Scientific community established multifactorial nature of mass mortality episodes all over the world. The only detection of *Vibrio* spp. in molluscs in fact doesn't mean the establishment of infection disease, because these microorganisms are ubiquitous in marine and brackish waters.

Study of several episodes of summer mortalities occurred in hatcheries allowed to identify two different subspecies within *V. aestuarianus* species: *V. aestuarianus* subsp. *aestuarianus* and *V. aestuarianus* subsp. *francensis*. *C. gigas* pathogen strains belong to *V. aestuarianus* subsp. *francensis* and they were identified only by experimental challenge (Garnier *et al*., 2008; EFSA, 2015).

Further studies hypothesized key role of *VarS* gene in *V. aestuarianus* pathogenicity, that codes for a transduction signal histidine-protein kinase. *VarS* gene might work in the

regulation of metalloprotease production (Vam), which is considered fundamental in pathogenic mechanisms modulation because it would compromise the host's immune defenses by damaging hemocytes functions. Further studies are needed to clarify action mechanism of Vam metalloproteases in modulation of hemocytes physiology (Labreuche *et al*., 2010; Madec *et al*., 2014; Goudenège *et al*., 2015).

Experimental challenges are also a valid method for assessing stress levels and disease resistance of oysters, as reported by De Decker *et al.* (2011) in a study on the difference in diseases susceptibility between diploid and triploid oysters.

Induction of triploidy in oysters is a common practice to increase production yield, because it causes a reduction in reproductive stress of molluscs and facilitates a concurrent increase in growth rate, due to energy resources relocation from gonadal development toward the somatic growth. De Decker *et al.* (2011) evidenced a big affinity of *Vibrio* towards gonadal tissue, which was identified as an optimal tissue for infective process by histological and immunohistochemical analysis. Energy distribution towards the reproductive system development rather than survival could increase oyster's vulnerability to vibriosis, most of the energy in diploid oysters, indeed, is used to gonadal development and sometimes they show deficient immune response.

The data recorded on the experimental challenges of the whole study period didn't show any survival improvement in triploid oysters compared to diploid oysters, nor better performances were observed, despite minor gonadal development in triploid ones.

Although triploid oysters showed physiological weakness mainly in winter season, this condition didn't lead to mass mortalities similarly to what happened in summer mass mortalities, due to a minor pathogens presence in winter season.

Anyway, because few studies on triploid molluscs physiology are available, there is the need of further study and investigation (De Decker *et al.*, 2011).

Previous studies on oysters infected with *V. aestuarianus* subsp. *francensis* mainly showed less reactivity on adductor muscle both in experimentally infected oysters and in naturally infected (Garnier *et al*., 2007; EFSA, 2015).

Histologically, few fragmentary information is available about tissue lesions and they are not attributable with certainty to *V. aestuarianus* infection. Some infected samples showed necrotic lesions in different connective tissues and in the adductor muscle, atrophy of the epithelium of the digestive gland, and the detection of bacteria in various tissues (Garnier *et al*., 2007). Additional reported findings were hemocytes necrosis and damages of basal membrane of epithelia and tissues. Furthermore, lysis of the sub-epithelial connective tissue of the mantle, atrophy of the digestive diverticula with expansion of the diverticula lumen, hemocytes lysis, infiltration and agglutination in hemolymphatic vessels were also observed. Moreover, moribund oysters showed high intensity of these lesions and *V. aestuarianus* was detected in all tissues (Parizadeh *et al*., 2018). In the work of Parizadeh *et al.* (2018) it was hypothesized that the infection route is as follow: early hemolymph colonization by virulent strain, bacterial multiplication, hemocytic recruitment and finally invasion of other connective tissues.

Vibrio aestuarianus and other pathogens role in oyster's mortality episodes is still unclear, in fact they often were detected together with other *Vibrio* species and OsHV-1.

This finding strengthens the idea of the multifactorial nature of the mass mortality episodes, bacause many factors may favor development of viral or bacterial infections, such as high water temperature, main environmental factors variations, stress conditions of molluscs and also genetic host factors. Further studies are needed to a better understanding of host-pathogens interactions related to genetic-environmental factors (Barbosa Solomieu *et al*., 2015).

1.3.3 Oyster parasites

Several parasites belonging to Protozoa can infect bivalve molluscs causing diseases and death; most of these included in OIE database (World Organization for Animal Health) because of economic damage inflicted to farmed molluscs. For example, since 1920 France culture of *O. edulis* were severely affected firstly by *Marteilia refringens* then by *Bonamia ostreae*: these events forced the farmers to replace *O. edulis* with *C. gigas* (EFSA, 2010).

Among protozoan parasites, *B. ostreae*, *Haplosporidium nelsoni*, *M. refringens* and *Perkinsus marinus* represent the most important pathogens of oysters (Table 1.5) (Gosling, 2003).

Bivalve trading and changes in environmental temperature have been proposed as two of the main causes for parasitic diseases diffusion in molluscs, and the speed of this diffusion depends on oyster's density and their resistance to parasites (Fernàndez Robledo *et al*., 2014).

Table 1.5 Main protozoan parasites of oysters (modified from Gosling, 2003).

Parasite	Disease	Host
Bonamia ostreae	Bonamiasis	*Ostrea edulis*
Haplosporidium nelsoni	MSX	*Crassostrea virginica*
Perkinsus marinus	Dermo disease	*Crassostrea virginica*
Marteilia refringens	Aber disease	*Ostrea edulis, Crassostrea gigas, Mytilus edulis*

Bonamia ostreae (Phylum Acetospora) infects European oyster *O. edulis*. The first description of *B. ostreae* disease was in France in 1979, where it spreaded in European west coast and then in United States and New Zealand coasts (Elston *et al*., 1986**;** Dinamani *et al*., 1987).

This parasite infects hemocytes and epithelial cells of gills and it diffuses through water to infect other oysters. Adhesion of *B. ostreae* to hemocytes and parasite phagocytosis is followed by proliferative stage and the destruction of hemocytes, with the release of new *B. ostreae* cells in the water (Montes *et al*., 1994). Detectable tissue lesions are mainly located in gills and mantle connective tissue, with yellow diffused discoloration (Arzul and Joly, 2011).

Main diagnostic methods to detect *B. ostreae* or its infection are histopathology and transmission electron microscopy (TEM), mainly used to surveillance programs in infected regions, and PCR analysis (Engelsma *et al*., 2014).

Another acetosporan parasite is *H. nelsoni*, that causes MSX disease (Multinucleated Sphere X) in *C. virginica* and it spread in USA causing severe mortality since late 1950. In some area oysters became resistant to the parasite, because, once infected, they were capable to contain the infection. *Haplosporidium nelsoni* has been also detected in *C. gigas* from California, Washington and China's coasts, but no mortality was observed (Wang *et al.* 2010).

Haplosporidium nelsoni infection begins in gills epithelium and it diffuses in the circulatory system to reach other organs. When the infection is confined to gills little consequences are observed in this tissue (Ford *et al*., 1999). In cases of severe systemic infection MSX disease developed, causing a reduction in feeding and the consequent decrease of meat condition index and fecundity. It is still unclear if the transmission occurs between oysters or it is necessary an intermediate host.

The disease develops in summer month, strongly conditioned by water temperature and salinity. In fact, it is unlikely that the disease could manifest at low salinity levels of water because of the low tolerance of parasites (Gosling, 2003).

Diagnostic methods to detect *H. nelsoni* are histocytology, histology techniques, standard PCR and *in situ* hybridization (ISH) (Lynch *et al*., 2013).

Crassostrea virginica can also be infected by *P. marinus* (Phylum Apicomplexa), that causes dermo disease. It is responsible for great mortalities in Gulf of Mexico and United States coasts since 1940.

The infection starts with trophozoites, which are in water and fare able to enter in oyster tissues exploiting their filtering activity. Subsequently parasites are released in water where they undergo a series of cellular divisions, thus forming zoospores able to infect other hosts. Main tissue damage is in the epithelium of gills, mantle and gut. The destructions of epithelia and membrane occurs and the parasite move to every tissue inside the hemocytes. Infected oysters appear emaciated with abscesses, exhibiting a slow growth and a reduced reproduction rate (Kennedy *et al*., 1995).

Temperature and salinity are the main factors to control the disease diffusion. Highest mortalities episodes occurred infact during summer months, when temperatures were up 20°C, and in the early autumn, confirming that parasites don't appreciate too low and too high salinity levels. Other factors that affect disease distribution are the age of oysters, the availability of food and the mollusk density (Gosling, 2003).

Histology, immunological assay, PCR and culture method represent the main methods used for diagnosis (Bower, 2013; Smolowitz, 2013).

Protozoan parasite *M. refringens* causes *aber disease* that affects the digestive gland. At the end of the 1960s *M. refringens* caused serious mortality episodes in Brittany, which subsequently spread to other European countries (Alderman, 1979). This disease occurs mainly in summer months from June to August (Berthe *et al*., 2004).

Marteilia refringens life cycle starts from gills or labial palps of the host, from which they infect digestive tubules. The cellular multiplication takes place starting from the primary cell, inside which a variable number of secondary cells are produced. They remain inside the cell until spore's maturation that, once mature, are released through the lumen of the digestive tubules and intestine where they can invade the epithelium of the digestive gland. The

transmission route is still unclear and maybe an intermediate host is needed (Berthe *et al*., 2004; De Vico and Carella, 2016).

Marteilia refringens infection consequences in oysters and mussels are the reduction of organic substances absorption from the digestive gland, leading to a total inability to absorb nutritive substances. As a consequence, the meat condition index decreases and the molluscs die (Berthe *et al.,* 2004).

Histologically, severe inflammatory reactions were observed, with hemocytes infiltration in tissues and the destruction of digestive ducts and tubules epithelium (Carella *et al.,* 2010).

Most used techniques to detect *M. refringens* are histopathology and PCR.

An opportunistic parasite belonging to Phylum Anellida (Spionids family) is *Polydora ciliata*. It can parasitise several reared bivalve molluscs, mainly oysters, throughout the world. It may cause reduction of condition index, the atrophy or the detachment of the abductor muscle and a great economic damage (Ambariyanto, 1991; Handley, 1995; Handley and Bergquist, 1997; Duault *et al.,* 2000).

Polydora ciliata can perforate the shell of the oyster both chemically and mechanically, by creating blisters on the internal surface of the shell, that can release anaerobic metabolites including hydrogen sulphide (H2S). Oyster reacts to this damage and tries to counteract this degradation process, by the secretion of a new nacreous layer in order to protect itself and to repair the damage.

Secretion of a new shell layer by parasitised oysters represents an extra work that contributes to a retarded growth, as most the of energy is spent to maintain the integrity of the shell (Spiga *et al*., 2007). Chambon *et al.* (2007) observed multifactorial damages associated to this stress. In fact, infected oysters undergone hyperventilation and increase of food intake, which have proved to be insufficient since mollusc lost weight over time (Chambon *et al*., 2007).

In ecological context, *P. ciliata* parasitism induces oxidative stress and it reduces oyster's resistance to other pathogen agents.

Most used diagnostic methods are macroscopic examination and wet observation.

1.3.4 Oyster mortality and diagnostic methods of diseases

Oysters mortality episodes occurred since 50'-60', but they are partially considered a natural event because of oyster's high reproduction rate, with a production of more than 40 million eggs for each oyster's spawn. The current legislation (Directive 95/70 CE) defines unusual mortality as *"sudden mortality that affects approximately 15% of the stock and that occurs during a short period between two observations (with confirmation within 15 days)".*

Severe episodes of mass mortality of *C. gigas* have occurred in Japan and the United States since the 1950's and in France since the 1980's (Imai *et al*., 1965; Perdue *et al*., 1981; Maurer *et al*., 1986). Japan episodes occurred in Matsushima Bay, and it was observed as a physiological disorder and metabolic disturbances in spawning oysters. These data were interpreted as consequences of high temperatures recorded. In France, mortalities have occurred in Arcachon Bay (Maurer *et al*., 1986); Marennes-Oléron (Bodoy *et al*., 1990), Brittany and Normandy (Fleury *et al*., 2001). In Europe, also other countries were affected by mortality episodes, such as Spain and Netherlands (Elanadaloussi *et al*., 2009; Van Banning, 1997).

These episodes concern spat, juveniles and adult oysters generally in summer months with the highest temperatures of the year and mainly in oysters involved in the sexual maturation phase. These characteristics are typical of "summer mortality" events, even if the cause is not clear yet, but it is certainly known its multifactorial nature (EFSA, 2010; Degremont *et al*., 2005; Barbosa Solomieu *et al*., 2015). Mortality outbreaks have been extensively studied and some risk factors have been identified. Physiological stress associated to gonad maturation have been frequently observed in summer mortality episodes, but other relevant factors were also identified, particularly environmental factors (increase of water temperature, reduction of

dissolved oxygen, reduction of water salinity) and interaction with pathogens (Soletchnik *et al*., 1998; Lacoste *et al*., 2001; Gay *et al*., 2004b; Garnier *et al*., 2008; Domeneghetti *et al*., 2014; Vezzulli *et al.* 2015).

Main pathogen species associated with mass mortality events are Ostreid herpesvirus (OsHV-1 and its variants), *V. aestuarianus* and *V. splendidus.*

Currently, the main methods for detection of oyster pathogens are biomolecular and microbiological techniques. Bivalve histopathology has recently become an important tool in aquatic organisms pathology, although only few studies have highlighted the importance of histopathological investigation to detect the presence of inflammatory reaction and tissue lesions associated to mollusc pathogens (Renault *et al*., 2000; Gay *et al*., 2004b; Friedman *et al*., 2005; Cuevas *et al*., 2015; Martenot *et al*., 2016; Sanmartin *et al*., 2016; Parizadeh *et al*., 2018; Carella *et al*., 2018).

Integrated approach to describe the health status of bivalve molluscs should be used to a better understand of viral, bacterial and combined infections and their dynamics. In particular studies on oyster's disease need a multidisciplinary strategy to better understand viral and bacterial pathogenesis and summer mortality episodes dynamics.

1.4 References

- Alderman D.J. (1979) Epizootiology of *Marteilia refringens* in Europe. Marine Fisheries Review 41, 67-69.
- Allam B. and Raftos D. (2015) Immune responses to infectious diseases in bivalves. Journal of Invertebrate Pathology 131, 121–136.
- Ambariyanto, R. Seed (1991). The infestation of *Mytilus edulis* Linnaeus by *Polydora ciliata* (Johnston) in the Conwy estuary, North Wales. Journal of Molluscan Studies 57, 413-424.
- Andrews, J. (1980) A review of introductions of exotic oysters and biological planning for new importations. Marine Fisheries Review 42, 1-11.
- Arzul I., Corbeil S., Morga B., Renault T. (2017) Viruses infecting marine molluscs. Journal of Invertebrate Pathology 147, 118–135.
- Arzul, I. and Joly J.P. (2011) EURL (European Union Reference Laboratory) for Molluscs Diseases: *Bonamia* sp.
- Arzul I., Renault T., Lipart C., Davison A.J. (2001) Evidence for interspecies transmission of oyster herpesvirus in marine bivalves. Journal of General Virology 82, 865-870.
- Arzul I., Renault T., Thébault A., Gérard A. (2002) Detection of oyster herpesvirus DNA and proteins in asymptomatic *Crassostrea gigas* adults. Virus Research 84, 151-160.
- Barbosa Solomieu V., Renault T., Travers M.A. (2015) Mass mortality in bivalves and the intricate case of the Pacific oyster, *Crassostrea gigas*. Journal of Invertebrate Pathology 131, 2–10.

- Batista F.M., Arzul I., Pepin J.F., Ruano F., Friedman C.S., Boudry P., Renault T. (2007) Detection of ostreid herpesvirus 1 DNA by PCR in bivalve molluscs: a critical review. Journal of Virological Methods 139, 1-11.
- Batista F.M., Taris N., Boudry P., Renault T. (2005) Detection of ostreid herpesvirus-1 (OsHV-1) by PCR using a rapid and simple method of DNA extraction from oyster larvae. Diseases of Aquatic Organisms 64, 1-4.
- Berthe Franck C.J., Le Roux Frédérique, Adlard Robert D. and Figueras Antonio (2004) Marteiliosis in molluscs: A review. Aquatic Living Resources 17, 433–448.
- Bodoy A., Garnier J., Razet D., Geairon P. (1990) Mass mortalities of oysters (*Crassostrea gigas*) during spring 1988 in the bay of Marennes–Oléron, related to environmental conditions: ICES CM 1990 / K 11, 1–23.
- Bower, S.M. (2013) Synopsis of Infectious Diseases and Parasites of Commercially Exploited Shellfish: *Perkinsus marinus* ("Dermo" Disease) of Oysters.
- Bueno R., Perrott M., Dunowska M., Brosnahan C., Johnston C. (2016) *In situ* hybridization and histopathological observations during ostreid herpesvirus-1 associated mortalities in Pacific oysters *Crassostrea gigas*. Diseases of Aquatic Organisms 122, 43-55.
- Burioli E.A.V., Varello K., Lavazza A., Bozzetta E., Prearo M., Houssin M. (2018) A novel divergent group of Ostreid herpesvirus 1 µVar variants associated with a mortality event in Pacific oyster spat in Normandy (France) in 2016. Journal of Fish Diseases 00, 1–11.
- Carella F., Aceto S., Mangoni O., Mollica M. P., Cavaliere G., Trinchese G., Aniello F., De Vico G. (2018) Assessment of the health status of mussels *Mytilus galloprovincialis* along the Campania coastal areas: a multidisciplinary approach. Frontiers in Physiology 9, 683.

- Carella F., Aceto S., Marrone R., Maiolino P. and De Vico G. (2010) *Marteilia refringens* infection in cultured and natural beds of mussels (*Mytilus galloprovincialis*) along the Campanian coast (Tirrenian sea, South of Italy). Bulletin of the European Association of Fish Pathologists 30(5), 189.
- Carella F., Sardo A., Mangoni O., Di Cioccio D., Urciuolo G., De Vico G., Zingone A. (2015) Quantitative histopathology of the Mediterranean mussel (*Mytilus galloprovincialis* L.) exposed to the harmful dinoflagellate *Ostreopsis* cf. *ovata*. Journal of Invertebrate Pathology 127, 130–140.
- Cataudella S. e Bronzi P. (2001) Acquacoltura responsabile verso le produzioni acquatiche del terzo millennio.
- Cataudella S. & Spagnolo M. (eds) (2011) - The state of Italian marine fisheries and aquaculture. Ministero delle Politiche Agricole, Alimentari e Forestali (MiPAAF), Rome (Italy), 620 p.
- Chambon C., Legeay A., Durrieu G., Gonzalez P., Ciret P., Massabuau J. C. (2007) Influence of the parasite worm *Polydora* sp. on the behaviour of the oyster *Crassostrea gigas*: a study of the respiratory impact and associated oxidative stress. Marine Biology 152, 329–338.
- Chang S-J., Tseng S-M. and Chou H-Y. (2005) Morphological characterization via light and electron microscopy of the hemocytes of two cultured bivalves: a comparison study between the Hard Clam (*Meretrix lusoria*) and Pacific Oyster (*Crassostrea gigas*). Zoological Studies 44(1), 144-153.
- Cognie, B., Haure, J., Barillé, L. (2006) Spatial distribution in a temperate coastal ecosystem of the wild stock of the farmed oyster *Crassostrea gigas* (Thunberg). Aquaculture 259, 249-259.
- Collin Rachel (2013) Phylogenetic Patterns and Phenotypic Plasticity of Molluscan Sexual Systems. Integrative and Comparative Biology 53(4), 723–735.

- Comps M., Bonami J.R. (1977) Viral infection associated with mortality in the oyster *Crassostrea gigas* Thunberg. Comptes rendus hebdomadaires des seances de l'Academie des sciences. Serie D: Sciences naturelles 285(11), 1139-40.
- Comps M. and Cochennec N. (1993) A herpes-like virus from the European oyster *Ostrea edulis* L. Journal of Invertebrate Pathology 62, 201-203.
- Cuevas N., Zorita I., Costa P. M., Franco J., Larreta J. (2015) Development of histopathological indices in the digestive gland and gonad of mussels: integration with contamination levels and effects of confounding factors. Aquatic Toxicology 162, 152-164.
- Davison A.J., Eberle R., Ehlers B., Hayward G.S., McGeoch D.J., Minson A.C., Pellett P.E., Roizman B., Studdert M.J. and Thiry E., (2009) The order Herpesvirales. Archives of Virology 154, 171-177.
- Davison A., Trus B., Cheng N., Steven A., Watson M., Cunningham C., Le Deuff R. and Renault T. (2005) A novel class of herpesvirus with bivalve hosts. Journal of General Virology 86, 41-53.
- De Decker S., Normand J., Saulnier D., Pernet F., Castagnet S., Boudry P. (2011) Responses of diploid and triploid Pacific oysters *Crassostrea gigas* to *Vibrio* infection in relation to their reproductive status. Journal of Invertebrate Pathology 106, 179–191.
- Dégremont L., Bédier E., Soletchnik P., Ropert M., Huvet A., Moal J., Samain J-F. and Boudry P. (2005) Relative importance of family, site, and field placement timing on survival, growth, and yield of hatchery-produced Pacific oyster spat (*Crassostrea gigas*). Aquaculture 249, 213-229.

- De Vico G. and Carella F. (2012) Morphological features of the inflammatory response in molluscs. Research in Veterinary Science 93, 1109–1115.
- De Vico G. and Carella F. (2016) Elementi di patologia comparata dei molluschi. Ed. Loffredo.
- Dinamani P., Hine P. M., Jones J. B. (1987) Occurrence and characteristics of the haemocyte parasite *Bonamia* sp. in the New Zealand Dredge Oyster *Tiostrea lutaria*. Diseases of Aquatic Organisms 3(1), 37-44.
- Domeneghetti S., Varotto L., Civettini M., Rosani U., Stauder M., Pretto T., Pezzati E., Arcangeli G., Turolla E., Pallavicini A. and Venier P. (2014) Mortality occurrence and pathogen detection in *Crassostrea gigas* and *Mytilus galloprovincialis* close-growing in shallow waters (Goro lagoon, Italy). Fish & Shellfish Immunology.
- Duault C., Gillet P. et Fleury P. G. (2000) Spatio-temporal variations of the infestation of oysters, Crassostrea gigas, by Polydora sp, (ANNELIDES POLYCHETES), observed in the IFREMER/REMORA network. Journal de Recherche Océanographique (JRO) de l'U.O.F.
- Dundon W.G., Arzul I., Omnes E., Robert M., Magnabosco C., Zambon M., Gennari L., Toffan A., Terregino C., Capua I., Arcangeli G. (2011) Detection of Type 1 Ostreid Herpes variant (OsHV-1 µvar) with no associated mortality in French origin Pacific cupped oyster *Crassostrea gigas* farmed in Italy. Aquaculture 314 (1–4), 49–52.
- EFSA (2015) Oyster mortality - EFSA Panel on Animal Health and Welfare (AHAW). EFSA Journal 13(6), 4122.
- EFSA (2010) Scientific Opinion on the increased mortality events in Pacific oysters, *Crassostrea gigas*. EFSA 8, 1894-1956.

- Elandaloussi L., Carrasco N., Andree K., Furones D., Roque A. (2009) Esdeveniments de mortalitat de l‟ostró del Pacific (*Crassostrea gigas*) en el delta de l‟Ebre- Estudi de cas. Proceedings of the II Simposi d'aqüicultura de Catalunya. Sant Carles de la Rapita, Spain.
- Elston R. A., Farley C. A., Kent M. L. (1986) Occurence and significance of bonamiasis in European flat oysters *Ostrea edulis* in North America. Diseases of Aquatic Organisms 2(1), 49-54.
- Engelsma Marc Y., Culloty Sarah C., Lynch Sharon A., Arzul Isabelle, Carnegie Ryan B. (2014) *Bonamia* parasites: a rapidly changing perspective on a genus of important mollusc pathogens. Diseases of aquatic organisms 110, 5–23.
- FAO - "FAO Fisheries & Aquaculture - *Crassostrea gigas*". www.fao.org
- FAO (2019) Fisheries and aquaculture software. FishStatJ - software for fishery statistical time series. In: FAO Fisheries and Aquaculture Department [online].
- FAO (2017) Regional review on status and trends in aquaculture development in Europe – 2015. FAO Fisheries and Aquaculture Circular No. 1135/1.
- FAO (2016) The State of World Fisheries and Aquaculture 2016 - Contributing to food security and nutrition for all. Rome. 200 pp.
- FAO (2018) The State of World Fisheries and Aquaculture 2018 - Meeting the sustainable development goals. Rome. Licence: CC BY-NC-SA 3.0 IGO.
- Farley C.A., Banfield W.G., Foster W.S. (1972) Oyster Herpes-Type virus. Science, 178(4062), 759-60.
- Fernandez Robledo J.A., Vasta G.R., Record N.R. (2014) Protozoan Parasites of Bivalve Molluscs: Literature Follows Culture. PLoS ONE 9(6), e100872.
- Fleury P.G., Goyard E., Mazurie J., Claude S., Bouget J.F., Langlade A. and le Coguic Y. (2001) The assessing of Pacific oyster (*Crassostrea gigas*) rearing performances by

the IFREMER/REMORA network: method and first results (1993-98) in Brittany (France). Hydrobiologia 465**,** 195-208.

- Ford S. Powell E., Klinck J. Hofmann E. (1999) Modeling the MSX Parasite in Eastern Oyster (*Crassostrea virginica*) Populations. I. Model Development, Implementation, and Verification Journal of Shellfish Research 18(2), 475-500.
- Friedman CS, Estes RM, Stokes NA, Burge CA, Hargove JS, Barber B.J., Elston R.A., Burreson E.M., Reece K.S. (2005) Herpes virus in juvenile Pacific oysters *Crassostrea gigas* from Tomales Bay, California, coincides with summer mortality episodes. Diseases of Aquatic Organisms 63, 33–41.
- Garnier M., Labreuche Y., Garcia C., Robert A. and Nicolas J.L. (2007) Evidence for the involvement of pathogenic bacteria in summer mortalities of the Pacific oyster *Crassostrea gigas*. Microbial Ecology 53, 187-196.
- Garnier M., Labreuche Y. and Nicolas J.L. (2008) Molecular and phenotypic characterization of *Vibrio aestuarianus* subsp. *francensis* subsp. nov., a pathogen of the oyster *Crassostrea gigas*. Systematic and Applied Microbiology 31(5), 358-365.
- Gay M., Berthe F.C.J., Le Roux F. (2004a) Screening of *Vibrio* isolates to develop an experimental infection model in the Pacific oyster *Crassostrea gigas*. Diseases of Aquatic Organisms 59, 49–56.
- Gay M., Renault T., Pons A.M., Le Roux F. (2004b) Two *Vibrio splendidus* related strains collaborate to kill *Crassostrea gigas*: taxonomy and host alterations. Diseases of Aquatic Organisms 62, 65–74.
- GLOBEFISH – Information and analysis on world fish trade (2018). www.fao.org
- Gosling Elizabeth (2003) Bivalve Molluscs – Biology, Ecology and Culture. Fishing News Books.

- Goudenège D., Travers M.A., Lemire A., Haffner P., Labreuche Y., Petton B., Mangenot S., Calteau A., Mazel D., Nicolas J.L., Jacq A. and Le Roux F. (2015) A single regulatory gene is sufficient to alter *Vibrio aestuarianus* pathogenicity in oysters. Environmental Microbiology 17(11), 4189-4199.
- Handley S. J. (1995) Spionid polychaetes in Pacific oysters, *Crassostrea gigas* (Thunberg) from Admiralty Bay, Marlborough Sounds, New Zealand. New Zealand Journal of Marine and Freshwater Research 29, 305-309.
- Handley S. J., Bergquist, P.R. (1997) Spionid polychaete infestations of intertidal Pacific oysters *Crassostrea gigas* (Thunberg), Mahurangi Harbour, northern New Zealand. Aquaculture 153(3), 191-205.
- Henshaw Jonathan M. (2018) Protandrous Hermaphroditism. J. Vonk, T.K. Shackelford (eds.), Encyclopedia of Animal Cognition and Behavior, https://doi.org/10.1007/978-3-319-47829-6_1972-1.
- Hine P.M., Wesney B. and Hay B.E. (1992) Herpesviruses associated with mortalities among hatchery-reared larval Pacific oysters *Crassostrea gigas.* Diseases of Aquatic Organisms 12, 135-142.
- Imai T., Numachi K., Oizumi J., Sato S. (1965) Studies on the mass mortality of the oyster in Matsushima Bay - II. Search of the cause of the mass mortality and the possibility to prevent it by transplantation experiment. Bulletin of Tohoku Regional Fisheries Research Laboratory 25, 27-38.
- ISMEA (2013) Check Up 2013 – Il settore ittico in Italia.
- Kennedy V. S., Newell R. I. E., Krantz G. E., Otto S. (1995) Reproductive capacity of the eastern oyster *Crassostrea virginica* infected with the parasite *Perkinsus marinus.* Diseases of aquatic organisms 23, 135-144.

- Labreuche Y., Le Roux F., Henry J., Zatylny C., Huvet A., Lambert C., Soudant P., Mazel D., Nicolas J.L. (2010) *Vibrio aestuarianus* zinc metalloprotease causes lethality in the Pacific oyster *Crassostrea gigas* and impairs the host cellular immune defenses. Fish & Shellfish Immunology 29, 753-758.
- Lacoste A., Jalabert F., Malham S., Cueff A., Gélébart F., Cordevant C., Lange M., Poulet S. A. (2001) A *Vibrio splendidus* strain is associated with summer mortality of juvenile oysters *Crassostrea gigas* in the Bay of Morlaix (North Brittany, France). Disease of Aquatic Organisms 46, 139–145.
- Le Deuff R. and Renault T. (1999) Purification and partial genome characterization of a herpes-like virus infecting the Japanese oyster, *Crassostrea gigas*. Journal of General Virology 80, 1317-1322.
- Lipp P.R., Brown B., Liston J., Chew K. (1976) Recent findings on the summer diseases of Pacific oysters. Proceedings of the National Shellfisheries Association in Garnier 65, 9–10.
- Lopez-Sanmartin M., Power D.M., Herran-José F., Navas I., Batista F.M. (2016) Experimental infection of European flat oyster *Ostrea edulis* with Ostreid Herpesvirus 1 microvar: mortality, viral load and detection of viral transcripts by in situ hybridization. Virus Research 217, 55-62.
- Lynch S.A., Villalba A., Abollo E., Engelsma M., Stokes N.A., Culloty S.C. (2013) The occurrence of haplosporidian parasites, *Haplosporidium nelsoni* and *Haplosporidium* sp., in oysters in Ireland. Journal of Invertebrate Pathology 112, 208–212.

- Madec S., Pichereau V., Jacq A., Paillard M., Boisset C., Guérard F., Paillard C., Nicolas J.L. (2014) Characterization of the secretomes of two vibrios pathogenic to mollusks. PLoS ONE 9(11), e113097.
- Mandas D. and Salati F. (2017) Ostreid herpesvirus: A pathogen of oysters. Virology Research Reviews 1(2), 1-5.
- Martenot C., Fourour S., Oden E., Jouaux A., Travaille E., Malas J.P. and Houssin M., (2012) Detection of the OsHV-1µVar in the Pacific oyster *Crassostrea gigas* before 2008 in France and description of two new microvariants of the Ostreid Herpesvirus 1 (OsHV-1). Aquaculture 338, 293-296.
- Martenot C., Oden E., Travaillé E., Malas J-P. and Houssin M. (2011) Detection of different variants of Ostreid Herpesvirus 1 in the Pacific oyster, *Crassostrea gigas* between 2008 and 2010. Virus Research 160, 25-31.
- Martenot C., Segarra A., Baillon L., Faury N., Houssin M., *et al*. (2016) In situ localization and tissue distribution of ostreid herpesvirus 1 proteins in infected Pacific oyster, *Crassostrea gigas*. Journal of Invertebrate Pathology 136, 124–135.
- Maurer D., Comps M. and His E. (1986) Caractéristiques des mortalités estivales de l'huître *Crassostrea gigas* dans le bassin d'Arcachon, Haliotis (Société Française de Malacologie) 15, 309–317.
- Montes J., Anadón R., Azevedo C. (1994) A Possible Life Cycle for *Bonamia ostreae* on the Basis of Electron Microscopy Studies. Journal of Invertebrate Pathology 63(1), 1-6.
- Nicolas J.L., Comps M., Cochennec N. (1992). Herpes-like virus infecting Pacific oyster larvae, *C. gigas*. Bulletin of the European Association of Fish Pathologists 12, 11–13.

- Oden E., Martenot C., Berthaux M., Travaillé E., Malas J.P., Houssin M. (2011) Quantification of ostreid herpesvirus 1 (OsHV-1) in *Crassostrea gigas* by real-time PCR: Determination of a viral load threshold to prevent summer mortalities. Aquaculture 317, 27–31.
- Olalemi A., Baker-Austin C., Ebdon J., Taylor H. (2016) Bioaccumulation and persistence of faecal bacterial and viral indicators in *Mytilus edulis* and *Crassostrea gigas*. International Journal of Hygiene and Environmental Health 219, 592–598.
- Parizadeh L., Tourbiez D., Garcia C., Haffner P., Dégremont L., Le Roux F. and Travers M.A. (2018) Ecologically realistic model of infection for exploring the host damage caused by *Vibrio aestuarianus*. Environmental Microbiology 00(00), 1–9.
- Perdue J.A., Beattie J.H., Chew K.K. (1981) Some relationships between gametogenic cycle and Summer Mortality phenomenon in the Pacific oyster (*Crassostrea gigas*) in Washington State. Journal of Shellfish Research 1, 9–16.
- Pila E.A., Sullivan J.T., Wu X.Z., Fang J., Rudko S.P., Gordy M.A., and Hanington P.C. (2016) Haematopoiesis in molluscs: a review of haemocyte development and function in gastropods, cephalopods and bivalves. Developmental & Comparative Immunology 58, 119–128.
- Prioli G. (2001) Censimento nazionale sulla molluschicoltura. UNIMAR Osservatorio tecnico-biologico.
- Prioli G. (2008) La molluschicoltura in Italia. En A. Lovatelli, A. Farias e I. Uriarte (eds). Estado actual del cultivo y manejo de moluscos bivalvos y su proyección futura: factores que afectan su sustentabilidad en América Latina. Taller Técnico Regional de la FAO. 20-24 de agosto de 2007, Puerto Montt, Chile. FAO Actas de Pesca y Acuicultura. No. 12. Roma, FAO. pp. 159-176.

- Quayle, O.B. (1980) Tropical oysters culture and methods. Ottawa, Ont., IDRC, 80 pp.
- Renault T. (2008) Shellfish viruses. Encyclopedia of virology 5, 560-567.
- Renault T., Arzul I. (2001) Herpes-like virus infections in hatchery-reared bivalve larvae in Europe: specific viral DNA detection by PCR. Journal of Fish Diseases 24, 161-167.
- Renault T., Arzul I., Lipart C. (2004) Development and use of an internal standard for oyster herpesvirus 1 detection by PCR. Journal of Virological Methods 121, 17-23.
- Renault T., Cochennec N., Le Deuff R.M., Chollet B. (1994a) Herpes-like virus infecting Japanese oyster (*Crassostrea gigas*) spat. Bulletin of the European Association of Fish Pathologists 14, 64–66.
- Renault T., Le Deuff R. M., Chollet B., Cochennec N. and Gérard A. (2000) Concomitant herpes-like virus infections in hatchery-reared larvae and nursery-cultured spat *Crassostrea gigas* and *Ostrea edulis*. Diseases of Aquatic Organisms 42, 173-183.
- Renault T., Le Deuff R.M., Cochennec N., Maffart P. (1994b) Herpesviruses associated with mortalities among Pacific oyster, *Crassostrea gigas*, in France - comparative study. Revue de Medecine Veterinaire 145, 735–742.
- Sanmartín M. L., Power D. M., De la Herrán R., Navas J. I., Batista F. M. (2016) Experimental infection of European flat oyster *Ostrea edulis* with ostreid herpesvirus 1 microvar (OsHV-1 var): mortality, viral load and detection of viral transcripts by in situ hybridization. Virus Research 217, 55–62.
- Sauvage C., Pépin J.F., Lapègue S., Boudry P., Renault T. (2009) Ostreid herpes virus 1 infection in families of the Pacific oyster, *Crassostrea gigas*, during a summer mortality outbreak: differences in viral DNA detection and quantification using real-time PCR. Virus Research 142, 181–187.

- Schikorski D., Renault T., Saulnier D., Faury N., Moreau P. and Pépin J-F. (2011) Experimental infection of Pacific oyster *Crassostrea gigas* spat by ostreid herpesvirus 1: demonstration of oyster spat susceptibility. Veterinary Research 42, 27-27.
- Segarra A., Pépin J.F., Arzul I., Morga B., Faury N. and Renault T. (2010) Detection and description of a particular Ostreid herpesvirus 1 genotype associated with massive mortality outbreaks of Pacific oysters, *Crassostrea gigas*, in France in 2008. Virus Research 153, 92-99.
- Séguin A., Caplat C., Serpentini A., Lebel J.M., Menet-Nedelec Florence, Costil K. (2016) Metal bioaccumulation and physiological condition of the Pacific oyster (*Crassostrea gigas*) reared in two shellfish basins and a marina in Normandy (northwest France). Marine Pollution Bulletin 106(1-2), 202-214.
- Smolowitz R. (2013) A Review of Current State of Knowledge Concerning *Perkinsus marinus.* Effects on *Crassostrea virginica* (Gmelin) (the Eastern Oyster). Veterinary Pathology 50(3), 404-411.
- Soletchnik P., Le Moine O., Faury N., Razet D., Geairon P., Goulletquer P. (1998) Summer mortality of the oyster in the Bay Marennes-Oleron: spatial variability of environnement and biology using a geographical information system (GIS). Aquatic Living Resources 12, 131–143.
- Spiga B., Fenzi G., Salati F. (2007) Treatment trials in *Crassostrea gigas* against *Polydora ciliata* infection. Ittiopatologia 4, 207-213.
- Sugumar G., Nakai T., Hirata Y., Matsubara D., Muroga K. (1998) *Vibrio splendidus* biovar II as the causative agent of bacillary necrosis of Japanese oyster *Crassostrea gigas* larvae. Diseases of Aquatic Organisms 33, 111-118.

- Thompson F.L., Iida T., Swings J. (2004) Biodiversity of vibrios. Microbiology and Molecular Biology Reviews 68, 403-431.
- Tison David L. and Seidler Ramon J. (1983) *Vibrio aestuarianus*: a new species from estuarine and waters and shellfish. International Journal of Systematic Bacteriology 33(4), 699-702.
- Usheva L. N., Vaschenko M. A. and Durkina V. B. (2006) Histopathology of the Digestive Gland of the Bivalve Mollusk *Crenomytilus grayanus* (Dunker, 1853) from Southwestern Peter the Great Bay, Sea of Japan. Russian Journal of Marine Biology 32(3), 166–172.
- Van Bannig (1997) Summer Mortality in the Netherlands in IFREMER meeting 6-9/10/1997.
- Vezzulli L., Pezzati E., Stauder M., Stagnaro L., Venier P. and Pruzzo C. (2015) Aquatic ecology of the oyster pathogens *Vibrio splendidus* and *Vibrio aestuarianus.* Environmental Microbiology 17(4), 1065–1080.
- Viale I., Olla G., Salati F. (2016) Acquacoltura in Sardegna – tradizioni, innovazione, sapori e ambiente. Agenzia Regionale LAORE Sardegna.
- Waechter M., Le Roux F., Nicolas J.L., Marissal E., Berthe F. (2002) Caractérisation de bactéries pathogènes de naissain d'huître creuse *Crassostrea gigas*. Comptes Rendus Biologies 325, 231–238.
- Wallace R.K., Waters P., Rikard F.S. (2008) Oyster hatchery Techniques. SRAC Publication No. 4302.
- Wang Zhongwei, Lu Xin, Liang Yubo, Wang Chunde (2010) *Haplosporidium nelsoni* and *H. costale* in the Pacific oyster *Crassostrea gigas* from China's coasts. Diseases of aquatic organisms 89, 223–228.

- Yang H., Simon N. and Sturmer L. (2018) Production and Performance of Triploid Oysters for Aquaculture. Fisheries and Aquatic Sciences (SFRC) Publication #FA208.
- Yonge C. M. (1926) Structure and physiology of the organs of feeding and digestion in *Ostrea edulis*. Journal of the Marine Biological Association 14(2).

Chapter 2

Sampling site and processing techniques of sampled oysters

2.1 Study area

Pacific oysters, belonging to *Crassostrea gigas* species, were sampled from 4 different sites: San Teodoro (north eastern Sardinia), Tortolì (eastern Sardinia), Calich (north western Sardinia) and Marceddì (western Sardinia) (Fig. 2.1). San Teodoro and Tortolì samples derived from aquaculture farms, while Calich and Marceddì oysters from lagoon production tests.

Fig. 2.1 Sampling sites.

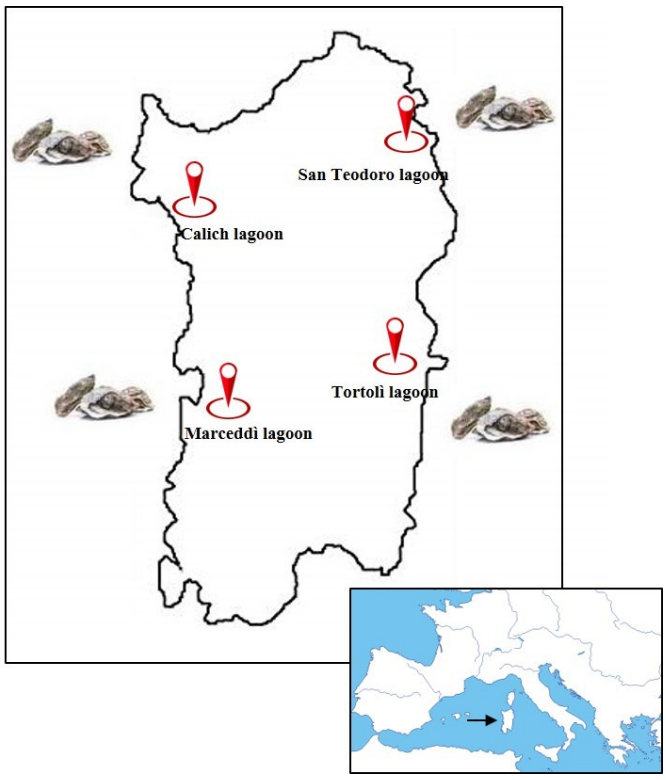

A total of 440 oysters were collected from October 2016 to June 2018 during a regular, once a month, or sporadic sampling program, as detailed in Table 2.1.

Oysters were sampled directly from poches or baskets and immediately transported within refrigerated containers to the laboratory.

Table 2.1 Sampled specimens of *Crassostrea gigas*.

Sampling date	Species	Sampling site	N° samples	Water temperature
October 2016	*Crassostrea gigas*	San Teodoro	23	22°C
November 2016	*Crassostrea gigas*	San Teodoro	16	16°C
December 2016	*Crassostrea gigas*	San Teodoro	30	14°C
January 2017	*Crassostrea gigas*	San Teodoro	24	13°C
February 2017	*Crassostrea gigas*	San Teodoro	24	14°C
March 2017	*Crassostrea gigas*	San Teodoro	24	16°C
April 2017	*Crassostrea gigas*	Tortolì	20	/
April 2017	*Crassostrea gigas*	San Teodoro	21	18°C
May 2017	*Crassostrea gigas*	San Teodoro	18	20°C
June 2017	*Crassostrea gigas*	San Teodoro	22	28°C
July 2017	*Crassostrea gigas*	San Teodoro	20	25,3°C
August 2017	*Crassostrea gigas*	San Teodoro	16	26°C
September 2017	*Crassostrea gigas*	Tortolì	24	24°C
September 2017	*Crassostrea gigas*	San Teodoro	26	22°C
October 2017	*Crassostrea gigas*	Calich	9	22°C
October 2017	*Crassostrea gigas*	San Teodoro	18	18,5°C
November 2017	*Crassostrea gigas*	San Teodoro	15	17,5°C
December 2017	*Crassostrea gigas*	San Teodoro	12	12°C
January 2018	*Crassostrea gigas*	San Teodoro	18	13°C
February 2018	*Crassostrea gigas*	San Teodoro	14	13°C
April 2018	*Crassostrea gigas*	Calich	4	/
April 2018	*Crassostrea gigas*	Marceddì	10	/
May 2018	*Crassostrea gigas*	Tortolì	15	20,5°C
June 2018	*Crassostrea gigas*	San Teodoro	17	24,4°C
Total			440	

2.2 Sampling sites

2.2.1 The San Teodoro lagoon

San Teodoro lagoon is located in the north eastern of Sardinia (40°47′51.71″N 9°40′00.05″E) (Fig. 2.2), it is bordered from ss125 in west coast and from Cinta beach in east coast. It's about 3,5 km long and total extension is about 218 hectares. Rio San Teodoro is the main tributary, which flows into lagoon. Seabed is partially muddy and sandy with some emerging rock.

The San Teodoro lagoon is characterized by a large variety of vegetal and animal species: it is considered an international importance site with protected species at risk of extinction. The town of San Teodoro often discharges into lagoon untreated wastewaters, thatcould represent a big source of pollution in the environment.

Three local companies have a fishing license: Cooperativa Peschiera fishes in lagoon with "lavorieri" systems; Società Cooperativa Fo.Ca. collects clams; Compagnia Ostricola Mediterranea breeds oysters with *poches* and baskets (Fenza *et al*., 2014).

Fig. 2.2 Oysters farm in San Teodoro lagoon.

2.2.2 The Tortolì lagoon

Tortolì lagoon is located in the eastern part of Sardinia (39°56'37.5"N 9°40'14.4"E) (Fig. 2.3) and it extends for about 289 hectares and has two outlets to the sea allowing water turnover. Water currents are fundamental factors to nutrients provision. Cooperativa Pescatori Tortolì has public concession on this lagoon, and practices fish catching with "lavorieri" systems located in outlets towards the sea. It has also been installed sea bass and gilt-head bream semi-intensive farming systems with floating cages, long line for mussels farming and *poches* for oysters farming.

Moreover, Cooperativa Pescatori Tortolì has an advanced depuration and shipment system for shellfish treatment (Fenza *et al*., 2014).

Fig. 2.3 Tortolì lagoon (Fenza *et al*., 2014).

2.2.3 The Marceddì lagoon

San Giovanni – Marceddì lagoon is in the west coast of Sardinia (39°42′40.01″N 8°31′06.53″E) (Fig. 2.4), near Oristano Gulf, and is an artificial delimited area which comprises 2 basins: San Giovanni lagoon of about 700 hectares with a fresh water watercourse flow (Rio Mogoro e il Rio Sitzerri), and Marceddì lagoon of about 900 hectares that communicates with the sea. In both basins, water depth is between 40 cm and 2 meters.

In this area, there are many zootechnical and agricultural farms that could represent a big problem for water pollution.

Consorzio Cooperative Riunite della Pesca di Marceddì has public concession of this lagoon and it practices fish trap, net fishing and mussel farming (Sardinian wetlands; Fenza *et al*., 2014). The main fish species present in this lagoon are mullets, eels, sea bream, and sea bass.

Fig. 2.4 San Giovanni-Marceddì lagoon (Fenza *et al*., 2014).

2.2.4 The Calich lagoon

In the Regional Natural Park of Porto Conte area, there is the Calich lagoon (40°36′N 8°18′E) (Fig. 2.5), near Alghero city and Fertilia town; it is about 92 hectares in extension and 1,2 m depth. Three freshwater watercourses flow into this lagoon, Rio Barca, Rio Calvia and Rio Oruni, with direct connection with the sea.

Originally, the lagoon was separated from the sea by a sandy area, then a connecting channel was created towards the sea, which determined an increase in water salinity. Further modifications have been made to improve water oxygenation, favorable factors for the development of new species of flora and fauna.

Previous analysis showed an increase of nitrogen and phosphorus, probably due to microalgae proliferation in this lagoon, a negative aspect for the ecosystem.

In Calich lagoon there is a good variety of fishing production: mullet, sea bass, sea bream, eel, sole, crabs represent the main fishing species. Advanced "lavoriero" system has been realized, but it is currently unused. Cooperativa Pescatori Algheresi "Il Golfo e la Laguna" has public concession since 1993 and it practices fishing mainly with nets and purse seine nets (Fenza *et al*., 2014).

Fig. 2.5 Calich lagoon (Fenza *et al*., 2014).

2.3 Material and methods

In this study, oysters were analyzed by means of microbiological, biomolecular and histopathological techniques.

Microbiological analyses were performed on hepatopancreas isolations of each specimen, in order to identify pathogens species by classical microbiological methods.

Moreover, specific biomolecular analyses, such as PCR reaction (Polymerase Chain Reaction) with specific oligonucleotides, were used to identify oyster pathogens from bacterial strains and tissue fragments.

Finally, histopathological analyses were performed on oyster tissue sections to detect and to correlate lesions with bacterial or viral infections.

2.3.1 Necropsy

Based on the following biometric features, oysters were categorized as a juvenile or adult:

- juvenile specimens ranged between 10-50 g in weight and 5-7 cm in length;
- adult oysters ranged between 50-150 g in weight and 8-15 cm in length (Fig. 2.6).

Fig. 2.6 Biometric evaluations: length and weight were evaluated using laboratory instruments.

Necropsy of oysters were performed according to NOAA manual (Howard *et al*., 2004): tissues were macroscopically examined to detect lesions or any anomalies. Firstly, oysters were opened by severing adductor muscle to evaluate muscle reactivity, subsequently pallial fluid presence and the integrity and pigmentation of gills and mantle tissues were evaluated as features of oyster's welfare, infection or disease process (Fig. 2.7).

Fig. 2.7 Sample of cupped oyster, *Crassostrea gigas*.

During necropsy, molluscs were transversally sectioned in the cephalic area and the hepatopancreas were collected (Fig. 2.8) for microbiological isolation under sterile condition (Kueh and Chan, 1985).

Fig. 2.8 Oyster transversal section.
In evidence, hepatopancreas (blue arrows), gills (*), mantle (**) and labial palps (***).

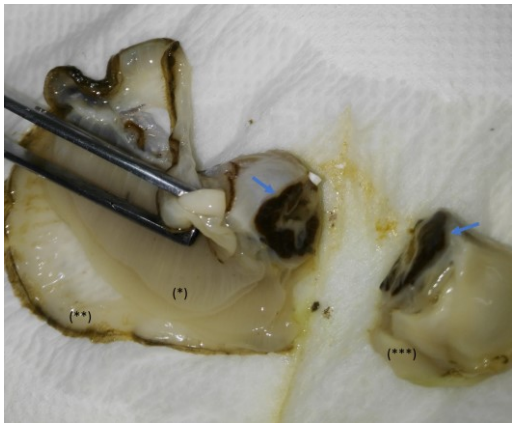

Gills and mantle were collected and subsequently DNA was extracted from these tissues in order to perform biomolecular analysis.

Histological sections were prepared with a transversal cut at the meeting point of the labial palps and the gills and the second cut was made 2-5 mm toward the adductor muscle side (Fig. 2.9).

Oyster sections were placed into labeled histological cassettes and fixed in 10% neutral formalin for histological analysis (Fig. 2.10).

Fig. 2.9 Parallel continuous lines indicate the cross-sections for histology.

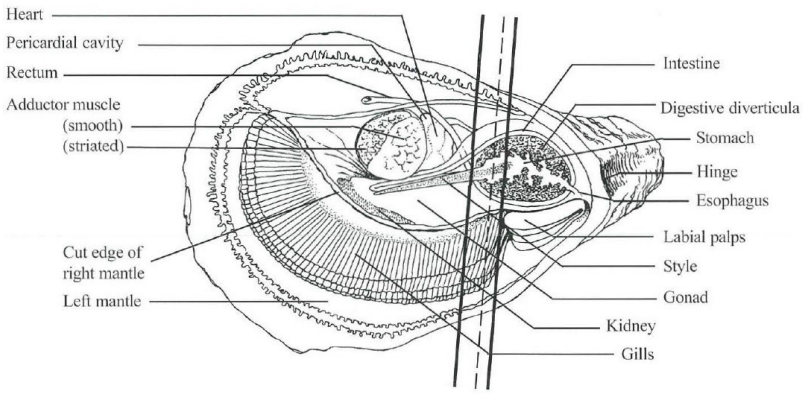

Fig. 2.10 Oyster sections into labeled histological cassettes.

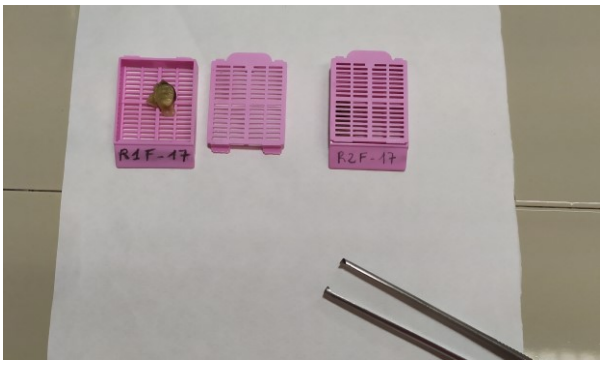

2.3.2 Microbiological analysis

Microbiological isolation from the hepatopancreas of each oyster was performed with a sterile inoculation loop. Bacterial strains were identified using a polyphasic approach including morphological and biochemical investigations and biomolecular analysis.

Bacterial cultures were grown on a generic culture medium (BHI: Brain Heart Infusion, Difco) added with 1.5% NaCl and purified until obtaining a pure culture (Colwell and Liston, 1960).

Morphological evaluations were performed by Gram staining of bacteria using a commercial kit (Becton Dickinson, France) and samples were examined by Olympus CX 31 optical microscope (Fig. 2.11).

Fig. 2.11 Optical microscope (Olympus CX 31).

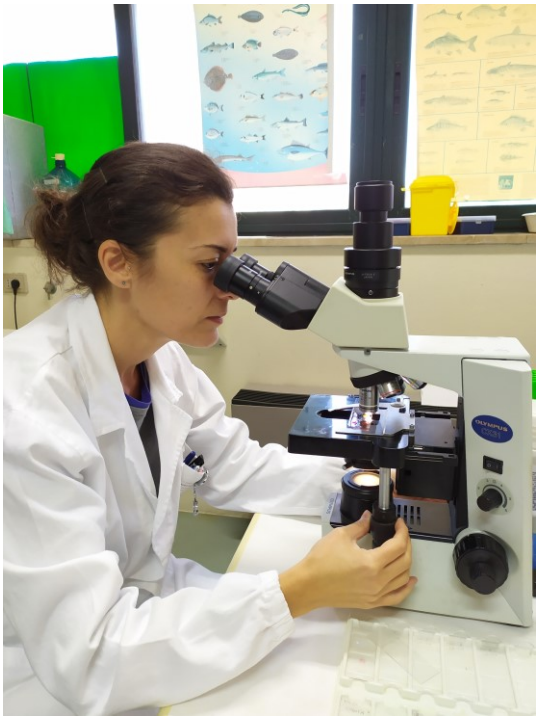

After fixing of the sample in a microscope slide, Gram stain method provided 4 phases (Fig. 2.12):

- 1 minute of Gram Crystal Violet;
- 1 minute of Stabilized Gram Iodine;
- 30 seconds of Gram Decolorizer;
- 30 seconds of Gram Basic Fuchsin.

After each phase, a washing step with tap water was performed.

Fig. 2.12 Gram staining kit (Becton Dickinson, France).

Subsequently, biochemical profile of isolated strains was determined using the following procedures (Fig. 2.13) (Garnier *et al*., 2008):

- API 20 NE: identification test for non-enteric Gram-negative rod bacteria that contains 8 conventional tests and 12 assimilation tests (Biomerieux, France);
- SIM: evaluates sulfide production, indole production and motility (SIM medium, Oxoid Limited, Hampshire, United Kingdom);
- O/F: determines the oxidative and/or fermentative metabolism (OF medium, Becton Dickinson, France);
- Oxidase test (Becton Dickinson, France);
- Catalase test.

Fig. 2.13 Bacterial strain in BHI agar culture medium and API 20 NE test.

The primary tests for the determination of biochemical characteristics were performed according to Manual of Methods for General Bacteriology (American Society for Microbiology, 1981).

2.3.3 Biomolecular analysis

2.3.3.1 DNA extraction

DNA extraction on bacterial strains was performed using a commercial kit (Nexttec GmbH, Germany). Bacterial culture was suspended in 0,5 ml of purified water, centrifuged and the supernatant was removed. The pellet was subjected to two lysis phases and to a final purification as followed:

- Buffer B, Lysozime, RNase A: 10 minutes at 56°C, 1200 rpm;
- SDS-solution, Proteinase K, DTT, EDTA: 30 minutes at 56°C, 1200 rpm;
- Small quantity of the lysate has been filtered in equilibrated cleanColumn.

Also, DNA of gills and mantle tissues was extracted using QIAamp DNA mini kit (Qiagen GmbH, Germany).

About 25 mg of tissue was finely cut and collected in 1.5 ml microcentrifuge tube. The other extraction phases are reported below:

- Adding lysis Buffer and Proteinase K at 56°C until complete lysis;
- Adding another lysis buffer and ethanol: 10 minutes at 70°C;
- Lysate was filtered in spin columns;
- DNA was washed with two wash-buffers;
- DNA was eluted with EA buffer (Elution buffer).

These protocols guarantee the purification of total DNA from bacteria and tissues, respectively. Extracted DNA from each sample was stored at -20°C for biomolecular analysis by PCR and real time PCR.

2.3.3.2 PCR

Polymerase Chain Reaction (PCR), also named end-point PCR, a molecular technique currently used as a diagnostic tool for the identification of diseases and microbial infections.

This technique amplifies specific DNA regions and can be performed on single or double stranded DNA template. It requires two oligonucleotide primers flanked the target fragment, short sequence-specific oligonucleotides studied on a specific gene region. This technique synthesizes a double-stranded DNA fragment from a single-stranded ones by using dNTPs, which link is based on complementarity with the DNA template.

PCR requires four fundamental elements: DNA polymerase enzyme, deoxyribonucleotide triphosphates (dNTPs), DNA template and gene-specific primers.

The PCR process takes place in a thermocycler instrument, which allows rapid changes of temperatures respecting times and number of pre-established cycles.

The reaction occurs in different phases:

- Denaturation phase: separation of two complementary strands of dsDNA; the breaking of nucleotide's hydrogen bonds occurs between 94° C and 99° C;
- Annealing phase: link the primers and the complementary sequence in the denatured DNA strand; annealing temperature depends on primers, generally ranging from 30° C to 55° C;
- Extension phase: an optimal temperature of 72° C allows the DNA-polymerase to extend the fragment starting from the primers, based on the sequence of a single DNA template.

As shown in Fig. 2.14, these phases are repeated for a variable number of cycles (generally 30 or 40) allowing the synthesis of new DNA fragments (final copy number is 2^n, n represents the cycle number) (Brock *et al*., 1998; Ishmael and Stellato, 2008).

Fig. 2.14 Exponential amplification of DNA fragment in PCR reaction.

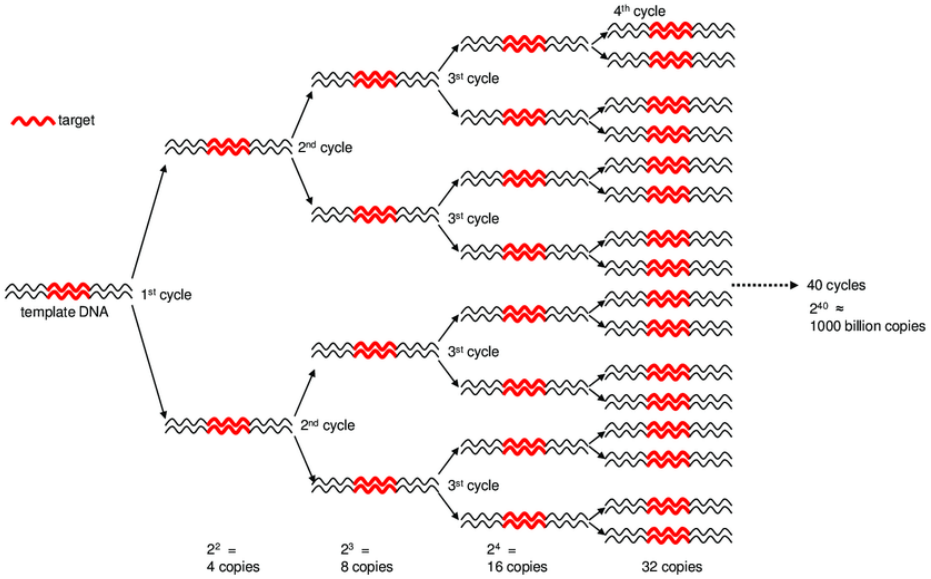

At the end of the reaction, conventional PCR requires a post-amplification phase, that consists of an electrophoretic run on agarose gel to view amplified fragment, thanks to the addition in the agarose gel of a fluorescent compound and its binding with dsDNA (ethidium bromide is powerful mutagen and it has often been replaced by other fluorescent substances, such as SYBRSafe). Addition of 100bp nucleotide marker (DNA Ladder) allows to quantify fragments lenght.

2.3.3.3 Real-time PCR

An accurate and sensitive method to quantify DNA is real-time PCR, that allows real-time detection and quantitation of DNA during amplification process (Higuchi R., *et al*., 1992; Higuchi R., *et al*., 1993). The addition of aromatic substances (SYBR Green) or specific oligonucleotide probes in the reaction mix (fluorescent dyes) and their integration or hybridization with the target DNA produces fluorescent signals whose intensity reflects the number of amplified molecules.

During the amplification process, a quantification curve based on the fluorescence detected by the system is created.

Fig. 2.15 Phases of quantification curve.

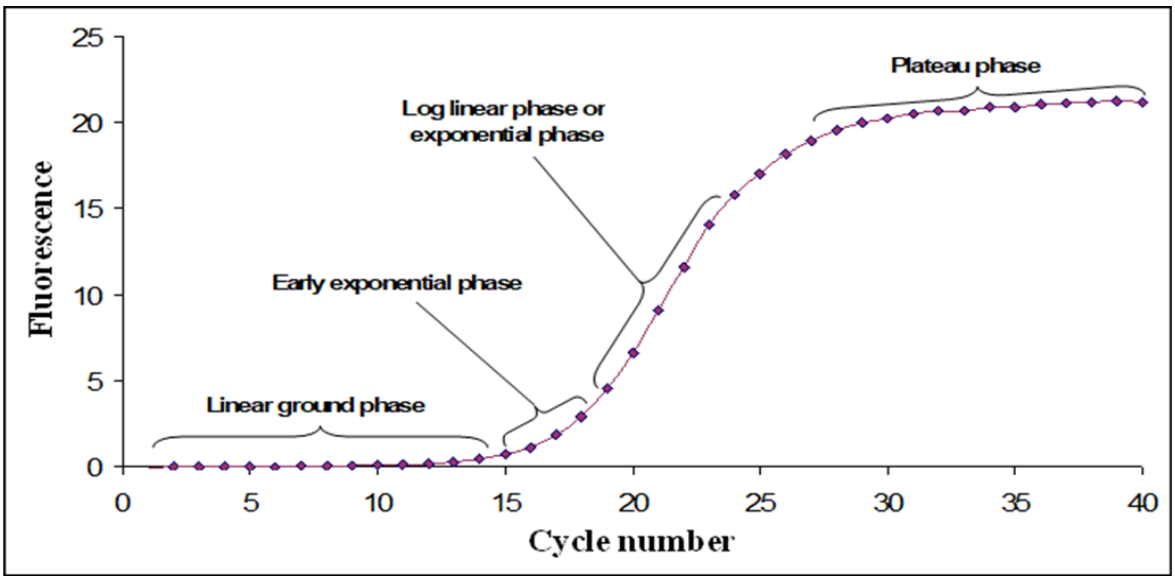

As shown in Fig. 2.15, fluorescence profile of a hypothetical quantification curve has 4 characteristic phases. A first linear phase involves the first 10-15 cycles and the system still failes to detect a significant increase in fluorescence. In this step occurs the calculation of the basic fluorescence of the reaction. During the next phase, the early exponential phase, there is a significant exponential increase in fluorescence detectable by the system, when it is possible to identify the Ct or threshold cycle. It represents the cycle in which the system starts fluorescence detection: a threshold line is set and Ct value of samples corresponds to intersection of curves with this line. This is an important value in quantification assays because a greater quantity of targets corresponds to lower Ct value. In exponential phase occurs an exponential increase of PCR products and the increase of fluorescence is detected by the system until the plateau phase. This is the last phase, in which the reaction stopped because components are exhausted and the fluorescence is no longer detectable.

In this reaction it is possible to observe the specificity of the primers by controlling the Melting curve, that allows to distinguish secondary products or primer-dimers from the specific amplification.

It occurs a slow and progressive increase in temperature and the fluorescence is continuously detected. This process is represented in a graph with temperature and fluorescence (Fig. 2.16).

Fig. 2.16 Melting curve representing the specific product in blue and secondary product in purple (primer-dimers) (Photo by Kubista *et al*., 2006).

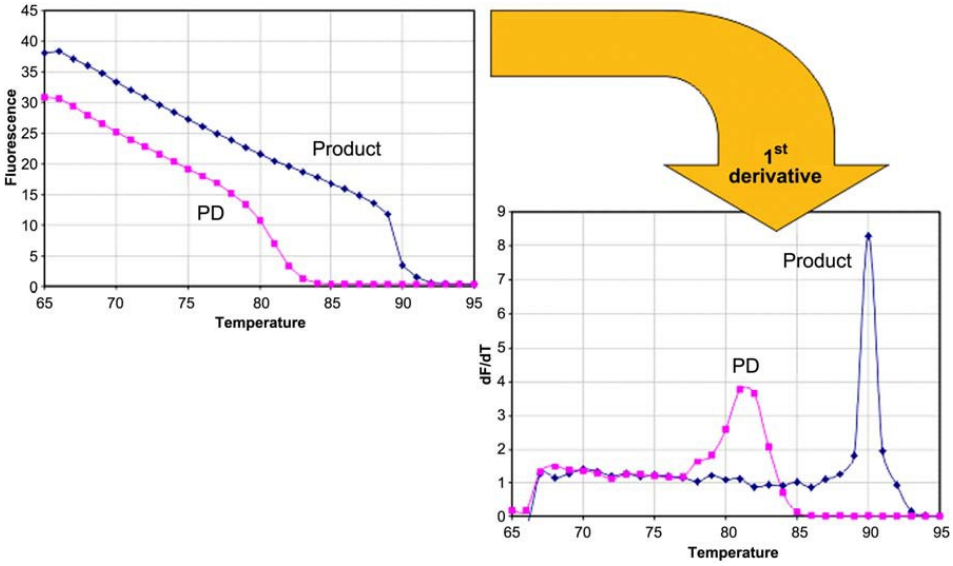

The peak of melting temperature (Tm) of a DNA sample (Tm: the temperature at which 50% of the DNA duplex is denatured) allows to distinguish the amplicon from secondary products or primer-dimers: they generally have a lower Melting temperature (Kubista *et al*., 2006).

Absolute quantitation of the PCR products can be performed by realizing a quantification curve using serial dilutions of known concentration sample. A standard curve produces a linear relationship between the threshold cycle of each quantitative standard and its initial quantity, and a linear regression line is obtained (it is represented by $y=mx+q$ equation). This regression line gives important information on the PCR reaction: the m value is the slope of the line that allows us to obtain the amplification efficiency (E). The success of the reaction

has a slope value between - 3.6 and -3.1, which corresponds to an efficiency of 90-100% (Fig. 2.17 and Fig. 2.18) (Kubista *et al*., 2006).

Fig. 2.17 Standard curve performed with serial dilutions of known bacterial concentration sample ($1,5x10^8$ copies/µl).

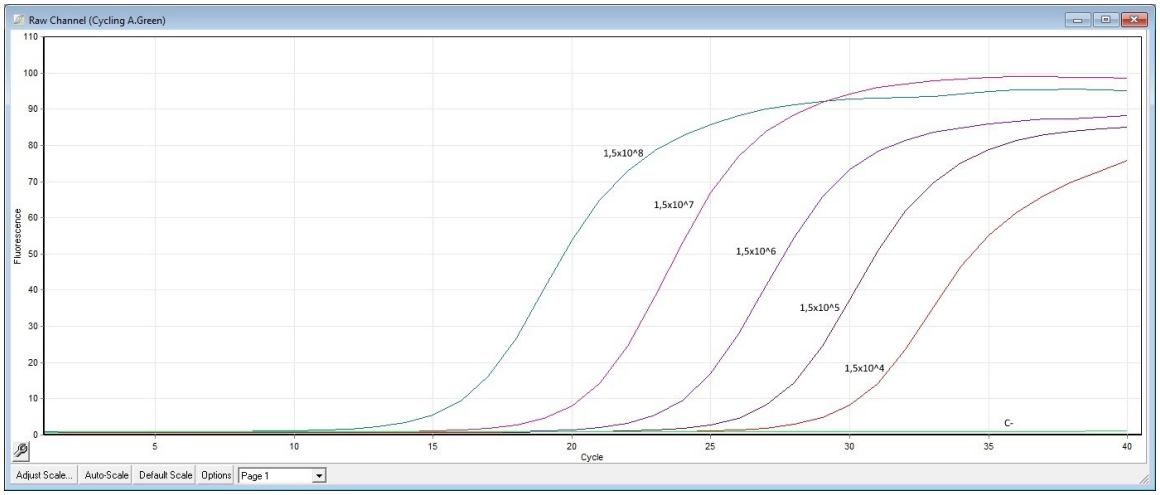

Fig. 2.18 Linear regression line of quantitative standards: the graph shows *m* value of 3,479 and good PCR efficiency of 94%.

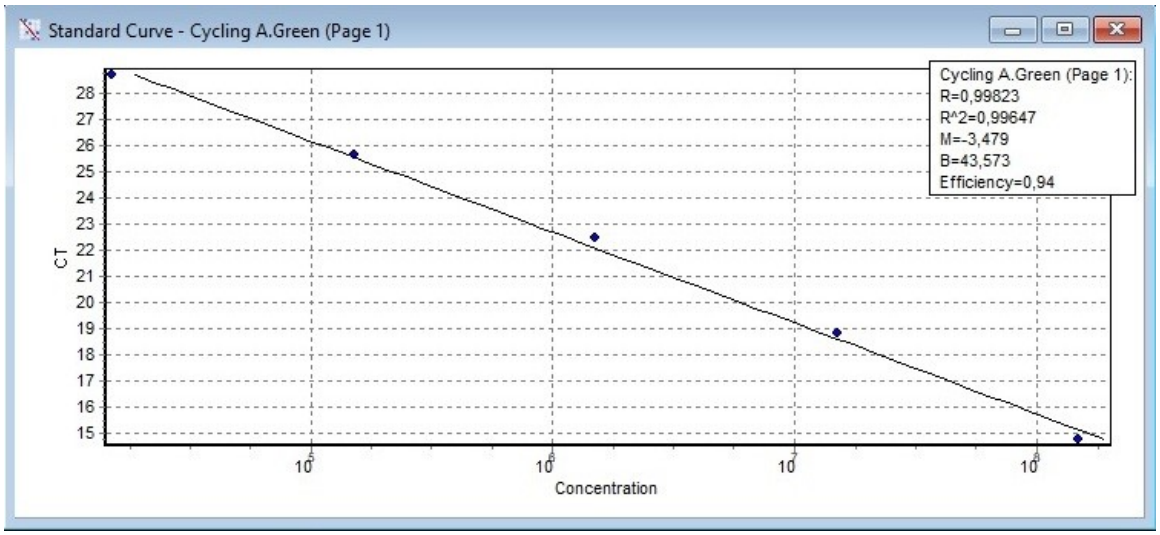

2.3.4 Histopathology

Transversal section of the cephalic area of each oyster was collected for subsequent histopathological examination of gills, mantle and hepatopancreas.

Each oyster section was identified with an identification number and it was created an Excel table containing relevant data of each sample: ID (identification number), analyzed tissue, distribution and intensity of hemocytes infiltration, hemocytes infiltration in hemolymphatic vessels, loss of gills epithelium, parasites, oysters sex. In this table were also recorded PCR results of *Vibrio aestuarianus, V. splendidus* and Ostreid herpesvirus-1 (OsHV-1) detection in hepatopancreas and in gills/mantle pools (Fig. 2.19).

Fig. 2.19 Database of histopathological and biomolecular data.

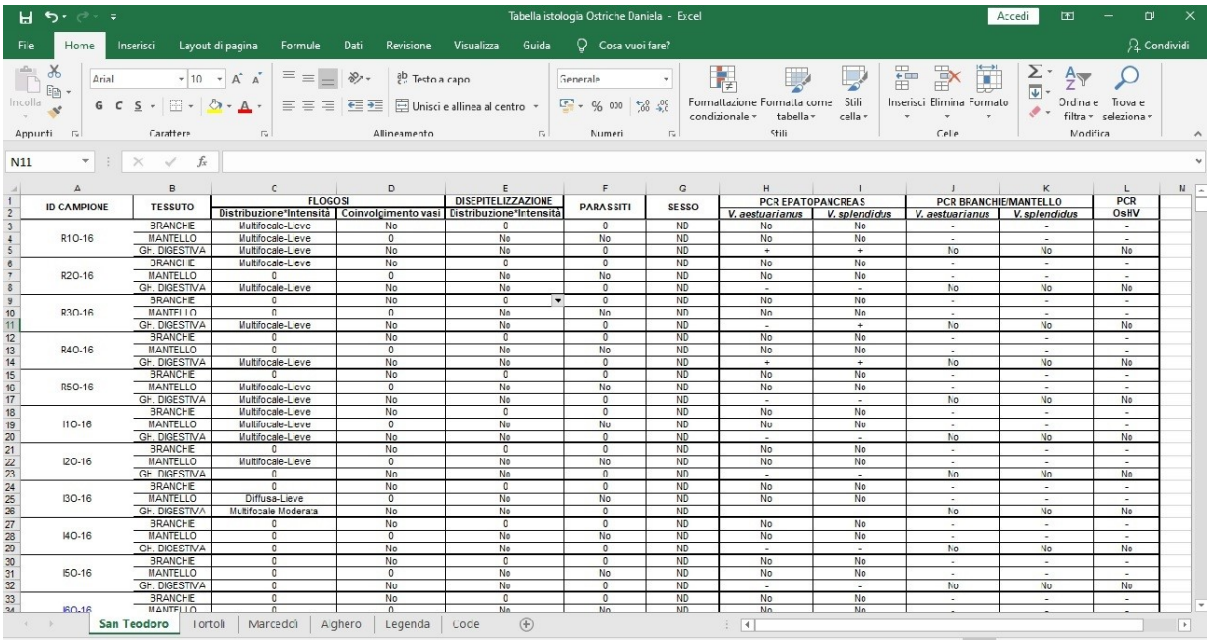

	A	B	C	D	E	F	G	H	I	J	K	L
1			FLOGOSI		DISEPITELIZZAZIONE			PCR EPATOPANCREAS		PCR BRANCHIE/MANTELLO		PCR
2	ID CAMPIONE	TESSUTO	Distribuzione*Intensità	Coinvolgimento vasi	Distribuzione*Intensità	PARASSITI	SESSO	*V. aestuarianus*	*V. splendidus*	*V. aestuarianus*	*V. splendidus*	OsHV
3	R10-16	BRANCHIE	Multifocale-Lieve	No	0	0	ND	No	No	-	-	-
4		MANTELLO	Multifocale-Lieve	0	No	No	ND	No	No	-	-	-
5		GH. DIGESTIVA	Multifocale-Lieve	No	No	0	ND	+	+	No	No	No
6	R20-16	BRANCHIE	Multifocale-Lieve	No	0	0	ND	No	No	-	-	-
7		MANTELLO	0	0	No	No	ND	No	No	-	-	-
8		GH. DIGESTIVA	Multifocale-Lieve	No	No	0	ND	-	-	No	No	No
9	R30-16	BRANCHIE	0	No	0	0	ND	No	No	-	-	-
10		MANTELLO	0	0	No	No	ND	No	No	-	-	-
11		GH. DIGESTIVA	Multifocale-Lieve	No	No	0	ND	-	+	No	No	No
12	R40-16	BRANCHIE	0	No	0	0	ND	No	No	-	-	-
13		MANTELLO	0	0	No	No	ND	No	No	-	-	-
14		GH. DIGESTIVA	Multifocale-Lieve	No	No	0	ND	+	+	No	No	No
15	R50-16	BRANCHIE	0	No	0	0	ND	No	No	-	-	-
16		MANTELLO	Multifocale-Lieve	0	No	No	ND	No	No	-	-	-
17		GH. DIGESTIVA	Multifocale-Lieve	No	No	0	ND	-	-	No	No	No
18	I10-16	BRANCHIE	Multifocale-Lieve	No	0	0	ND	No	No	-	-	-
19		MANTELLO	Multifocale-Lieve	0	No	No	ND	No	No	-	-	-
20		GH. DIGESTIVA	Multifocale-Lieve	No	No	0	ND	-	-	No	No	No
21	I20-16	BRANCHIE	0	No	0	0	ND	No	No	-	-	-
22		MANTELLO	Multifocale-Lieve	0	No	No	ND	No	No	-	-	-
23		GH. DIGESTIVA	0	No	No	0	ND	-	-	No	No	No
24	I30-16	BRANCHIE	0	No	0	0	ND	No	No	-	-	-
25		MANTELLO	Diffusa-Lieve	0	No	No	ND	No	No	-	-	-
26		GH. DIGESTIVA	Multifocale Moderata	No	No	0	ND			No	No	No
27	I40-16	BRANCHIE	0	No	0	0	ND	No	No	-	-	-
28		MANTELLO	0	0	No	No	ND	No	No	-	-	-
29		GH. DIGESTIVA	0	No	No	0	ND	-	-	No	No	No
30	I50-16	BRANCHIE	0	No	0	0	ND	No	No	-	-	-
31		MANTELLO	0	0	No	No	ND	No	No	-	-	-
32		GH. DIGESTIVA	0	No	No	0	ND	-	-	No	No	No
33		BRANCHIE	0	No	0	0	ND	No	No	-	-	-
34		MANTELLO	0	0	No	No	ND	No	No	-	-	-

Histologically, each tissue was evaluated and scored according to:

- tissues distribution of hemocytes infiltration (multifocal, diffuse or nodular);
- intensity of hemocytes infiltration (mild, moderate or severe).

Furthermore, hemocytes infiltrate in mantle hemolymphatic vessels as well as the presence of degenerative lesions, including the loss of epithelium in gills, and parasitic structures in both

the hepatopancreas and the gills were evaluated.

Sections were placed in histological cassettes and all collected samples were fixed in 10% neutral formalin for 48h. Subsequently, tissue sections were dehydrated with increasing concentrations of alcohol and xylene, using an automatic tissue processor (HISTO-PRO 200); finally, they were paraffin embedded (Fig. 2.20).

Fig. 2.20 Automatic tissue processor (HISTO-PRO 200).

The histological proceedings were performed according to Mazzi (1977):

- Fixation: Formaldehyde 40% was buffered with CaCO3 and 10% neutral formalin was used to fix the tissues. Firstly, tissue sections were placed in histological cassettes, then they were fixed in 10% neutral formalin which penetrates tissue causing chemical and physical changes increasing their hardness, preventing autolysis and degradation process. Fixation process lasted 48 h.
- Dehydration: in this phase water was removed from samples by treatment with increasing concentration of ethanol solutions (2 h 50% ethanol, 2 h 70% ethanol, 2 h 90% ethanol, 2 h 100% ethanol, 2 h 100% ethanol). Afterward, melted paraffin infiltrated the tissues.

- Clearing: in this phase xylene removed a substantial amount of fat from the tissue which appeared translucent, so this is called clearing agent. Xylene treatments were two (2 h xylene, 2 h xylene).
- Wax infiltration: tissues were immersed in 3 steps of paraffin (a mixture of hydrocarbons with a melting point at 60°C) until the paraffin entirely infiltrated the tissue and replaced xylene. Wax infiltration treatments were three (2 h wax infiltration, 2 h wax infiltration, 2 h wax infiltration).
- Embedding or blocking out: in this phase, tissues were embedded within a block of paraffin by using a mould. This process was performed using an embedding centre (ACM 50; Fig. 2.21). In this phase a correct positioning of the samples is crucial to obtain a well oriented plane of section.

Fig. 2.21 (a) Embedding centre (ACM 50); (b) mould used to create paraffin block.

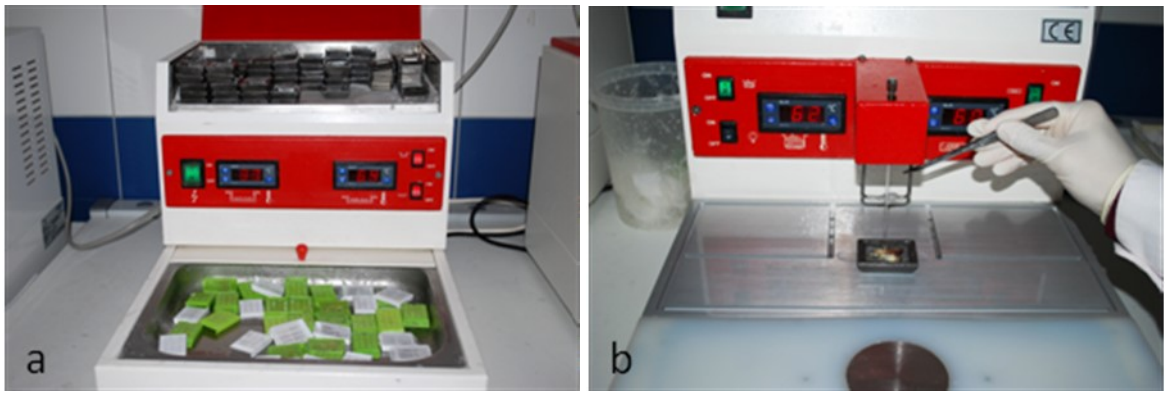

- Cut and stained: the paraffin solidified blocks were removed from the mould and 3µm sections of each sample were cut using the microtome (Leica RM 2245) (Fig. 2.22). Sections were then stained in an automatic multistainer (ST5020, Leica Biosystems) (Fig. 2.23) with Hematoxylin and Eosin (HE), set according to a standard method (Mazzi 1977). Sections were mounted on a glass slide and they were then evaluated at light microscopy (Nikon Eclipse 80i).

Fig. 2.22 Microtome (Leica RM 2245).

Fig. 2.23 Automatic multistainer (ST5020, Leica Biosystems).

Protocols for Haematoxylin and Eosin (H&E) and Gram staining of histological sections are reported below:

Haematoxylin and Eosin (H&E)

1. Slides were deparaffinized and rehydrated through graded alcohols;
2. Harris' hematoxylin (3 min);
3. Washed in running tap water (5 min x 2);
4. Rinsed in distilled water;
5. Eosin (2 min);
6. Rinsed in distilled water;
7. Dehydrated, cleared and mounted.

Gram stain (Peck and Badrick, 2017)

1. Slides were deparaffinized and rehydrated through graded alcohols;
2. Gram crystal violet 1% (1 minute);
3. Rinse using stabilized Gram Lugol solution;
4. Stabilized Gram Lugol solution (1 minute);
5. Wash with distilled water;
6. Gram decolorizer (10-15 seconds);
7. Wash with distilled water;
8. Gram safranin solution (1 minute);
9. Wash with distilled water;
10. Picric acid in acetone (5-10 seconds);
11. Alcohol 100%;
12. Alcohol 100%;
13. Xylene;
14. Xylene.

2.3.4.1 Digestive gland atrophy evaluation

Tubular *lumen areas* of oyster digestive gland were computed by image analysis to evaluate gland atrophy in *V. aestuarianus* PCR positive and PCR negative samples, as previously described by Carella *et al*., 2015. In particular images of H&E-stained sections were randomly captured at 10× magnification and 100 tubules areas of each sample were calculated. 10 PCR positive samples and 10 PCR negative samples were finally evaluated.

The images were analyzed using the *ImageJ* software (version 1.52a, Rasband, 1997–2018). Each image was reduced to an 8-bit greyscale and a *threshold* of the image was set to

highlight only the tubular lumen. Afterward, evidenced tubular lumen were measured using *Analyze particle* tool (Fig. 2.24).

For each sample, area percentage of the selected tubular lumen was calculated and data were transferred to a spreadsheet software (Excel) and statistical software (Stata 11.2 software, StataCorp LP) for further analysis.

Fig. 2.24 Eight-bit greyscale of digestive gland tubules of *V. aestuarianus* PCR negative (a) and positive (b) samples, and respective tubular lumen evidenced with *threshold* tool (c, d).

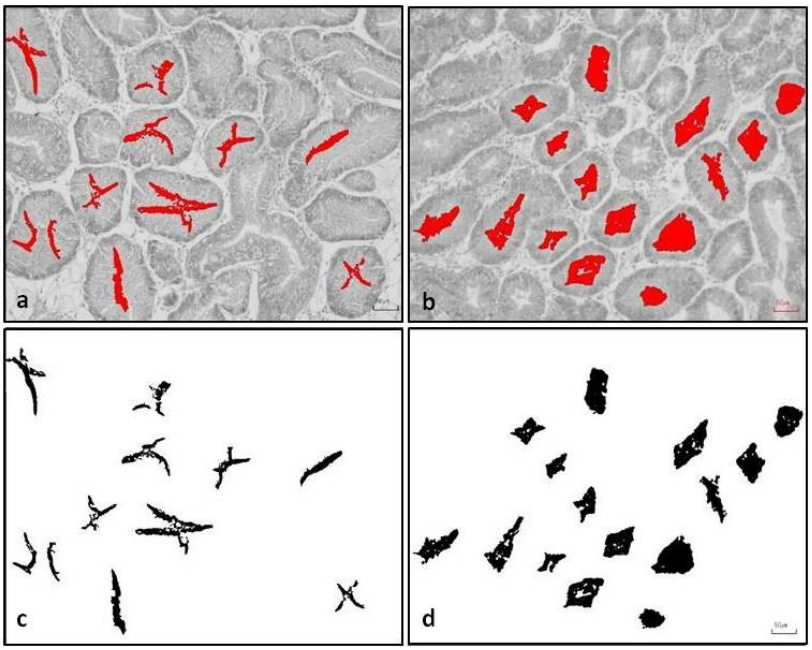

2.3.5 Statistical analysis

Statistical analysis of the obtained data was carried out using Stata 11.2 software (StataCorp LP). Fisher and Chi-square ($\chi 2$) tests were used to evaluate the correlation between pathogen agents detection results (by PCR) and histological lesions observed in the examined tissues. After checking the normality with Shapiro-Wilk test, results of tubular lumen areas of digestive diverticula evaluation were analyzed using Student *t-test*. A *P*-value <0.05 was considered significant.

2.4 Results

Four-hundred and forty oyster specimens (*C. gigas)* were sampled from October 2016 to June 2018. Three hundred and fifty-eight oysters were sampled from San Teodoro lagoon, 59 from Tortolì lagoon, 10 from Marceddì lagoon and 13 from Calich lagoon (Table 2.2).

Gills, mantle and digestive gland from each specimen were analyzed.

Eighty oysters were males (74 from San Teodoro, 3 from Tortolì, 2 from Marceddì, 1 from Calich lagoons); forty-one oysters were females (31 from San Teodoro, 2 from Tortolì, 7 from Marceddì, 1 from Calich lagoons); five oysters show ovotestis (both oocytes and sperm), it means they were in transition phase from male to female (or conversely), 3 oysters were in San Teodoro lagoon and 2 oysters were in Tortolì lagoon. Finally, 314 specimens were not sexually determined (250 from San Teodoro, 52 from Tortolì, 1 from Marceddì, 11 from Calich lagoons) (Fig. 2.25).

Fig. 2.25 Male (a) and female (b) gonads. Oyster showing ovotestis (c). Bar (a) = 100 µm; Bar (b, c) = 50 µm.

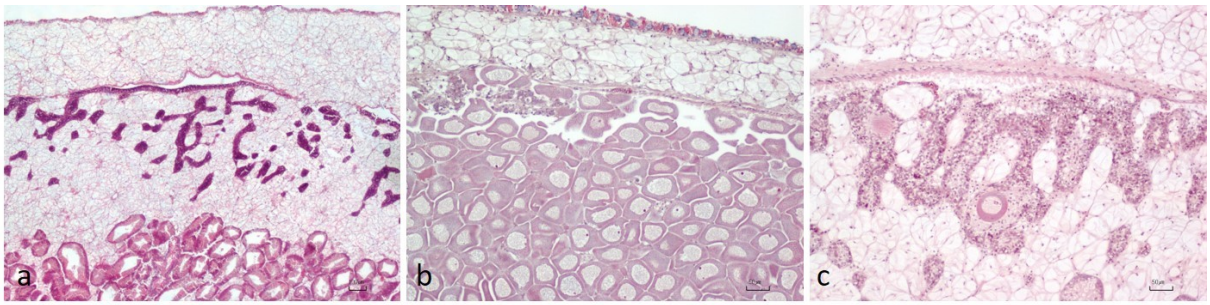

Table 2.2 Total analyzed oysters.

Sampling site	Species	N° oysters	Sex			
			Male	Female	M/F	ND
San Teodoro	*Crassostrea gigas*	358	74	31	3	250
Tortolì	*Crassostrea gigas*	59	3	2	2	52
Marceddì	*Crassostrea gigas*	10	2	7	-	1
Calich	*Crassostrea gigas*	13	1	1	-	11
Total		440	80	41	5	314

2.4.1 San Teodoro lagoon

Three hundred and fifty-eight oysters were sampled from San Teodoro lagoon from October 2016 to February 2018 once a month, with an additional sampling in June 2018. Specimens were in juvenile and adult phase (Table 2.3).

Overall, 74 oysters were males, 31 were females, 3 oysters were classified as M/F (both oocytes and sperm) and 250 were not sexually determined.

Table 2.3 Oysters from San Teodoro lagoon.

Sampling date	Species	Sampling site	N° oysters
October 2016	*Crassostrea gigas*	San Teodoro	23
November 2016	*Crassostrea gigas*	San Teodoro	16
December 2016	*Crassostrea gigas*	San Teodoro	30
January 2017	*Crassostrea gigas*	San Teodoro	24
February 2017	*Crassostrea gigas*	San Teodoro	24
March 2017	*Crassostrea gigas*	San Teodoro	24
April 2017	*Crassostrea gigas*	San Teodoro	21
May 2017	*Crassostrea gigas*	San Teodoro	18
June 2017	*Crassostrea gigas*	San Teodoro	22
July 2017	*Crassostrea gigas*	San Teodoro	20
August 2017	*Crassostrea gigas*	San Teodoro	16
September 2017	*Crassostrea gigas*	San Teodoro	26
October 2017	*Crassostrea gigas*	San Teodoro	18
November 2017	*Crassostrea gigas*	San Teodoro	15
December 2017	*Crassostrea gigas*	San Teodoro	12
January 2018	*Crassostrea gigas*	San Teodoro	18
February 2018	*Crassostrea gigas*	San Teodoro	14
June 2018	*Crassostrea gigas*	San Teodoro	17
Total			358

2.4.2 Tortolì lagoon

Fifty-nine oysters were examined from Tortolì lagoon. Specimens were taken in three different sampling periods, in April 2017, in September 2017 and the last sampling was in May 2018. As shown in the table below, the life stage of all samples was juvenile and adult stage (Table 2.4).

In total, 3 oysters were males, 2 were females, 2 oysters were in the transition phase (both oocytes and sperm) and 52 were not sexually determined.

Table 2.4 Oysters from Tortolì lagoon.

Sampling date	Species	Sampling site	N° oysters
April 2017	*Crassostrea gigas*	Tortolì	20
September 2017	*Crassostrea gigas*	Tortolì	24
May 2018	*Crassostrea gigas*	Tortolì	15
Total			59

2.4.3 Marceddì lagoon

Only 10 specimens were analyzed from Marceddì lagoon; they were sampled in April 2018 and they were juvenile/adult oysters (Table 2.5).

Of these specimens, 7 were females, 2 oysters were males and 1 oyster wasn't sexually determined.

Table 2.5 Oysters from Marceddì lagoon.

Sampling date	Species	Sampling site	N° oysters
April 2018	*Crassostrea gigas*	Marceddì	10
Total			10

2.4.4 Calich lagoon

Nine oysters from Calich lagoon were sampled in October 2017, and 4 oysters were sampled in April 2018. They were juvenile and adult oysters (Table 2.6).

Overall, 11 oysters were sexually not determined, 1 oyster was male and 1 was female.

Table 2.6 Oysters from Calich lagoon.

Sampling date	Species	Sampling site	N° oysters
October 2017	*Crassostrea gigas*	Calich	9
April 2018	*Crassostrea gigas*	Calich	4
Total			13

2.5 References

- Brock D. T., Madigan D. M., Martinko M.J., Parker J. (1998) Microbiologia. IV edizione 1998. Città Studi Edizioni.
- Carella F., Sardo A., Mangoni O., Di Cioccio D., Urciuolo G., De Vico G., Zingone A. (2015) Quantitative histopathology of the Mediterranean mussel (*Mytilus galloprovincialis* L.) exposed to the harmful dinoflagellate *Ostreopsis* cf. *ovata*. Journal of Invertebrate Pathology 127, 130–140.
- Colwell, R.R. and Liston, J. (1960) Microbiology of shellfish; bacteriological study of the natural flora of Pacific oysters (*Crassostrea gigas*). Applied Microbiology 8, 104–109.
- Fenza A., Olla G., Salati F., Viale I. (2014) Stagni e lagune produttive della Sardegna. Tradizioni, sapori e ambiente. Agenzia Regionale LAORE Sardegna.
- Garnier M., Labreuche Y. and Nicolas J.L. (2008) Molecular and phenotypic characterization of *Vibrio aestuarianus* subsp. *francensis* subsp. nov., a pathogen of the oyster *Crassostrea gigas*. Systematic and Applied Microbiology 31(5), 358-365.
- Higuchi R., Dollinger G., Walsh P.S., Griffith R. (1992) Simultaneous amplification and detection of specific DNA sequences. Biotechnology (N Y) 10(4), 413-7.
- Higuchi R., Fockler C., Dollinger G., Watson R. (1993) Kinetic PCR analysis: real-time monitoring of DNA amplification reactions. Biotechnology (N Y) 11(9), 1026-30.
- Howard, D. W., Lewis E. J., Keller B. J., and Smith C. S. (2004) Histological techniques for marine bivalve mollusks and crustaceans. NOAA Technical Memorandum NOS NCCOS 5, 218 pp.

- Ishmael F. T., Stellato C. (2008) Principles and applications of polymerase chain reaction: basic science for the practicing physician. Annals of Allergy, Asthma & Immunology 101(4), 437-43.
- Kubista M., Andrade J.M., Bengtsson M., Forootan A., Jonak J., Lind K., Sindelka R., Sjoback R., Sjogreen B., Strombom L., Stahlberg A., N. Zoric (2006) Review - The real-time polymerase chain reaction. Molecular Aspects of Medicine 27, 95–125.
- Kueh C.S.W. and Chan K.Y. (1985) Bacteria in bivalve shellfish with special reference to the oyster. Journal of Applied Bacteriology 59, 41–47.
- Mazzi V. (1977) Tecniche Istologiche e Istochimiche. Piccin Editore.
- Peck M. and Badrick T. (2017) A review of contemporary practice and proficiency with Gram staining in anatomical pathology laboratories. Journal of Histotechnology 40(2), 54-61.
- Rasband, W.S. (1997–2018) ImageJ U.S. National Institutes of Health, Bethesda, Maryland, USA <http://rsb.info.nih.gov/ij/>.

Chapter 3

Vibrio bacteria and related tissue lesions in oysters (*Crassostrea gigas*) from Sardinia

3.1 Introduction

Losses of Pacific Oysters (*Crassostrea gigas*) have occurred for over 5 decades a with heavy impact on oyster aquaculture. Several studies have identified as probably triggers of these episodes both oyster's physiological factors, environmental factors (water temperature and salinity) and the presence of pathogens (viral and bacterial infections) (Garnier *et al*., 2007; Burge *et al*., 2006; Martenot *et al.,* 2011; Barbosa Solomieu *et al*., 2015).

In particular, bacterial diseases are reported in several bivalve species: *Vibrio* genus represents the main responsible of these episodes (Paillard *et al*., 2004; Beaz-Hidalgo *et al*., 2010; Lacoste *et al*., 2001; Le Roux *et al*., 2002; Waechter *et al*., 2002; Gay *et al*., 2004b; Garnier *et al*., 2008; Vezzulli *et al*., 2015).

Since 80s some bacteria belonging to the *Vibrio* genus were isolated from the lagoon's water and from molluscs with evident signs of damage, such as anomalies in swimming larvae and tissue necrosis (Jeffries, 1982; Elston and Leibovitz, 1980). More specific analysis established the identity of these bacterial species, belonging to the family of Vibrionaceae. Several strains were related to *Vibrio splendidus* clade (Baumann *et al*. 1980; Sugumar *et al*., 1998; Le Roux *et al*., 2002; Le Roux *et al*., 2004; Gay *et al*., 2004a) and a new emerging species *V. aestuarianus*, was detected (Tison and Seidler, 1983).

In the following years, numerous studies in oysters affected by episodes of mortality were carried out and *V. aestuarianus* was identified as the main pathogen of adult oysters, sometimes in synergy with *V. splendidus* (Garnier *et al*., 2007; Garnier *et al*., 2008; Travers *et al*., 2015; Travers *et al*., 2017).

Vibrio species are Gram negative bacteria, curved-rod in shape with a unique flagellum, about 0.4-0.5 µm in width and 1-1.5 µm in length. They are facultative anaerobe and no spore forming bacteria (Gomez-Leon *et al*., 2005; Garnier *et al*., 2008; Zhang X. J. *et al*., 2011).

Due to uncertain results of cultural methods, biomolecular analyses are used to detect bacterial DNA in samples, such as conventional PCR and real time PCR (Saulnier *et al*., 2009; Saulnier *et al*., 2017).

The detectable symptoms of infected oysters were mainly weakness of the adductor muscle and moribund appearance of the molluscs (EFSA, 2015). Little information are available about the dynamics and transmission of these bacterial species, whose infection is closely linked to host- dependent (i.e. immune deficiency) and environmental factors (Barbosa Solomieu *et al*., 2015). Gay *et al*., 2004a described histological alterations observed in *V. splendidus* infected oysters, and they showed mainly muscular damages and sometimes hemocyte infiltrations in the gills and connective tissues (Gay *et al*., 2004a).

Furthermore, histological analysis on *V. aestuarianus* infected oysters showed mainly necrosis of the mantle subepithelial connective tissue, atrophy of the digestive diverticula, and hemocytic infiltration in the hemolymphatic vessels. It has been suggested that *V. aestuarianus* colonized firstly the hemolymph with hemocytes recruitment after a multiplication growth and finally invades the connective tissues of digestive gland and mantle, in which tissue lesions were observed (Parizadeh *et al*., 2018).

The aim of this work was to investigate the presence of *V. aestuarianus* and *V. splendidus* and associated lesions in hepatopancreas, gills and mantle tissues of *C. gigas* samples collected from Sardinian lagoons, by the use of PCR and real time PCR and histopathological analyses.

Moreover, according to Parizadeh *et al*. tubular lumen areas of oyster's digestive glands were measured by image analysis to evaluate gland atrophy (Carella *et al*., 2015; Parizadeh *et al*., 2018).

3.2 Material and methods

3.2.1 Study area

Samples were collected from 4 lagoons: San Teodoro lagoon (North-Eastern Sardinia), Tortolì lagoon (Eastern Sardinia), Marceddì lagoon (Western Sardinia), Calich lagoon (North-Western Sardinia) (Fenza *et al*., 2014). Sites details are described in Chapter 2.

3.2.2 Sampling

Four hundred and forty samples of juvenile and/or adult cupped oysters, *C. gigas*, were collected from October 2016 to June 2018: 358 samples were from San Teodoro lagoon, 59 from Tortolì, 10 from Marceddì and 13 samples were from Calich lagoon. Details of sampling are reported in Chapter 2.

3.2.3 Gross pathology evaluation

Gross examination of oyster samples in order to verify physiological status and vitality of molluscs was carried out.

During necropsy, microbiological isolation was carried out from hepatopancreas, in aseptic conditions to prevent environmental contaminations. Fragments of target tissues (gills and mantle) were collected and stored at -20°C for subsequent molecular analysis. In total, 434 oyster's hepatopancreas and 440 oyster's gills and mantle tissues were analyzed. For details see Chapter 2.

3.2.4 Microbiological analysis

Microbiological isolation on 434 hepatopancreas samples by using Brain Heart Infusion Agar (Difco) growth medium was performed. After 24-48 h of incubation at 17-20°C, growth

colonies were isolated to purify the bacteria; their morphology was microscopically examined after Gram staining and biochemical tests were carried out on purified colonies, according to Manual of Methods for General Bacteriology (American Society for Microbiology, 1981) (Garnier *et al*., 2008). For a detailed description of bacteriological analysis see Chapter 2.

3.2.5 Biomolecular analysis

DNA extraction on 434 isolated strains of hepatopancreas by using Nexttec DNA isolation kit for Bacteria (Nexttec GmbH, Germany) was carried out. DNA extraction on 440 gills/mantle tissue pools were carried out by using QIAamp DNA mini kit (Qiagen GmbH, Germany), according to manufacturer instructions.

PCR was performed on each sample, to detect *V. aestuarianus* and *V. splendidus*, both in DNA extracted from hepatopancreas isolated strains and in DNA extracted from gill/mantle tissues.

V. aestuarianus and *V. splendidus* PCR reactions were performed with 25 µl reaction mix containing 1 mM $MgCl_2$, 3 µl of Mastermix (Larova), 0,2 µM of each primer, 1 µl of extracted DNA and distilled water.

Primers were designed by Prof. A. Alberti (Infectious Disease, Department of Veterinary Medicine, University of Sassari) to amplify fragments of *toxR*, gene for transmembrane regulatory protein, of both *V. aestuarianus* and *V. splendidus*.

PCR amplification was performed with the following thermal conditions: 1 cycle of initial denaturation at 94°C for 2 min; denaturation at 94°C for 20 sec, primer annealing at 55°C for 20 sec and elongation at 72°C for 20 sec, the last 3 steps were repeated for 30 times; the last step was 1 cycle of final elongation at 72°C for 10 min.

Fig. 3.1 *V. aestuarianus* primers.

ID primers	Sequence	bp
VesToxRF	5' CAAAGAACCGGTGGTCGAGC 3'	259 bp
VesToxRR	5' ATTGTAGACAGCCAATTGCC 3'	

Fig. 3.2 *V. splendidus* primers.

ID primers	Sequence	bp
VspToxF	5' TTTGCAACGCCTACAATGAC 3'	182 bp
VspToxR	5' ATTGGCATGATGAAAGCCGC 3'	

Post-amplification analyses of amplified fragments were carried out by 2% gel electrophoresis (Sigma-Aldrich, St. Louis, MO, USA) with 10000X SYBR Safe as DNA staining (Invitrogen, Carlsbad, CA, USA), Blue Loading Buffer (Invitrogen) and 100 bp DNA Ladder (Invitrogen). Transilluminator Safe Imager was used to highlight amplified fragments and images were acquired by Photodoc system (Invitrogen).

Real-time PCR was performed on DNA extracted from gills/mantle tissues in order to quantify *V. aestuarianus* and *V. splendidus* positive samples. These PCR reactions were both carried out with 25 µl reaction mix containing 1,5 mM $MgCl_2$, 15 µl of Crystal Taq Master (Larova), 1 µl Sybr Green, 0,2 µM of each primer (VesToxRF and VesToxRR for *V. aestuarianus* amplification, Fig. 3.1; VspToxF and VspToxR for *V. splendidus* amplification, Fig. 3.2), 1 µl of extracted DNA and distilled water.

Thermal conditions were: 1 cycle of initial denaturation at 95°C for 2 min; denaturation at 95°C for 10 sec, primer annealing at 60°C for 15 sec and extension at 72°C for 60 sec, the last 3 steps were repeated for 40 times; the melting curve was performed at 95°C, 45°C, 95°C for

0 seconds, and the temperature increased by increments of 1ºC, waiting for 5 seconds before each acquisition. Finally, the system cooling down until 35°C.

The quantification of the samples was based on a standard curve with five dilution points from 1,5 x 10^8 copies/µl stock of genomic DNA extracted from reference strains (*V. aestuarianus* DSM 19606; *V. splendidus* DSM 19640), as shown in Fig. 3.3 and Fig. 3.4. Real-time PCR assays exhibited good correlation coefficient values (r^2), between 0,975 and 0,985, and acceptable PCR reaction efficiency, between 0,92 and 1,06 (Takahashi *et al*., 2005; Saulnier *et al*., 2009).

Fig. 3.3 Standard curve: the graphs show the log cell numbers and the relative threshold cycles (Ct) of each *V. aestuarianus* diluition. Standard curve r^2 is 0,97 and its efficiency is 1,05.

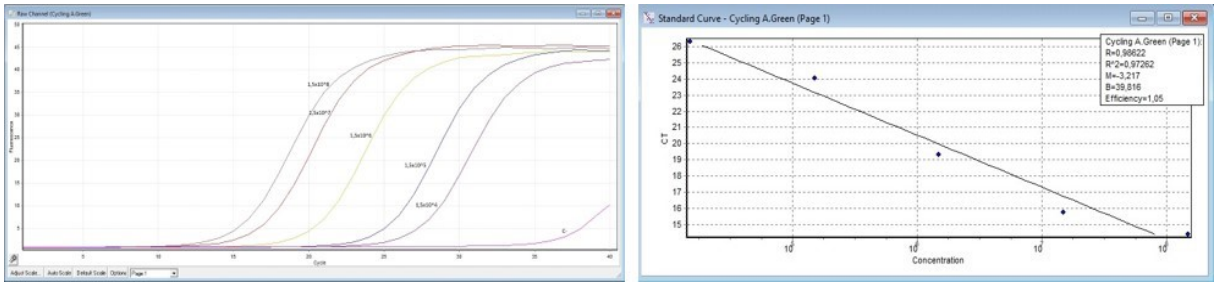

Fig. 3.4 Standard curve: the graphs show the log cell numbers and the relative threshold cycles (Ct) of each *V. splendidus* diluition. Standard curve r^2 is 0,99 and its efficiency is 0,94.

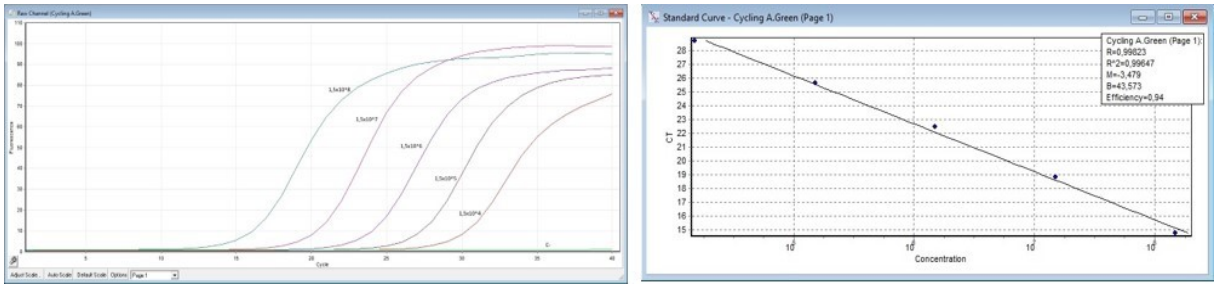

3.2.6 Histopathology

Each oyster was sectioned and samples of target tissues (hepatopancreas, gills and mantle) were fixed in 10% neutral buffered formalin; tissues were dehydrated through alcohol and xylene, using an automatic tissue processor, and paraffin-embedded according to standard techniques (Mazzi, 1977). Sections of 3 µm thick were stained with Haematoxylin and Eosin and examined with a light microscope. More details are reported in Chapter 2.

3.2.7 Digestive diverticula atrophy evaluation

Evaluation of tubular lumen areas of oyster's hepatopancreas digestive diverticula were carried out by image analysis to measure gland atrophy in 10 *V. aestuarianus* PCR positive and 10 *V. aestuarianus* PCR negative samples. *ImageJ* software (version 1.52a, Rasband, 1997–2018) was used to highlight lumen areas (Carella *et al*., 2015). For a detailed description of method see Chapter 2.

3.2.8 Statistical analysis

Histopathological and biomolecular data were analyzed using Stata 11.2 software (StataCorp LP). Fisher and Chi-square ($\chi 2$) tests have been used to compare histopathological results, biomolecular results and to correlate histopathological-biomolecular results. A *P*-value <0,05 indicated significant data. Moreover, tubular lumen areas of digestive diverticula were analyzed using Student *t-test*.

3.3 Results

During sampling in San Teodoro lagoon, a mortality outbreak was reported from December 2016 to March 2017: it caused more than 80% of oyster mortality in the farm. In these months water temperatures were the lowest of the year (13-16°C) and water salinity decreased from 40% to 10% because of heavy rains.

3.3.1 Microbiology

Several bacterial colonies from 434 samples of hepatopancreas were isolated; 122 out of 434 were Gram-negative and curved-rod in shape, they were biochemically characterized by positivity for oxidase and catalase tests and both aerobe and anaerobe metabolism. These strains were identified as *Vibrio* spp. by API 20 NE test (Fig. 3.5A, B). Remaining isolated strains have not been identified.

However, the results of biochemical tests for the identification of the isolated strains did not allow a clear identification of the species, then all isolated strains were subjected to molecular analysis.

Fig. 3.5 Strain on BHI agar growth medium (A); API 20 NE test (B).

A 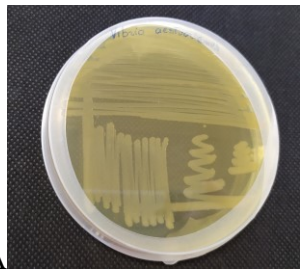

B 

3.3.2 Molecular biology

Hepatopancreas isolated strains by microbiological methods were also evaluated by PCR to detect oyster's pathogens, *V. aestuarianus* (Fig. 3.6A) and *V. splendidus* (Fig. 3.6B). Furthermore, gills and mantle tissues were firstly evaluated by PCR and subsequently real time PCR was performed on positive samples to quantify bacterial loads in tissues.

Hepatopancreas PCR results: *V. aestuarianus* PCR analysis performed on 434 strains isolated from oysters showed 79/434 positive samples (18,2%) and 355 negative ones (81,8%). *V. splendidus* PCR showed positivity in 206/434 analyzed samples (47,5%), while 228/434 were PCR negative (52,5%).

Gills and mantle PCR results: *V. aestuarianus* and *V. splendidus* PCR were performed on 440 oyster samples. *V. aestuarianus* PCR positive samples were 33/440 (7,5%), the remaining 407/440 samples were PCR negative (92,5%) (Fig. 3.6A). *V. splendidus* was detected in 10/440 oyster gills and mantle pools (2,3%), while 430/440 samples were negative (97,7%) (Fig. 3.6B).

Both *V. aestuarianus* and *V. splendidus* were more frequently discovered in the hepatopancreas compared to the pools of gills and mantle tissue (X^2=22.4013 P=0.000; X^2=172.9177 P=0.000).

Fig. 3.6 *V. aestuarianus* (A) and *V. splendidus* (B) amplified fragments.

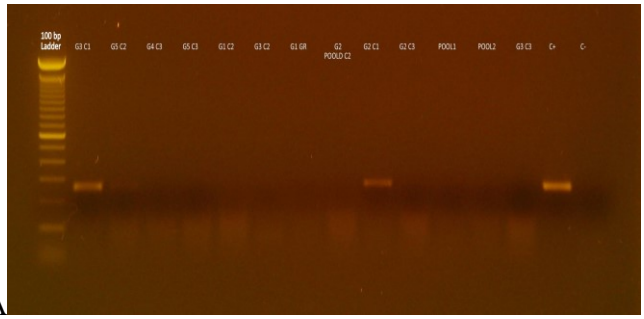

A

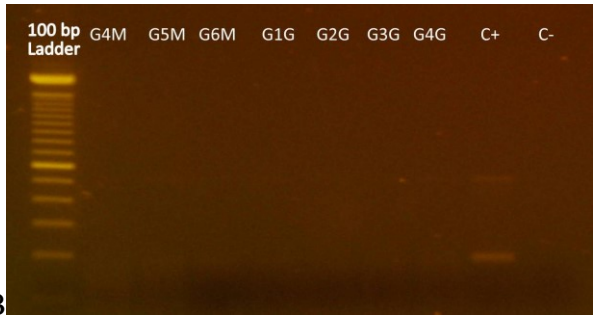

B

Gills and mantle real time PCR results: a standard curve was designed to quantify *V. aestuarianus* and *V. splendidus* in gills and mantle tissues (Fig. 3.7A, B and Fig. 3.8A, B).

Fig. 3.7 Standard curve (A) and linear regression line (B) of *V. aestuarianus* quantitative standards.

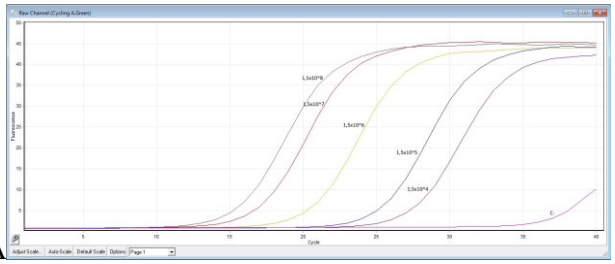

A

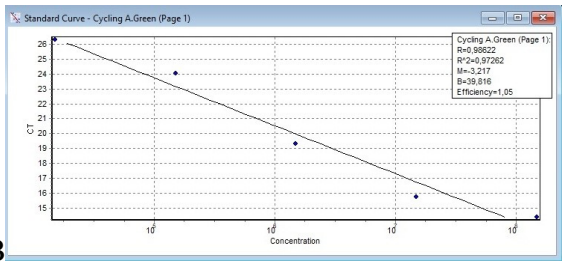

B

Fig. 3.8 Standard curve (A) and linear regression line (B) of *V. splendidus* quantitative standards.

A

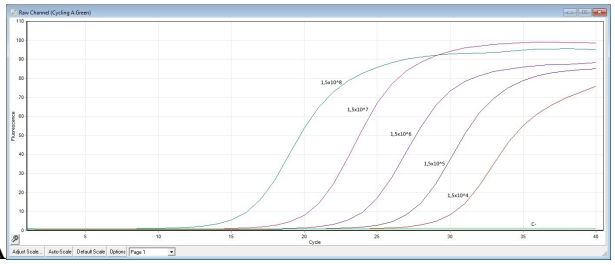

B

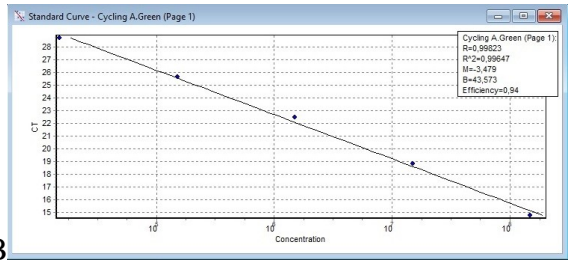

Based on this standard curve (Fig. 3.7A, B), *V. aestuarianus* was quantified on 33 samples: bacterial load ranged from 6,05x10^2 copies/µl to 7,55x10^6 copies/µl. (Fig. 3.9A, B, C).

Five out 33 samples were 10^2 copies/µl, 12/33 were 10^3 copies/µl, 9/33 were 10^4 copies/µl, 6/33 were 10^5 and 1/33 sample was 10^6 bacterial load.

Fig. 3.9A Quantification analysis of *V. aestuarianus* in oyster samples.

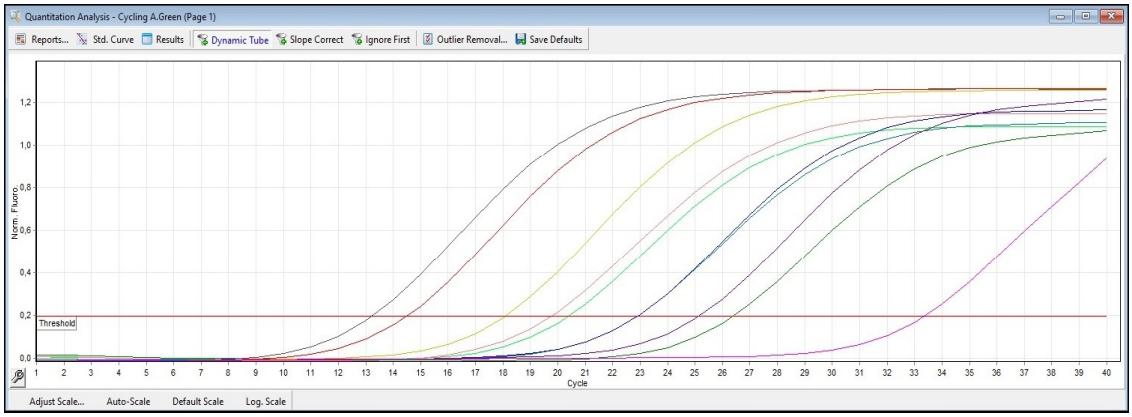

Fig. 3.9B Standard curve of *V. aestuarianus* in oyster samples.

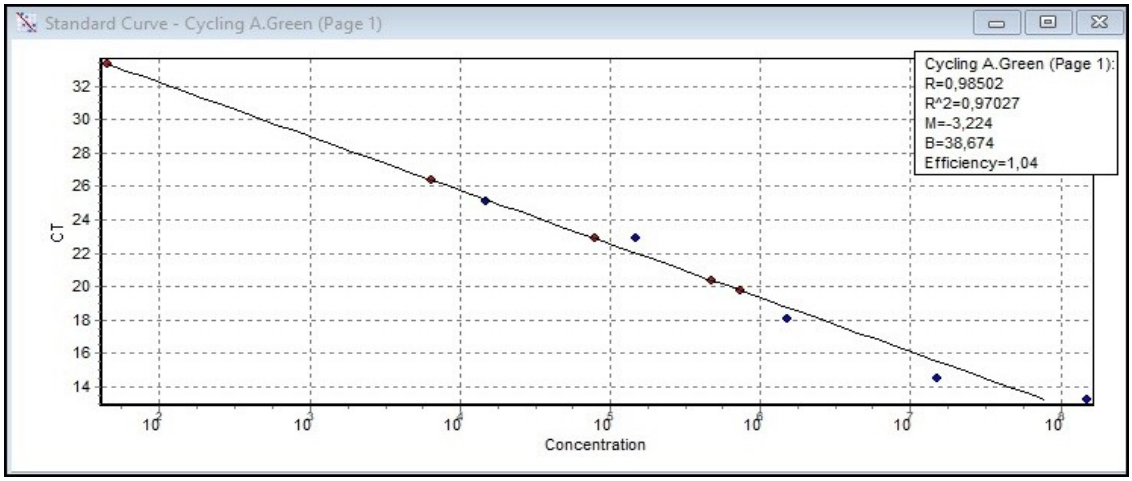

Fig. 3.9C Quantification results of *V. aestuarianus* in oyster samples.

Quant. Results - Cycling A.Green (Page 1)

No.	Name	Type	Ct	Ct Comment	Given Conc (cop	Calc Conc (copie	% Var	Rep. Ct	Rep. Ct Stc	Rep. Ct (95
1	G1T 05/18 C1	Unknown	20,37			4,75E+05		20,37		
2	G2T 05/18 C1	Unknown	22,88			7,93E+04		22,88		
3	G6T 05/18 C1	Unknown	19,75			7,38E+05		19,75		
4	G5T 05/18 C2	Unknown	26,37			6,53E+03		26,37		
5	10E6	Standard	13,21		1,50E+08	7,90E+07	47,4%	13,21		
6	10E5	Standard	14,49		1,50E+07	3,17E+07	111,1%	14,49		
7	10E4	Standard	18,08		1,50E+06	2,44E+06	62,5%	18,08		
8	10E3	Standard	22,89		1,50E+05	7,87E+04	47,5%	22,89		
9	10E2	Standard	25,13		1,50E+04	1,58E+04	5,6%	25,13		
10	C-	Negative	33,35			4,49E+01		33,35		

V. splendidus PCR positive samples were 10: the quantification of these samples, based on *V. splendidus* standard curve (Fig. 3.8A, B), range from 1,47x10^4 copies/µl to 1,22x10^5 copies/µl (Fig. 3.10A, B, C). Nine out of 10 samples were 10^4 copies/µl bacterial load and one sample was 10^5 copies/µl.

Fig. 3.10A Quantification analysis of *V. splendidus* in oyster samples.

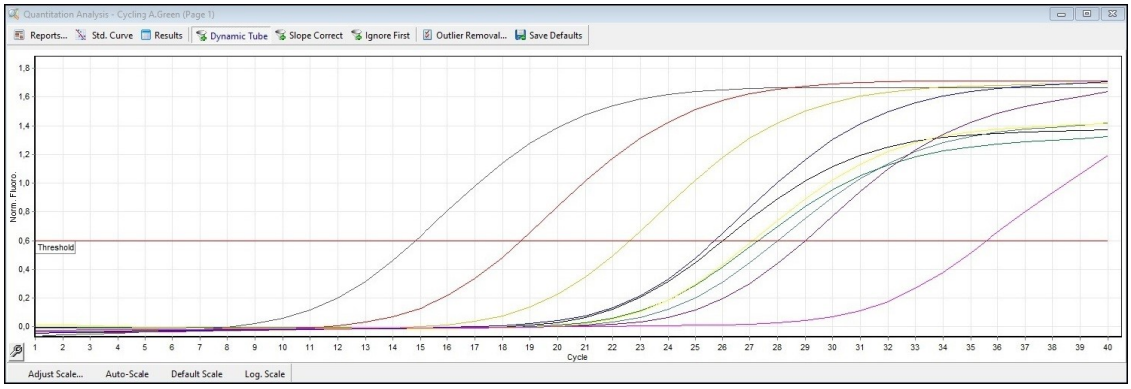

Fig. 3.10B Standard curve of *V. splendidus* in oyster samples.

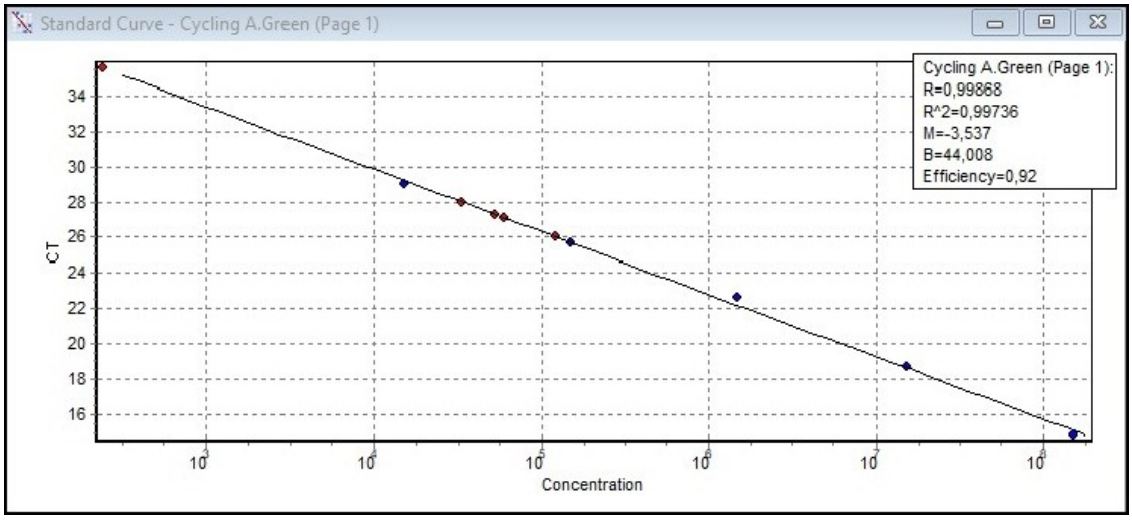

Fig. 3.10C Quantification results of *V. splendidus* in oyster samples.

Quant. Results - Cycling A.Green (Page 1)

No.	Name	Type	Ct	Ct Comment	Given Conc (cop	Calc Conc (copie	% Var	Rep. Ct	Rep. Ct Stc	Rep. Ct (9E
4	G4 MARC	Unknown	27,30			5,29E+04		27,30		
6	G6 MARC	Unknown	26,01			1,22E+05		26,01		
8	G8 MARC	Unknown	28,00			3,35E+04		28,00		
10	G10 MARC	Unknown	27,11			5,98E+04		27,11		
11	10E6	Standard	14,82		1,50E+08	1,78E+08	18,8%	14,82		
12	10E5	Standard	18,68		1,50E+07	1,45E+07	3,3%	18,68		
13	10E4	Standard	22,61		1,50E+06	1,12E+06	25,2%	22,61		
14	10E3	Standard	25,71		1,50E+05	1,49E+05	0,8%	25,71		
15	10E2	Standard	28,99		1,50E+04	1,76E+04	17,3%	28,99		
16	C-	Negative	35,58			2,41E+02		35,58		

To exclude PCR incorrect amplification, the melting curve of each real-time PCR reaction was evaluated, and Tm values of samples corresponded to Tm value of the positive control (Fig. 3.11).

Fig. 3.11 Melting curve of negative (NEG) and positive (POS) samples.

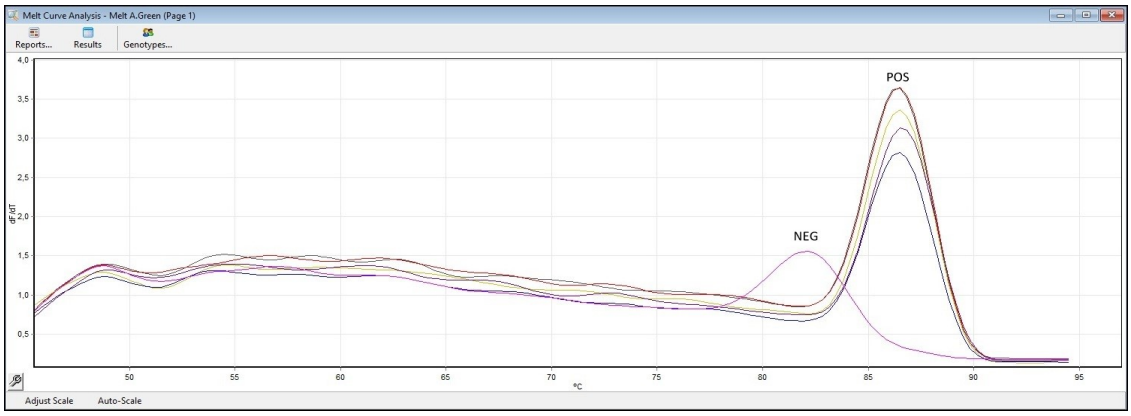

3.3.3 Histopathology

Hepatopancreas results: hemocytes infiltration was observed in the interstitial spaces among digestive tubules, mainly around the intestinal lumen and digestive ducts with different degree of severity (mild, moderate and severe).

Based on the histological pattern, 434 samples of hepatopancreas were evaluated. Histopathologic examinations showed 252/434 samples (58,1%) with mild hemocytes infiltration, 64/434 samples had a moderate amount of hemocyte (14,7%) and only 13/434 oyster specimens displayed severe hemocytes infiltration (3%). Instead, hemocytes were not detected in 103/434 hepatopancreas samples (23,7%). Two remaining samples were not evaluable.

Gills results: the immune response was characterized by hemocytic infiltrations, with multifocal, diffuse or nodular distribution of hemocytes (Fig. 3.12). Gills damage were mostly characterized by loss of lamellar surface epithelium.

Fig. 3.12 Gills: normal (A); mild (B), moderate (C), severe (D) hemocytes infiltration in gills tissue. Bar A-C-D = 50 µm; Bar B = 10 µm.

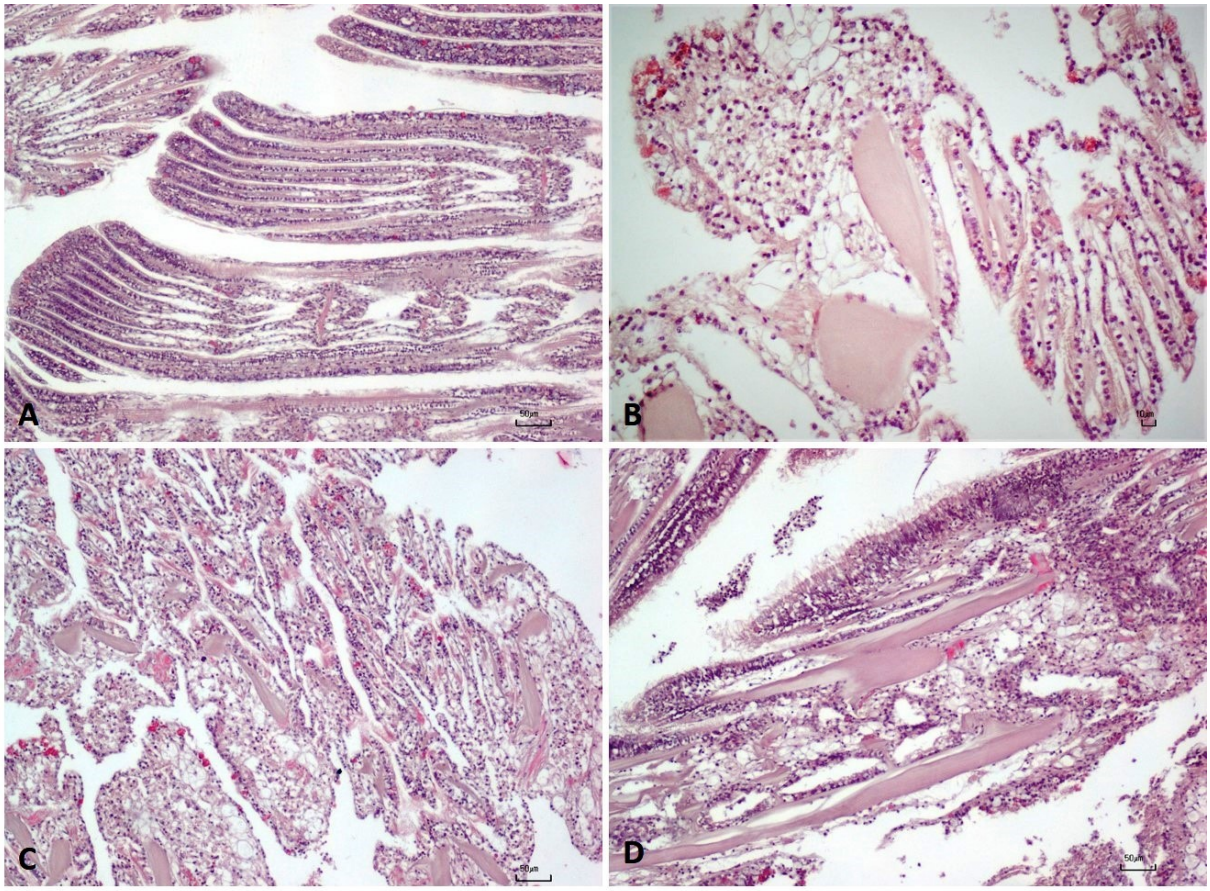

Histologically, 440 gills samples were evaluated: 185/440 showed mild (42%), 58/440 moderate (13,2%) and 12/440 (2,7%) severe hemocytes infiltration, respectively. Hemocytes were no detected in 142/440 samples (32,3%), while 43/440 samples were histologically not evaluable, due to technical issues.

Mantle results: hemocytes were mainly located at the margins of the tissue and their distribution was multifocal, diffuse or nodular. Nodular aggregation was mostly observed in association with severe infiltration of the mantle where hemocytes were often placed within hemolymphatic vessels or around them (Fig. 3.13).

Fig. 3.13 Mantle: normal tissue (A); mild (B), moderate (C), severe (D) hemocytes infiltration with a nodular distribution (D-E). Hemocytes infiltration in hemolymphatic vessel (F). Bar A-B-C-D-F = 50 µm; Bar E = 10 µm.

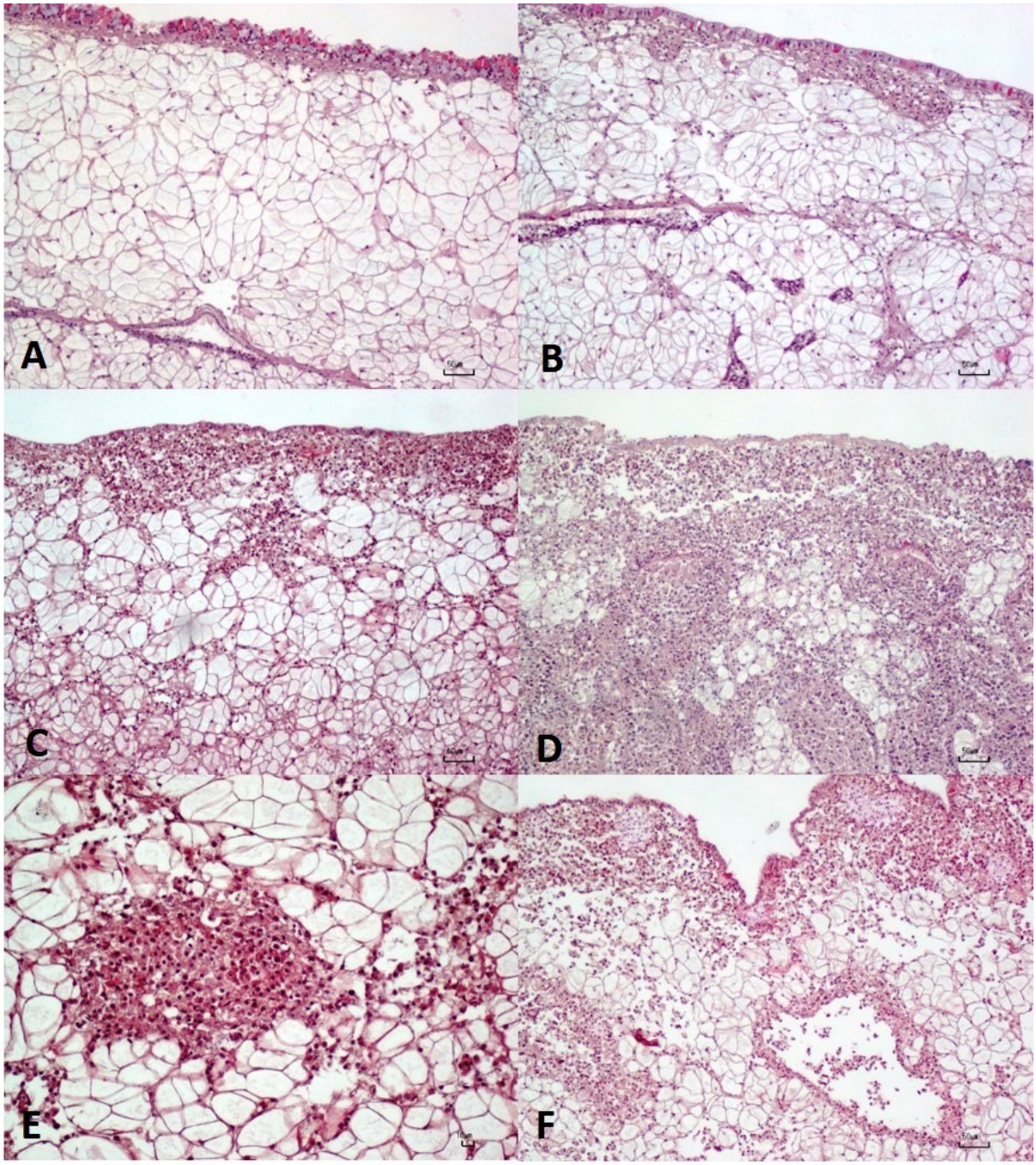

One-hundred and sixty-two out 440 mantle samples showed mild hemocytes infiltration (36,8%), 57/440 had a moderate infiltration (13%) and 14/440 samples had severe hemocyte infiltration (3,2%). Hemocytes were not observed on 173 out of 440 samples (39,3%). Remaining 34 samples were histologically not evaluable.

No statistically significant difference was observed in hemocytes infiltration between mantle, gills and digestive glands (X^2 =3.9677 P= 0.410).

3.3.4 PCR and histopathology correlation

Hepatopancreas results: accordingly, to the molecular biology results, 79/434 hepatopancreas samples were *V. aestuarianus* PCR positive (Table 3.1).

Histologically, 58 out of 79 *V. aestuarianus* PCR positive samples displayed hemocytes infiltration; 38/79 were characterized by a mild infiltration (48,1%), 15/79 showed moderate (19%) and 5/79 samples had a severe hemocytes infiltration (6,3%) (Table 3.1). No hemocytes infiltration was detected in 20 PCR positive samples (25,3%), and one sample was histologically not evaluable. Furthermore, among PCR negative samples (355/434), 271 out 355 (76,3%) showed hemocytes infiltration (Table 3.1).

Negative PCR samples were more consistently associated with hemocytes infiltration of high intensity compared to the positive one's (X^2=6.5004 P=0.039).

Regarding *V. splendidus*, 206/434 hepatopancreas samples were PCR positive; 159 out of 206 showed hemocytes infiltration, of which 115/206 showed mild (55,8%), 37/206 showed moderate (18%) and 7/206 showed severe infiltration (3,4%); 46 samples had no hemocytes infiltration and one sample was histologically not evaluable (Table 3.1). *V. splendidus* PCR negative samples were 228/434, 170/228 showed hemocytes infiltration (74,6%). The remaining 57/228 samples were negative (25%). One hepatopancreas sample was histologically not evaluable (Table 3.1).

No statistically significant difference in the degree of hemocytes infiltration was noticed comparing negative and positive *V. splendidus* PCR samples (X^2=3.1958 P=0.202).

Table 3.1 Hepatopancreas: *V. aestuarianus* and *V. splendidus* PCR and hemocytes infiltration in oysters.

	Analyzed samples	N° positive samples			
		PCR	Histology*^		
			Mild	Moderate	Severe
**V. aestuarianus*	434	79	38	15	5
^*V. splendidus*	434	206	115	37	7

[*] *V. aestuarianus* PCR positive samples (n=20) were histologically negative and 1 sample was histologically not evaluable;

^ *V. splendidus* PCR positive samples (n=46) were histologically negative and 1 sample was histologically not evaluable.

Gills and mantle results: 440 gills and mantle tissues were evaluated and 33 were *V. aestuarianus* PCR positive (Table 3.2).

Histologically, 28 out of 33 *V. aestuarianus* PCR positive samples displayed hemocytes infiltration in gills. Seventeen out of 33 PCR gills positive samples showed mild hemocytes infiltration (51,5%); 7/33 samples had moderate hemocytes infiltration (21,2%) and 4/33 samples were characterized by severe hemocytes infiltration (12,1%). Two out of 33 PCR positive samples do not show any infiltration (6,1%). Remaining 3 PCR positive samples were histologically not evaluable, due to technical issues. PCR negative samples were 367/440 (83,4%) of which 227/367 (61,9%) showed hemocytes infiltration and 140 out of 367 remaining samples (38,1%) were negative. Forty gills tissue samples out of 440 were histologically not evaluable (Table 3.2).

The hemocytes infiltration was more frequently observed in negative PCR samples compared to *V. aestuarianus* positive (X^2=6.8116 P=0.033).

In mantle tissue 33/440 samples were *V. aestuarianus* PCR positive (7,5%); 4/33 samples displayed mild hemocytes infiltration (12,1%), 22/33 had moderate hemocytes infiltration (66,7%); severe hemocytes infiltration was observed in 7/33 PCR positive samples (21,2%). PCR negative samples were 407/440 (92,5%), 200/407 showed hemocytes infiltration

(49,1%) and 173/407 were negative (42,5%). Remaining 34/407 samples were histologically not evaluable (8,4%).

Gram staining was performed on severe infiltrated mantle samples and red bacteria were showed (Fig. 3.14).

Fig. 3.14 Gram negative bacteria stain red (Gram staining). Bar = 10 µm.

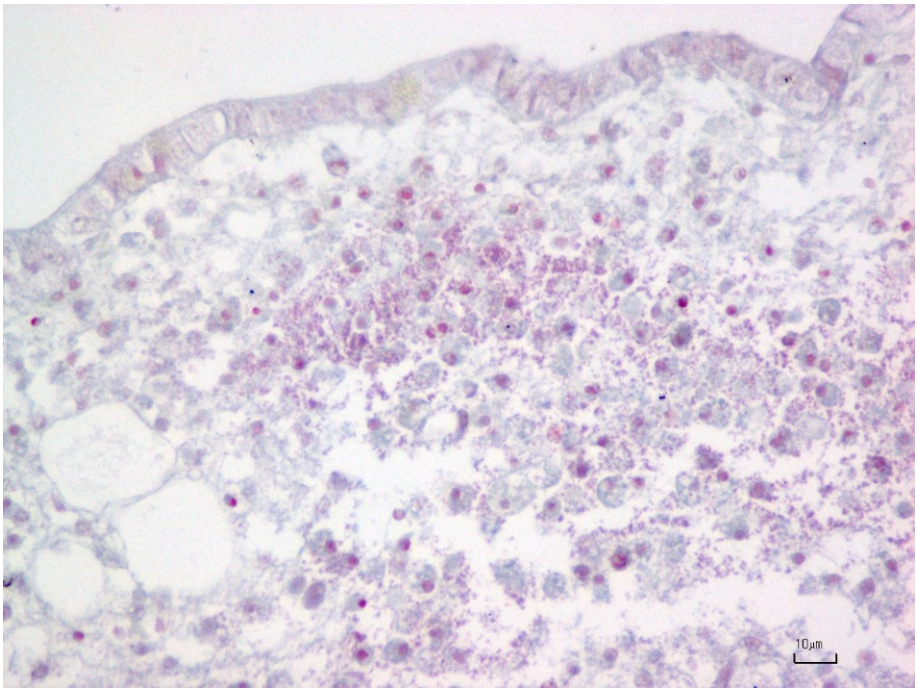

The hemocytes infiltration was more frequently observed in negative PCR samples compared to *V. aestuarianus* positive (X^2= 61.0025 P=0.000); however, in PCR positive samples, 7 out 33 (21.2%) showed a severe degree of hemocytes infiltration, while most of the samples (22) were characterized by a moderate infiltration (X^2= 61.0025 P=0.000).

Table 3.2 Gills and mantle: *V. aestuarianus* PCR and hemocytes infiltration in oysters.

Tissues	Analyzed samples	N° positive samples			
		PCR	Histology*^		
			Mild	Moderate	Severe
*Gills	440	33	17	7	4
Mantle	440	33	4	22	7

*Two PCR positive samples were histologically negative, and 3 samples were histologically not evaluable;

V. splendidus PCR positive gill samples were 10 out of 440 (2,3%): hemocytes infiltration was mild in 7/10 samples (70%), while 2/10 samples had respectively moderate (10%) and severe hemocytes infiltration (10%). One PCR positive sample was histologically negative (10%). *V. splendidus* PCR negative samples were 430/440 (97,7%): hemocytes infiltration has been observed in 246 out of 430 PCR negative samples (57,2%), and 141/430 samples were negative (32,8%). Remaining 43 samples were histologically not evaluable (Table 3.3).

No statistically significant differences were observed comparing the hemocytes infiltration in PCR positive and negative samples (X^2=1.4037 P=0.496).

Similarly, in mantle 10/440 samples were *V. splendidus* PCR positive (2,3%). Four out of 10 showed mild hemocytes infiltration (40%), 2/10 samples had moderate (20%) and only one sample (10%) showed the severe intensity of hemocytes. Three out of 10 *V. splendidus* PCR positive samples displayed no hemocytes. PCR negative samples were 430/440 (97,7%) and histological analysis showed hemocytes infiltration in 224/430 samples (52,1%). One hundred seventy-two out of 430 samples had no hemocytes infiltration (40%) and 34/430 samples were histologically not evaluable. No statistically significant differences were observed comparing the hemocytes infiltration in PCR positive and negative samples (X^2=1.5726 P=0.456).

Table 3.3 Gills and mantle: *V. splendidus* PCR and hemocytes infiltration in oysters.

Tissues	Analyzed samples	N° positive samples			
		PCR	Histology*^		
			Mild	Moderate	Severe
*Gills	440	10	7	1	1
^Mantle	440	10	4	2	1

*One PCR positive sample was histologically negative;
^Three PCR positive samples were histologically negative.

Real time analysis: real time quantification of *V. aestuarianus* showed 17/33 (51,5%) samples with low bacterial load, ranging between $6,05x10^2$ copies/µl and $7,81x10^3$ copies/µl. Histologically, 3/17 samples had a mild intensity of hemocytes infiltration (17,6%), 12/17 samples showed moderate number of hemocytes (70,6%) and 2/17 samples (11,8%) severe hemocytes infiltration was observed.

Sixteen out of 33 samples (48,5%) had high bacterial load, ranging between $1,31x10^4$ copies/µl and $7,55x10^6$ copies/µl; histologically, all these samples showed hemocytes infiltration, 1/16 was of mild intensity (6,3%), 10/16 were of moderate (62,5%) and 5/16 were severe intensity (31,3%).

Low bacterial load of *V. aestuarianus* was more commonly associated with moderate hemocytes infiltration (70,6%), while higher bacterial load showed moderate (62,5%) to severe (31,3%) infiltration of hemocytes (X^2= 2.4395 P=0.295).

Instead, real-time PCR of *V. splendidus* showed high bacterial load in 10/10 quantified samples (100%), ranging between $1,47x10^4$ copies/µl and $1,22x10^5$ copies/µl. Histologically, 4/10 samples had mild hemocytes infiltration (40%), 2/10 samples showed moderate hemocytes (20%) and only 1 sample displayed severe intensity hemocytes infiltration (10%). Three out of 10 samples didn't show any infiltrate (30%).

3.3.4.1 San Teodoro lagoon

Hepatopancreas results: a total of 358 oyster specimens was analyzed; 71/358 samples were *V. aestuarianus* PCR positive (19,8%).

Histologically, 52 out of 71 (73,2%) *V. aestuarianus* PCR positive samples showed an hemocytes infiltration ranging from mild to severe intensity [33 mild intensity (46,5%), 15 moderate intensity (21,1%), 4 severe intensity (5,6%)]. Instead, 18 remaining samples didn't show hemocytes infiltration (25,4%) (Table 3.4). One sample was histologically not evaluable.

V. aestuarianus PCR negative samples were 287/358: 215 out of 287 samples showed hemocytes infiltration (74,9%) and 72/287 were negative (25,1%).

Both positive and negative samples were more commonly associated with a mild intensity of infiltration (X^2=6.4767 P=0.039).

V. splendidus PCR positive samples were 166/358 (46,4%) and 126/166 (75,9%) *V. splendidus* PCR positive hepatopancreas samples showed mild to severe hemocytes infiltration at histological observation. In particular, mild hemocytes infiltration were observed in 88/166 samples (53%), 33/166 samples had moderate infiltration (19,9%) and 5/166 samples showed severe hemocytes infiltration (3%); 39/166 samples were histologically negative (23,5%). One sample was histologically not evaluable. Instead, 192/358 samples were PCR negative (53,6%); 141/192 of these samples showed hemocytes infiltration (73,4%) and 51/192 were histologically negative (26,6%) (Table 3.4).

Percentage of hemocytes infiltration in *V. splendidus* PCR negative samples (73,4%) was comparable to the observed in PCR positive samples (75,9%). In hepatopancreas, differences in hemocytes infiltration between PCR positive and PCR negative samples were not statistically significant (both in the case of *V. aestuarianus* and *V. splendidus*).

Table 3.4 San Teodoro lagoon: *V. aestuarianus* and *V. splendidus* PCR and hemocytes infiltration in oysters hepatopancreas.

	Analyzed samples	N° positive samples			
		PCR	Histology*^		
			Mild	Moderate	Severe
**V. aestuarianus*	358	71	33	15	4
^*V. splendidus*	358	166	88	33	5

* *V. aestuarianus* PCR positive samples (n=18) were histologically negative and one sample was histologically not evaluable;

^ *V. splendidus* PCR positive samples (39) were histologically negative and one sample was histologically not evaluable.

Gills and mantle results: three hundred fifty-eight samples were analyzed. In gills, *V. aestuarianus* PCR positive samples were 28/358 (7,8%) and 24/28 (85,7%) showed hemocytes infiltration: 16/28 samples had mild hemocytes infiltration (57,1%), 7/28 samples displayed a moderate number of hemocytes (25%) and one sample (3,6%) showed severe infiltration of hemocytes in gills tissue. Two out of 28 samples were negative (7,1%) and remaining 2/28 PCR positive samples were histologically not evaluable. Mild to moderate loss of gill epithelium was also observed in 4 out of 28 PCR positive samples (14,3%) (Table 3.5).

In gills, PCR negative samples were 330 and 178/330 showed hemocytes infiltration (53,9%); 122/330 samples were histologically negative (37%) and 30/330 samples were histologically not evaluable. The differences in hemocytes infiltration between PCR positive and PCR negative samples were statistically significant (Fisher's Exact test $P< 0.05$).

In mantle, *V. aestuarianus* PCR positive samples were 28/358 (7,8%); 28/28 samples (100%) showed mild to severe hemocytes infiltration: 3/28 had mild hemocytes infiltration (10,7%), 22/28 were moderately (78,6%) and 3/28 were severely infiltrated (10,7%), respectively.

Moreover, 12/28 (42,9%) PCR positive samples were characterized by infiltration of hemolymphatic vessels (Table 3.6).

Hemocytes infiltration was observed also in 157/330 PCR negative samples (47,6%), whereas 154 out of 330 samples were negative (46,7%) and 19/330 samples were histologically not evaluable.

Hemocytes infiltration was more frequently observed in *V. aestuarianus* PCR positive samples compared to PCR negative samples (X^2= 23.448 P<0.05), while a mild infiltration was most frequently recorded in negative samples (80,3%).

PCR failed to identify *V. splendidus* in all the gills and mantle pools examined.

Table 3.5 San Teodoro lagoon: *V. aestuarianus* and *V. splendidus* PCR and hemocytes infiltration in oysters gills.

	N° analyzed samples	PCR positive samples	Gills positive samples			
			Histology*			Loss of gills ephitelium
			Mild	Moderate	Severe	
**V. aestuarianus*	358	28	16	7	1	4
V. splendidus		-	-	-	-	-

*Two *V. aestuarianus* PCR positive samples were histologically negative and 2 samples were histologically not evaluable;

Table 3.6 San Teodoro lagoon: *V. aestuarianus* and *V. splendidus* PCR and hemocytes infiltration in oysters mantle.

	N° analyzed samples	PCR positive samples	Mantle positive samples			
			Histology*			Mantle vessels infiltration
			Mild	Moderate	Severe	
V. aestuarianus	358	28	3	22	3	12
V. splendidus		-	-	-	-	-

3.3.4.2 Tortolì lagoon

Hepatopancreas results: a total of 53/59 hepatopancreas tissue samples were analyzed. Eight samples out of 53 (15,1%) were *V. aestuarianus* PCR positive. *V. aestuarianus* PCR positive samples showed hemocytes infiltration in 6/8 samples (75%): 5 with mild infiltrate (62,5%) and one with severe infiltrate (12,5%). Two remaining samples had no hemocytes infiltration (25%) (Table 3.7). PCR negative samples were 45/53 (84,9%), of which 38 samples showed hemocytes infiltration.

No statistically significant differences were observed comparing the hemocytes infiltration in PCR positive and negative samples (X^2=1.0721 P=0.585).

Twenty five out of 53 samples were PCR positive to *V. splendidus* (47,2%). Histologically, 21/25 *V. splendidus* PCR positive samples showed hemocytes infiltration, 17 with mild (68%), 2 with moderate (8%) and 2 samples with severe infiltration (8%) (Table 3.7). Four PCR positive samples were histologically negative (16%).

V. splendidus PCR negative samples were 27/53 samples (50,9%), and hemocytes infiltration was observed in 23/27 samples (85,2%). One sample was histologically not evaluable.

No statistically significant differences were observed comparing the hemocytes infiltration in PCR positive and negative samples (X^2=0.7778 P=0.678).

Table 3.7 Tortolì lagoon: *V. aestuarianus* and *V. splendidus* PCR and hemocytes infiltration in oysters hepatopancreas.

	Analyzed samples	N° positive samples			
		PCR	Histology*^		
			Mild	Moderate	Severe
**V. aestuarianus*	53	8	5	-	1
^*V. splendidus*	53	25	17	2	2

*Two *V. aestuarianus* PCR positive samples were histologically negative.
^Four *V. splendidus* PCR positive samples were histologically negative.

Gills and mantle results: 59 samples were analyzed and *V. aestuarianus* PCR positive gills samples were 4 out of 59 (6,8%) and 3/4 PCR positive samples (75%) showed both severe hemocytes infiltration and severe loss of epithelium (Table 3.8). Remaining 1/4 sample was histologically not evaluable (25%). PCR negative samples were 55/59 (93%) and 29/55 showed hemocytes infiltration (52,7%).

The hemocytes infiltration was more frequently observed in negative PCR samples compared to *V. aestuarianus* positive ones; moreover, positive samples were more commonly associated with a severe degree of infiltrate, while most of negative one's (79.3%) showed a mild infiltrate (X^2=32.0000 P=0.000).

Four out 59 mantle samples were *V. aestuarianus* PCR positive: all positive samples showed a severe hemocytes infiltration (100%), 2 of these samples (50%) showed also hemocytes infiltration in hemolymphatic vessels (Table 3.9). *V. aestuarianus* PCR negative samples were 55 and 25/55 PCR negative samples showed hemocytes infiltration (45,5%). Interestingly, as previously described in gills, the hemocytes infiltration was more frequently observed in negative PCR samples compared to *V. aestuarianus* positive, but positive samples were more commonly associated with a severe hemocytes infiltration (100% of cases), while negative one's (76%) showed a mild infiltrate (X^2=17.7867 P=0.000).

In gills and in mantle tissues, 1/59 sample was *V. splendidus* PCR positive (1,7%): remarkably, this case was also *V. aestuarianus* PCR positive, and histologically was characterized by a severe hemocytes infiltration, gills loss of epithelium and hemocytes infiltration in mantle vessels (Table 3.8 and Table 3.9).

Table 3.8 Tortolì lagoon: *V. aestuarianus* and *V. splendidus* PCR and hemocytes infiltration in oysters gills.

	N° analyzed samples	PCR positive samples	Gills positive samples			
			Histology*^			Loss of gills epithelium
			Mild	Moderate	Severe	
**V. aestuarianus*	59	4	-	-	3	3
V. splendidus		1^	-	-	1	1

*One *V. aestuarianus* PCR positive sample was histologically not evaluable;
^ One *V. aestuarianus*-*V. splendidus* co-infection.

Table 3.9 Tortolì lagoon: *V. aestuarianus* and *V. splendidus* PCR and hemocytes infiltration in oysters mantle.

	N° analyzed samples	PCR positive samples	Mantle positive samples			
			Histology^			Mantle vessels infiltration
			Mild	Moderate	Severe	
V. aestuarianus	59	4	-	-	4	2
V. splendidus		1^			1	1

^One *V. aestuarianus*-*V. splendidus* co-infection.

3.3.4.3 Marceddì lagoon

Hepatopancreas results: 10/10 samples were *V. aestuarianus* negative, while *V. splendidus* was detected in 7/10 samples (70%).

Four out of 7 *V. splendidus* PCR positive samples showed mild hemocytes infiltration (57,1%) and 3/7 PCR positive samples had no hemocytes infiltration (42,9%) (Table 3.10).

Remaining 3/10 samples were PCR negative (30%) and, histologically, only one sample showed immune cells infiltrate, whereas the others were negative.

No statistically significant differences were observed comparing the hemocytes infiltration in PCR positive and negative samples (Fisher's exact=0.200).

Table 3.10 Marceddì lagoon: *V. aestuarianus* and *V. splendidus* PCR and hemocytes infiltration in oysters hepatopancreas.

	Analyzed samples	N° positive samples			
		PCR	Histology^		
			Mild	Moderate	Severe
V. aestuarianus	10	-	-	-	-
^*V. splendidus*	10	7	4	-	-

^Three *V. splendidus* PCR positive samples were histologically negative.

Gills and mantle results: 1/10 sample was *V. aestuarianus* PCR positive (10%) and 9/10 samples were *V. splendidus* PCR positive (90%). In gills tissue, *V. aestuarianus* PCR positive sample showed mild hemocytes infiltration (Table 3.11). Remaining 9/10 samples were PCR negative (90%) and characterized by hemocytes infiltration.

In mantle tissue, the single PCR positive sample displayed mild hemocytes infiltration (Table 3.12), that was also observed in 3 out of 9 PCR negative samples (33,3%). As expected, no statistical difference was noticed (Fisher's exact=1.000).

Gills tissue positive samples for *V. splendidus* were 9/10 (90%) and characterized by mild hemocytes infiltration in 7/9 samples (77,8%) and by moderate infiltration in 1/9 positive samples (11,1%) (Table 3.11). One PCR positive sample was histologically negative.

In mantle tissue, mild hemocytes infiltration was observed in 4/9 PCR positive samples (44,4%), 2/9 samples had moderate infiltration (22,2%) while 3/9 PCR positive samples (33,3%) didn’t show any hemocytes infiltration (Table 3.12). One sample showed co-infection *V. aestuarianus*-*V. splendidus* by PCR analysis, but no histological abnormalities were observed.

Table 3.11 Marceddì lagoon: *V. aestuarianus* and *V. splendidus* PCR and hemocytes infiltration in oysters gills.

	N° analyzed samples	PCR positive samples	Gills positive samples			
			Histology*^			Loss of gills ephitelium
			Mild	Moderate	Severe	
V. aestuarianus	10	1^	1	-	-	-
**V. splendidus*		9	7	1	-	-

*One *V. splendidus* PCR positive sample was histologically negative;
^One *V. aestuarianus*-*V. splendidus* co-infection.

Table 3.12 Marceddì lagoon: *V. aestuarianus* and *V. splendidus* PCR and hemocytes infiltration in oysters mantle.

	N° analyzed samples	PCR positive samples	Mantle positive samples			
			Histology*^			Mantle vessels infiltration
			Mild	Moderate	Severe	
V. aestuarianus	10	1^	1	-	-	-
**V. splendidus*		9	4	2	-	-

*Three *V. splendidus* PCR positive samples were histologically negative;
^ One *V. aestuarianus*-*V. splendidus* co-infection.

3.3.4.4 Calich lagoon

Hepatopancreas results: 13 oysters were analyzed. *V. aestuarianus* was not detected by PCR, while *V. splendidus* was detected in 8/13 samples (61,5%).

Six out of 8 *V. splendidus* PCR positive samples showed mild hemocytes infiltration (75%) and 2/8 samples had moderate hemocytes infiltration (25%) (Table 3.13). PCR negative samples were 5/13 (38,5%) and showed hemocytes infiltration. No statistical difference was noticed (Fisher's exact=1.000).

Table 3.13 Calich lagoon: *V. aestuarianus* and *V. splendidus* PCR and hemocytes infiltration in oysters hepatopancreas.

	Analyzed samples	N° positive samples			
		PCR	Histology		
			Mild	Moderate	Severe
V. aestuarianus	13	-	-	-	-
V. splendidus	13	8	6	2	-

Gills and mantle results: 13 samples were *V. aestuarianus* and *V. splendidus* PCR negative (Table 3.14 and Table 3.15). Nevertheless, in gills tissue 8/13 samples showed mild hemocytes infiltration (61,5%), and 4/13 samples had moderate hemocytes infiltration (30,8%); one sample didn't show infiltration. Instead, in mantle tissue 10/13 samples had mild hemocytes infiltration (76,9%) and 3/13 moderate hemocytes infiltration (23,1%).

Table 3.14 Calich lagoon: *V. aestuarianus* and *V. splendidus* PCR and hemocytes infiltration in oysters gills.

	N° analyzed samples	PCR positive samples	Gills positive samples			
			Histology			Loss of gills ephitelium
			Mild	Moderate	Severe	
V. aestuarianus	13	-	-	-	-	-
V. splendidus		-	-	-	-	-

Table 3.15 Calich lagoon: *V. aestuarianus* and *V. splendidus* PCR and hemocytes infiltration in oysters mantle.

	N° analyzed samples	PCR positive samples	Mantle positive samples			
			Histology			Mantle vessels infiltration
			Mild	Moderate	Severe	
V. aestuarianus	13	-	-	-	-	-
V. splendidus		-	-	-	-	-

3.3.5 Digestive gland atrophy

Image analysis was used to estimate the atrophy of digestive tubules in 10 *V. aestuarianus* PCR positive and 10 *V. aestuarianus* PCR negative samples. As shown in Table 3.17, PCR positive samples have a higher area% of digestive tubules (mean and SD: 2.67 ±1.53) compared to negative ones (Table 3.16) (mean and SD: 2.65±0.766) (Fig. 3.15). Furthermore, the difference was not statistically significative (Student's *t*-test P=0.9).

Table 3.16 Evaluation of the lumen of digestive tubules in terms of % area in *V. aestuarianus* PCR negative samples (mean ± SD).

Sample	%Area	Standard deviation
B1 APR 17	2.4219	0.4180376
B1 GIU 17	2.6027	0.5680769
B2 GIU 17	2.9986	0.9613602
I4 MARZO	1.6646	0.350737
R1 APR 17	2.3308	0.390482
R1 MARZO	3.0971	0.9581212
R2 APR 17	3.1196	0.7004826
R2 MARZO	2.6173	0.5062518
R4 MARZO	3.1586	0.7436114
R6 MARZO	2.5327	0.6201413
Total	2.65439	0.7662136

Table 3.17 Evaluation of the lumen of digestive tubules in terms of % area in *V. aestuarianus* PCR positive samples (mean ± SD).

Sample	%Area	Standard deviation
(A2)4 GIU-18	1.2075	0.7357158
(A2)5 GIU-18	1.294	0.5319074
(B2)2 GIU-18	1.794571	0.7010487
(B2)4 GIU-18	1.3755	0.6442434
G1 MARZO	3.1967	0.5477933
G1 VERDE	3.0624	1.009686
G2 MARZO	2.3805	0.635564
G2 VERDE	4.1946	1.230794
G6 VERDE	2.5223	1.124745
R1F-17	5.2891	1.075243
Total	2.671813	1,530453

Fig. 3.15 Digestive tubules of *V. aestuarianus* PCR positive (A) and negative samples (Bar = 50 µm).

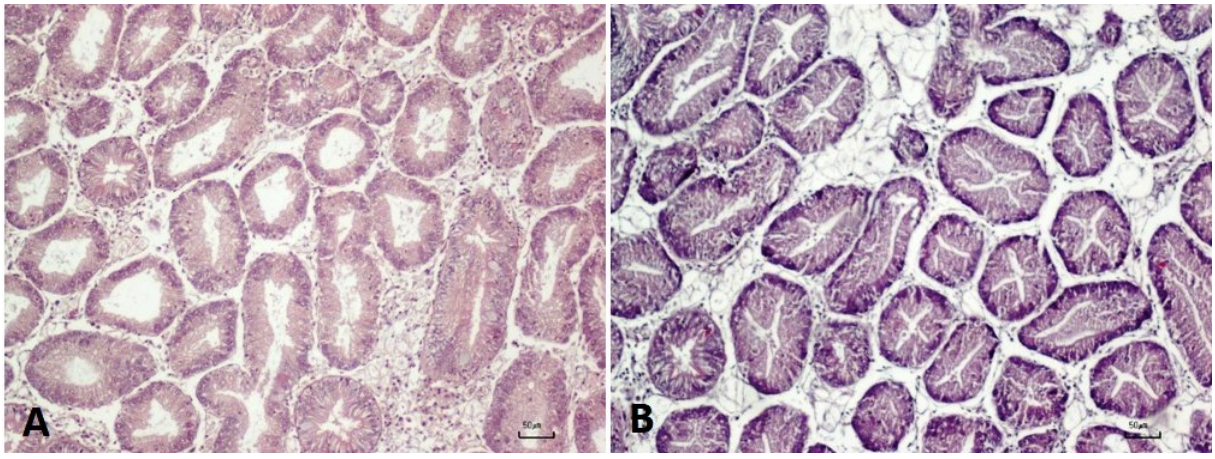

3.4 Discussion

In this study, the presence of *V. aestuarianus* and *V. splendidus* in hepatopancreas, gills and mantle tissues of *C. gigas* samples collected from four Sardinian lagoons was investigated.

In addition, histological analysis on *V. aestuarianus* and *V. splendidus* infected oysters were carried out in order to evaluate the relationship between hemocytes infiltration, glandular atrophy and presence of pathogens.

The hepatopancreas has a detoxifying role and it is the primary organ responsible for absorption and storage of ingested materials in molluscs. Therefore, it incorporates many elements from water as food particles, chemical substances and pathogens (Gold-Bouchot *et al*., 2007; Anacleto *et al*., 2014). Many genes coding for recognition receptors expressed in the hepatopancreas suggesting the role of the digestive system as the first line of defense. Hemocytes in hepatopancreas promote capture, neutralization and endocytosis of pathogens (Allam *et al*., 2015; De Vico and Carella, 2016). Furthermore, antimicrobial substances are involved in defensive responses, such as members of the lysozyme family which play a dual role in immunity and digestion causing the degradation of food particles and providing immune protection from microbial agents (Allam *et al*., 2015).

However, to date, few studies on host-associated microbial communities ("microbiota") have been carried out to identify bacterial populations in the digestive gland of *C. gigas*. The most commonly identified bacteria in digestive gland of oysters belong to *Vibrio* genus and it has been observed that *Vibrio* spp. might play a contrasting role in health and disease of different bivalve species (Hernandez-Zarate and Olmos-Soto, 2006; Fajardo *et al*., 2014; Vezzulli *et al*., 2018).

In our study, 434 isolated strains were subjected to molecular analyses and 79/434 (18,2%) of *V. aestuarianus* and 206/434 (47,5%) of *V. splendidus* strains were identified.

Histologically, 73,4% PCR positive samples of *V. aestuarianus* showed hemocytes infiltration mostly with a mild degree of severity. Negative PCR samples also showed hemocytes infiltration (76,3%).

Hemocytes infiltration was also observed in 77,2% *V. splendidus* PCR positive samples, mostly associated with mild hemocytic infiltration and in 74,6% PCR negative samples.

These findings clearly demonstrate that the proliferation of immune cells in the digestive gland of the oysters is not related to the presence of *Vibrio* spp. Hemocytes infiltration in the digestive gland could be interpreted as an independent factor from *V. aestuarianus* and *V. splendidus* and from their pathogenicity. These data agree with what previously reported by several authors, considering that the increase number of immune cells in the hepatopancreas could be considered a constant, because of the functions of this organ and its continuous interaction with pathogenic and not-pathogenic agents (Gold-Bouchot *et al*., 2007; Anacleto *et al*., 2014).

Based on these findings we postulate that the digestive gland does not represent the ideal target organ to investigate the specific role of a given pathogen during mortality episodes.

Gills/mantle tissues pools were also analyzed to detect *V. aestuarianus* and *V. splendidus* by PCR. These organs were considered target tissues to detected pathogens in oysters (Aboubaker *et al*., 2013; Burioli *et al*., 2017; Travers *et al*., 2017).

As previously reported by Burioli *et al*. (2017) and Parizadeh *et al*. (2018) we associated histopathological investigation to molecular detection of pathogens, in order to observe tissue lesions in positive samples and to better understand the pathogenesis of the bacteria infection.

In our report, *V. aestuarianus* was detected in 7,5% and *V. splendidus* in 2,3% of gills/mantle tissue samples by PCR analysis.

In gills, histology showed hemocytes infiltration in 85% *V. aestuarianus* PCR positive samples, mostly with mild degree of severity. A statistically significant difference was

observed when comparing hemocytes infiltration in PCR positive with PCR negative samples in gills.

In mantle hemocytes infiltration was mainly moderate (66,7%) to severe degree (21,2%), in *V. aestuarianus* PCR positive samples.

In particular, histological damages associated with *V. aestuarianus* detection were observed in San Teodoro and Tortolì lagoons. *V. aestuarianus* PCR positive samples had mainly moderate hemocytes infiltrate in San Teodoro lagoon and all positive samples had severe hemocytes infiltrate in Tortolì lagoon, in mantle tissue. It was also observed the presence of samples with hemocytes infiltration in mantle hemolymphatic vessels. PCR positive samples were commonly associated with an increase of hemocytes infiltration in the mantle. In particular, in San Teodoro and Tortolì lagoons positive samples were associated with a moderate and severe intensity of immune cells infiltration, respectively. Hemocytes infiltration was localized in sub-epithelial connective tissue of the mantle with multifocal to diffuse distribution, both around and within hemolymphatic vessels.

Interestingly, in San Teodoro hemocytes infiltration was detected in 100% of mantle *V. aestuarianus* PCR positive samples, mostly showing moderate to severe hemocytes infiltration. Conversely, *V. aestuarianus* PCR negative samples, were mostly associated to mild hemocytes infiltration.

In addition, in positive samples the highest bacterial loads were found in samples associated with mantle moderate to severe hemocytes infiltration.

Few data are reported in the literature about *V. aestuarianus*-oysters interaction in field, and most known data derives from experimental challenges. To the best of our knowledge our study is one of the few reports about molecular and histopathological investigation of farmed oysters.

Experimental challenges performed by several authors investigated the oysters-*V. aestuarianus* interactions and infection route. They suggested that *V. aestuarianus* infection

activity starts from hemolymph with inhibition of hemocytes functions (Labreuche *et al*., 2006a; Labreuche *et al*., 2006b). More recently, Parizadeh *et al*. (2018) hypothesized *V. aestuarianus* infection route, firstly with early hemolymph colonization by virulent strain, followed by bacterial multiplication in hemolymph, hemocytic recruitment and finally invasion of other connective tissues (Parizadeh *et al*., 2018).

Regarding histological analysis of *V. splendidus* PCR positive samples, it showed mainly mild intensity of hemocytes infiltration both in gills and mantle tissues. High bacterial load was detected in positive samples, but histologically no lesions were detected. Most positive samples were detected in Marceddì lagoon (90%), but no statistically significant data were obtained because of inadequate number of samples. Molecular and histopathological results of *V. splendidus* detection confirmed the hypothesis of multifactorial nature of infection and confirmed also the unclear role of pathogenicity/opportunism of strains belonging to *V. splendidus* clade (Gay *et al*., 2004a; Barbosa Solomieu *et al*., 2015).

An increase of oyster mortality outbreaks associated with *V. aestuarianus* has been recorded since 2012, causing great losses in oyster farms (Garcia *et al*., 2014; Barbosa Solomieu *et al*., 2015; Parizadeh *et al*., 2018), but in Italy only few reports on *Vibrios* detection in oysters have been performed (Domeneghetti *et al*., 2014; Burioli *et al*., 2017).

As reported in literature, water persistence and pathogenesis of *V. aestuarianus* and *V. splendidus* were strongly influenced by environmental factors, like temperature and salinity (Vezzulli *et al*., 2015; Barbosa Solomieu *et al*., 2015) and physiological factors (De Decker and Saulnier, 2011).

In this work we observed a mortality outbreak from December 2016 to March 2017 recorded in San Teodoro lagoon: it caused the loss of more than 80% of farmed oysters. In these months were also recorded the lowest water temperatures of the year (13-16°C) and water salinity suffered a drastic decrease (from 40 to 10‰) due to heavy rains. Most *V. aestuarianus* positive oysters (70%) were collected during this mortality episode. This

fundamental additional information demonstrates the importance of several factors interaction (pathogen bacteria and environmental factors), as previously reported by Barbosa Solomieu *et al*. (2015), Burioli *et al.* (2017) and Parizadeh *et al*. (2018).

Atrophy of digestive gland's diverticula in *V. aestuarianus* infected oysters was evaluated.

Image analysis method was already used to measure atrophy or cellular lesions in the glandular epithelium of mollusc species associated with pathogens or contaminants (Usheva *et al*., 2006; Cajara Ville *et al*., 1990; Cajara Ville *et al*., 1992; Lowe 1988; Marigomez *et al.*, 1990; Carella *et al*., 2015; Parizadeh *et al*., 2018).

The digestive epithelium is normally subjected to morphological changes during digestive cycle, it follows absorption, holding and disintegration phases (Owen, 1996). However, pathological destructive changes of morphology of digestive gland can occur, due to environmental factors. Several authors described these pathological changes on connective tissue and digestive tubules of digestive gland associated to water pollution and environmental stress (Cajara Ville *et al*. 1990; Cajara Ville *et al*. 1992; Usheva *et al*. 2006; Marigomez *et al*., 1990).

Carella *et al*. (2015) observed an increase of atrophic tubules in *Mytilus galloprovincialis* exposed to dinoflagellate *Ostreopsis* cf. *ovata* by using image analysis. We used the same method to estimate the atrophy of digestive tubules in *V. aestuarianus* infected samples (Carella *et al*., 2015; Parizadeh *et al*., 2018). Comparative analysis between positive and negative samples was carried out: PCR positive samples and negative one's had a similar area% of digestive tubules and difference was not statistically significative (Student's *t*-test P=0.9).

Our results are in contrast with data previously reported in which bacterial exposure was associated to epithelial atrophy of digestive diverticula with dilation of the lumen (Parizadeh *et al*., 2018).

3.5 References

- Aboubaker M. H., Sabrie´ J., Huet M., Koken M. (2013) Establishment of stable GFP-tagged *Vibrio aestuarianus* strains for the analysis of bacterial infection-dynamics in the Pacific oyster, *Crassostrea gigas*. Veterinary Microbiology 164, 392–398.
- Allam B. and Raftos D. (2015) Immune responses to infectious diseases in bivalves. Journal of Invertebrate Pathology 131, 121–136.
- Anacleto P., Maulvault A. L., Nunes M. L., Carvalho M. L., Rosa R., Marques A. (2014) Effects of depuration on metal levels and health status of bivalve molluscs. Food Control 47, 493-501.
- Barbosa Solomieu V., Renault T., Travers M.A. (2015) Mass mortality in bivalves and the intricate case of the Pacific oyster, *Crassostrea gigas*. Journal of Invertebrate Pathology 131, 2–10.
- Baumann P., Baumann L., Bang S.S., Woolkalis M.J. (1980) Reevaluation of the taxonomy of *Vibrio, Beneckea*, and *Photobacterium*: abolition of the genus *Beneckea*. Current Microbiology 4, 127–132.
- Beaz-Hidalgo R., Balboa S., Romalde J.L., Figueras M.J. (2010) Diversity and pathogenicity of *Vibrio* species in cultured bivalve molluscs. Environmental Microbiology Reports 2, 34–43.
- Burge C.A., Griffin F.J. and Friedman C.S. (2006) Mortality and herpesvirus infections of the Pacific oyster *Crassostrea gigas* in Tomales Bay, California, USA. Diseases of Aquatic Organisms 72, 31-43.
- Burioli E. A. V., Varello K., Trancart S., Bozzetta E., Gorla A., Prearo M., Houssin M. (2017) First description of a mortality event in adult Pacific oysters in Italy associated with infection by a *Tenacibaculum soleae* strain. Journal of Fish Diseases 00, 1–7.

- Cajaraville M.P., Díez G., Marigómez J.A. and Angulo E. (1990) Responses of basophilic cells of the digestive gland of mussels to petroleum hydrocarbon exposure. Diseases of Aquatic Organisms 9, 221–228.
- Cajaraville M.P., Marigómez I., Díez G., and Angulo E. (1992) Comparative effects of the water accommodated fractions (WAF) of three oils on mussels. 2. Quantitative alterations in the structure of the digestive tubules. Comparative Biochemistry Physiology 102, 113–123.
- Carella F., Sardo A., Mangoni O., Di Cioccio D., Urciuolo G., De Vico G., Zingone A. (2015) Quantitative histopathology of the Mediterranean mussel (*Mytilus galloprovincialis* L.) exposed to the harmful dinoflagellate *Ostreopsis* cf. *ovata*. Journal of Invertebrate Pathology 127, 130–140.
- De Decker S., Saulnier D. (2011) Vibriosis induced by experimental cohabitation in *Crassostrea gigas*: evidence of early infection and down-expression of immunerelated genes. Fish and Shellfish Immunology 30, 691–699.
- De Vico G. and Carella F. (2016) Elementi di patologia comparata dei molluschi. Ed. Loffredo.
- Domeneghetti S., Varotto L., Civettini M., Rosani U., Stauder M., Pretto T., Pezzati E., Arcangeli G., Turolla E., Pallavicini A. and Venier P. (2014) Mortality occurrence and pathogen detection in *Crassostrea gigas* and *Mytilus galloprovincialis* close-growing in shallow waters (Goro lagoon, Italy). Fish & Shellfish Immunology.
- EFSA (2015) Oyster mortality - EFSA Panel on Animal Health and Welfare (AHAW).
- Elston R. and Leibovitz L. (1980) Pathogenesis of experimental vibriosis in larval American oysters, *Crassostrea virginica*. Canadian Journal of Fisheries and Aquatic Sciences 37, 964–978.

- Fajardo P., Atanassova M., Garrido-Maestu A., Wortner-Smith T., Cotterill J., Cabado A.G. (2014) Bacteria isolated from shellfish digestive gland with antipathogenic activity as candidates to increase the efficiency of shellfish depuration process. Food Control 46, 272-281.
- Fenza A., Olla G., Salati F., Viale I. (2014) Stagni e lagune produttive della Sardegna. Tradizioni, sapori e ambiente. Agenzia Regionale LAORE Sardegna.
- Garcia C., Arzul I., Chollet B., Robert M., Omnes E., Ferrand S., Faury N., Tourbiez D., Haffner P., Miossec L., Joly J.P., Francois C. (2014) *Vibrio aestuarianus* and Pacific Oysters *Crassostrea gigas* mortality in France: a new chapter in their relation. Proceedings of the National Shellfish Association, Jacksonville, Florida, USA.
- Garnier M., Labreuche Y., Garcia C., Robert A. and Nicolas J.L. (2007) Evidence for the involvement of pathogenic bacteria in summer mortalities of the Pacific oyster *Crassostrea gigas*. Microbial Ecology 53, 187-196.
- Garnier, M., Labreuche, Y., and Nicolas, J.L. (2008) Molecular and phenotypic characterization of *Vibrio aestuarianus* subsp. *francensis* subsp. nov., a pathogen of the oyster *Crassostrea gigas*. Systematic and Applied Microbiology 31, 358–365.
- Gay M., Berthe F.C., and Le Roux F. (2004b) Screening of *Vibrio* isolates to develop an experimental infection model in the Pacific oyster *Crassostrea gigas*. Diseases of Aquatic Organisms 59, 49–56.
- Gay M., Renault T., Pons A.M., and Le Roux F. (2004a) Two *Vibrio splendidus* related strains collaborate to kill *Crassostrea gigas*: taxonomy and host alterations. Diseases of Aquatic Organisms 62, 65–74.
- Gold-Bouchot G., Zapata-Pérez O., Ceja-Moreno V., Rodríguez-Fuentes G., Simá-Alvarez R., Aguirre-Macedo M. L. and Vidal-Martínez V. M. (2007) Biological effects of environmental pollutants in American Oyster, *Crassostrea virginica*: A field

study in Laguna de Terminos, Mexico. International Journal of Environment and Health 1(2).

- Gomez-Leon J., Villamil L., Lemos M.L., Novoa B., and Figueras A. (2005) Isolation of *Vibrio alginolyticus* and *Vibrio splendidus* from Aquacultured Carpet Shell Clam (*Ruditapes decussatus*) Larvae Associated with Mass Mortalities. Applied and environmental microbiology 71(1), 98–104.
- Hernandez-Zarate G. and Olmos-Soto J. (2006) Identification of bacterial diversity in the oyster *Crassostrea gigas* by fluorescent in situ hybridization and polymerase chain reaction. Journal of Applied Microbiology 100, 664–672.
- Jeffries V.E. (1982) Three *Vibrio* strains pathogenic to larvae of *Crassostrea gigas* and *Ostrea edulis*. Aquaculture 29, 201–226.
- Labreuche Y., Lambert C., Soudant P., Boulo V., Huvet A., Nicolas J.-L. (2006b) Cellular and molecular hemocyte responses of the Pacific oyster, *Crassostrea gigas*, following bacterial infection with *Vibrio aestuarianus* strain 01/32. Microbes and Infections 8, 2715–2724.
- Labreuche Y., Soudant P., Goncalves M., Lambert C., Nicolas J.L. (2006a) Effects of extracellular products from the pathogenic *Vibrio aestuarianus* strain 01/32 on lethality and cellular immune responses of the oyster *Crassostrea gigas*. Developmental and Comparative Immunology 30, 367–379.
- Lacoste A., Jalabert F., Malham S., Cueff A., Gélébart F., Cordevant C., Lange M., Poulet S.A. (2001) A *Vibrio splendidus* strain is associated with summer mortality of juvenile oysters *Crassostrea gigas* in the Bay of Morlaix (North Brittany, France). Diseases of Aquatic Organisms 46, 139–145.
- Le Roux F., Gay M., Lambert C., Nicolas J.L., Gouy M., Berthe F. (2004) Phylogenetic study and identification of *Vibrio splendidus*-related strains based on *gyrB* gene sequences. Diseases of aquatic organisms 58, 143-150.

- Le Roux F., Gay M., Lambert C., Waechter M., Poubalanne S., Chollet B., Nicolas J. L., Berthe F. (2002) Comparative analysis of *Vibrio splendidus*-related strains isolated during *Crassostrea gigas* mortality events. Aquatic Living Resources 15**,** 251–258.
- Lowe D.M. (1988) Alterations in cellular structure of *Mytilus edulis* resulting from exposure to environmental contaminants under field and experimental conditions. Marine Ecology Progress Series 46, 91–100.
- Marigomez J. A., Saez V., Cajaraville M. P., Angulo E. (1990) A planimetric study of the mean epithelial thickness (MET) of the molluscan digestive gland over the tidal cycle and under environmental stress conditions. Helgolander Meeresunters. 44, 81-94.
- Martenot C., Oden E., Travaillé E., Malas J-P. and Houssin M. (2011) Detection of different variants of Ostreid Herpesvirus 1 in the Pacific oyster, *Crassostrea gigas* between 2008 and 2010. Virus Research, 160, 25-31.
- Mazzi V. (1977) Tecniche Istologiche e Istochimiche. Piccin Editore.
- Owen G. (1996) Feeding. In: Wilburn K.M., Yonge C.M. (Eds.), Physiology of Mollusca. Academic Press, New York. 2, 1–5.
- Paillard C., Le Roux F., Borrego J.J., 2004. Bacterial disease in marine bivalves, a review of recent studies: trends and evolution. Aquatic Living Resources 17, 477–498.
- Parizadeh L., Tourbiez D., Garcia C., Haffner P., Dégremont L., Le Roux F. and Travers M.A. (2018) Ecologically realistic model of infection for exploring the host damage caused by *Vibrio aestuarianus*. Environmental Microbiology (2018) 00(00), 1–9.
- Saulnier D., De Decker S. and Haffner P. (2009) Real-time PCR assay for rapid detection and quantification of *Vibrio aestuarianus* in oyster and seawater: A useful tool for epidemiologic studies. Journal of Microbiological Methods 77, 191-197.

- Saulnier D., De Decker S., Tourbiez D., Travers M.A. (2017) Development of a duplex Taqman real-time PCR assay for rapid identification of *Vibrio splendidus*-related and *V. aestuarianus* strains from bacterial cultures. Journal of Microbiological Methods 140, 67–69.
- Sugumar G., Nakai T., Hirata Y., Matsubara D., Muroga K. (1998) *Vibrio splendidus* biovar II as the causative agent of bacillary necrosis of Japanese oyster *Crassostrea gigas* larvae. Diseases of Aquatic Organisms 33, 111-118.
- Takahashi H., Hara-Kudo Y., Miyasaka J., Kumagai S., Konuma H. (2005) Development of a quantitative real-time polymerase chain reaction targeted to the toxR for detection of *Vibrio vulnificus*. Journal of Microbiological Methods 61, 77–85.
- Tison David L. and Seidler Ramon J. (1983) *Vibrio aestuarianus*: a new species from estuarine and waters and shellfish. International Journal of Systematic Bacteriology 33(4), 699-702.
- Travers M.A., Boettcher Miller K., Roque A., Friedman C.S. (2015) Bacterial diseases in marine bivalves. Journal of Invertebrate Pathology 131, 11–31.
- Travers M.A., Tourbiez D., Parizadeh L., Haffner P., Kozic-Djellouli A., Aboubaker M., Koken M., Dégremont L. and Lupo C. (2017) Several strains, one disease: experimental investigation of *Vibrio aestuarianus* infection parameters in the Pacific oyster, *Crassostrea gigas*. Veterinary Research 48,32.
- Usheva L. N., Vaschenko M. A. and Durkina V. B. (2006) Histopathology of the Digestive Gland of the Bivalve Mollusk *Crenomytilus grayanus* (Dunker, 1853) from Southwestern Peter the Great Bay, Sea of Japan. Russian Journal of Marine Biology 32(3), 166–172.

- Vezzulli L., Pezzati E., Stauder M., Stagnaro L., Venier P. and Pruzzo C. (2015) Aquatic ecology of the oyster pathogens *Vibrio splendidus* and *Vibrio aestuarianus.* Environmental Microbiology 17(4), 1065–1080.
- Vezzulli L., Stagnaro L., Grande C., Tassistro G., Canesi L., Pruzzo C. (2018) Comparative 16SrDNA Gene-Based Microbiota Profiles of the Pacific Oyster (*Crassostrea gigas*) and the Mediterranean Mussel (*Mytilus galloprovincialis*) from a Shellfish Farm (Ligurian Sea, Italy). Microbial Ecology 75(2), 495-504.
- Waechter M., Le Roux F., Nicolas J.L., Marissal E. and Berthe F. (2002) Characterization of *Crassostrea gigas* spat pathogenic bacteria. C.R. Biologies Academie des Sciences 325, 231–238.
- Zhang X.J., Qin G.M., Bing X.W., Yan B.L., Liang L.G. (2011) Molecular and phenotypic characterization of *Vibrio aestuarianus*, a pathogen of the cultured tongue sole, *Cynoglossus semilaevis* Gunther. Journal of Fish Diseases 34,57–64.

Chapter 4

Ostreid herpesvirus-1 and parasites in oysters (*Crassostrea gigas*) from Sardinia

4.1 Introduction of OsHV-1

Ostreid herpesvirus-1 (OsHV-1) has been associated with high mortalities in larvae and juvenile molluscs species and less in adult bivalves, including Pacific oyster (*Crassostrea gigas*) (Le Deuff and Renault, 1999; Friedman *et al.,* 2005).

In the 1990s, a herpes-like virus was observed in Pacific Oysters farms during the mortality episodes and electron microscopy techniques revealed the presence of cellular abnormalities in larvae and spat of oysters (Renault *et al*., 1994). This herpes-like virus was identified as Ostreid herpesvirus-1 (OsHV-1), assigned to the *Herpesviral*es order and to the *Malacoherpesviridae* family (Davison *et al*., 2009).

Constant detection of OsHV-1 and some genomic variant of this virus occurred during most mortality events, showing different rates of pathogenicity (Martenot *et al*., 2011). The virus was isolated from infected larvae and the entire genome of Ostreid herpesvirus-1, length estimated of 207 kbp, was completely sequenced (Genbank AY509253) (Le Deuff and Renault, 1999; Davison *et al*., 2005). In the last years there was an increase of control actions on oyster farms and several variants of OsHV-1 have been identified, showing some mutations in genome sequence compared to reference genome (Martenot *et al*., 2011; Martenot *et al*., 2012).

Significant detection of new variant (OsHV-1 µVar), was reported in France coasts during a severe episodes of oyster mortality (Segarra *et al*., 2010).

Nowadays, traditional histopathological methods and biomolecular techniques are used for the diagnosis of herpesvirus infection. Numerous different PCR methods are available for the detection of OsHV-1, but specific are the primers C2 and C6 which bracket a region of 709 bp (Martenot *et al*., 2016; Lopez-Sanmartin *et al*., 2016; Arzul *et al*., 2002; Moss *et al*., 2007).

Immunohistochemistry (IHC) and *in situ* hybridization (ISH) were also performed to analyze the localisation and distribution of OsHV-1 in affected samples (Bueno *et al*., 2016; Martenot *et al*., 2016).

Furthermore, few authors described the typical histopathological features of a viral infection, such as pyknosis of connective cells, nuclear changes with marginated chromatin and intranuclear inclusion bodies (Renault *et al*., 1994; Renault *et al*., 2000; Burge *et al.,* 2006; Vásquez-Yeomans *et al*., 2010).

Recently Burioli *et al.* described severe hemocytosis in the connective tissue of mantle, gills, and adductor muscle, as well as atrophy of the diverticular epithelium, in oysters affected by OsHV-1; Burioli *et al.,* 2018).

In our work, the occurrence of OsHV-1 infection in oysters collected from 4 Sardinian lagoons was investigated by PCR and histopathology techniques to detect tissue infiltration or cell abnormalities associated with viral infection.

4.2 Materials and methods

4.2.1 Sampling areas

Four hundred and forty samples of cupped oysters, *C. gigas*, were collected from October 2016 to June 2018. Sampling sites (San Teodoro lagoon, Tortolì lagoon, Marceddì lagoon and Calich lagoon) are described in detail in Chapter 2. A total of 358 oysters were collected from San Teodoro lagoon, 59 from Tortolì lagoon, 10 from Marceddì lagoon and 13 samples from Calich lagoon.

4.2.2 PCR

Mantle and gills tissue samples were collected from each specimen and total DNA was extracted using QIAamp DNA mini kit (Qiagen GmbH, Germany), according to manufacturer instructions. Extracted DNA was finally stored at -20°C until molecular analysis. More details are reported in Chapter 2.

DNA obtained from each oyster was analyzed by PCR to detect OsHV-1. It was performed by using C2 and C6 primers (Renault and Arzul, 2001), which amplified a 709 bp fragment (Fig. 4.1).

Fig. 4.1 Ostreid herpesvirus-1 primers (C2-C6).

Primers	Sequence	bp
OsHV-1 (C2)	5' CTCTTTACCATGAAGATACCCACC 3'	709 bp
OsHV-1 (C6)	5' GTGCACGGCTTACCATTTTT 3'	

PCR reaction was carried out using MJ Mini Thermal Cycler (BioRad, Hercules, CA, USA). PCR reaction mix volume of 25 µl contained 1X reaction buffer, 3 mM $MgCl_2$, 2 mM of each dNTP, 2U/µl Taq Polymerase (Life Technologies, US), 0,2 pmol/µl of each primer (MWG-Biotech, Ebersberg, Germany), 1 µl of extracted DNA and distilled water.

Thermal conditions of PCR reaction have been set as follow: 1 cycle of initial denaturation at 94°C for 2 min; denaturation at 94°C for 30 sec, primer annealing at 54°C for 30 sec and elongation at 72°C for 1 min, the last 3 steps were repeated for 35 times; finally, the last step was 1 cycle of final elongation at 72°C for 7 min.

Post amplification analysis was carried out by 2% gel electrophoresis (Sigma-Aldrich, St. Louis, MO, USA) with 10000X SYBR Safe as DNA staining (Invitrogen, Carlsbad, CA, USA), Blue Loading Buffer (Invitrogen) and 100 bp DNA Ladder (Invitrogen). Transilluminator Safe Imager was used to highlight amplified fragments and images were acquired by Photodoc system (Invitrogen).

4.2.3 Histopathology

Each oyster was sectioned and samples of target tissues (hepatopancreas, gills, and mantle) were fixed in 10% neutral buffered formalin. Specimens were dehydrated through alcohol and xylene and then paraffin-embedded, according to standard techniques (Mazzi, 1977). Sections of 3μm thickness were obtained with a microtome and then stained with Haematoxylin and Eosin. Histological examination using light microscopy was performed. Detailed procedures are described in Chapter 2.

4.2.4 Statistical analysis

Histopathological and biomolecular data were analyzed using Stata 11.2 software (StataCorp LP) and they were compared using the Chi-square ($\chi 2$) test. A *P*-value <0,05 was considered significant.

4.3 Results

All samples examined from San Teodoro, Marceddì and Calich lagoons were negative for the presence of OsHV-1 infection. Tortolì lagoon showed 28 out of 59 (47,5%) PCR positive samples to OsHV-1 infection (Fig. 4.2).

Fig. 4.2 Agarose gel electrophoresis: OsHV-1 positive samples (1, 2, 4, 5, E) and negative one's (3, 6, A, B, C, D, F); positive control (C+) and negative control (C-); 100 bp DNA Ladder.

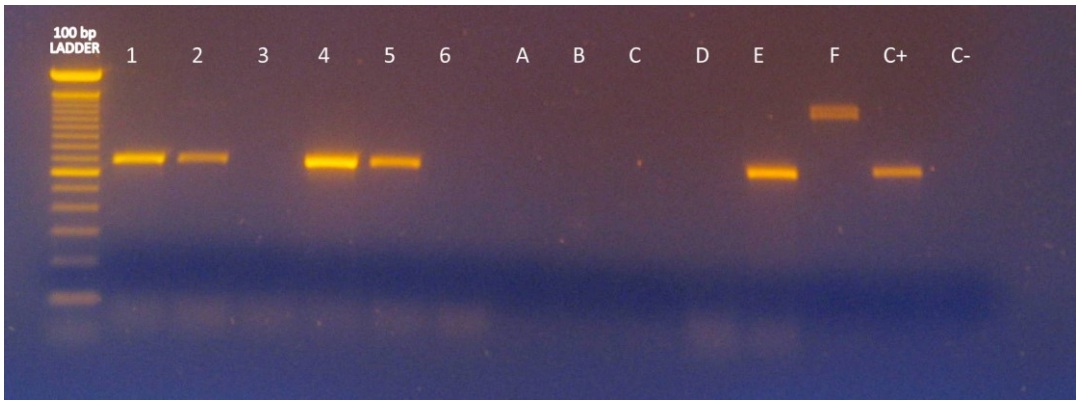

At histopathological examination, 13/28 (46,4%) gill samples showed infiltration of immune cells, 10/28 (35,7%) and 3/28 (10,7%) samples showed mild and moderate hemocytes infiltration, respectively. One sample with moderate hemocytes infiltration also showed multifocal loss of surface epithelium in gills (Table 4.1). Six out of 28 PCR positive samples did not show immune cells (21,4%). Remaining 9 PCR positive samples were histologically not evaluable. PCR negative samples were 31/59 (52,5%), 19/31 (61,3%) of which showed hemocytes infiltration and 10 out of 31 samples (32,3%) were negative. Two gills tissue samples out of 31 were histologically not evaluable.

No differences in terms of hemocytes infiltrate were observed considering negative and positive PCR samples (X^2=2.3489 P=0.309). However, both positive and negative samples were more consistently associated with hemocytes infiltration of mild intensity.

In mantle tissue, 15/28 OsHV-1 PCR positive samples showed an increase of hemocytes infiltration, ranging from mild (n=11, 39,3%), to moderate (n=3, 10,7%) and severe (n=1, 3,6%). Furthermore, samples with severe hemocytes infiltration also showed infiltration within vessels and in the connective tissue around mantle vessels (Table 4.2). Seven out of 28 PCR positive samples did not show hemocytes cells (25%). Remaining 6 PCR positive samples were histologically not evaluable. No differences in terms of infiltrate of immune

cells were observed considering negative and positive PCR samples, and both were more consistently associated with mild hemocytes infiltration (X^2=4.1108 P=0.128). Abnormalities of cells, as well as lesions of mantle connective tissue, were not detected in affected oysters.

Table 4.1 Gills: biomolecular and histopathological results of OsHV-1.

Sampling site	N° analyzed samples	Gills positive samples				
		PCR OsHV-1	Histology			Loss of ephitelium
			Mild	Moderate	Severe	
San Teodoro	358	-	-	-	-	-
Tortolì	59	28	10	3	-	1*
Marceddì	10	-	-	-	-	-
Calich	13	-	-	-	-	-

*One sample showed both moderate infiltrate and loss of epithelium.

Table 4.2 Mantle: biomolecular and histopathological results of OsHV-1.

Sampling site	N° analyzed samples	Mantle positive samples				
		PCR OsHV-1	Histology			Hemocytes infiltration in vessels
			Mild	Moderate	Severe	
San Teodoro	358	-	-	-	-	-
Tortolì	59	28	11	3	1	1*
Marceddì	10	-	-	-	-	-
Calich	13	-	-	-	-	-

*One sample showed both severe infiltrate and hemocytes infiltration in vessels.

4.4 Discussion

In this study, the presence of OsHV-1 in gills and mantle tissues of *C. gigas* samples collected from four Sardinian lagoons was investigated by PCR and histopathology.

Because oyster mortality depends from several factors, such as water temperature and age of oysters, as reported by several authors (Renault *et al*., 2008; Sauvage *et al*., 2009; Renault *et al*., 2014; Barbosa Solomieu *et al.,* 2015; EFSA, 2015), it is not possible to assume the potential role of OsHV-1 straight from a mortality episode.

In this work OsHV-1 infection was observed only in oysters from Tortolì lagoon. OsHV-1 PCR positive samples were 48% and all samples were histologically examined. Mainly mild hemocytes infiltration in gills and in mantle connective tissue was observed in PCR positive samples. Only one sample showed severe hemocytes infiltration involving vessels.

Briefly, from our results clearly appears that no differences in terms of hemocytic infiltrate were observed considering negative and positive PCR OsHV-1 samples in all examined target organs. Samples were more consistently associated with infiltration of hemocytes of mild intensity. Histopathological cells abnormalities and connective tissue lesions were not evident, differently from what have been reported by several authors (Prado-Alvarez *et al*., 2016; Friedman *et al*., 2005; Bueno *et al*., 2016; Martenot *et al*., 2016; Burioli *et al*., 2018).

In addition, there is an important difference that should be considered in oyster OsHV-1 infection when comparing the viral load in oyster tissue to lesions and mortality rates. In our work, we did not quantify viral load in infected oysters, and this issue could be linked with the absence of abnormalities in oyster samples. Another aspect that has to be considered is the ability of the OsHV-1 to persist in host after the primary infection without inducing disease and mortality (Arzul *et al*., 2002; Oden *et al*., 2011; Martenot *et al*., 2011).

OsHV-1 pathogenesis is still unclear: Schikorski *et al.* (2011) hypothesized that virus particles could enter through the digestive gland and the hemolymphatic system and could be

then transported to different target organs. In these organs the viral particles replicate giving start to disease development (Schikorski *et al.*, 2011; Martenot *et al*., 2016).

As reported by Burioli *et al.* (2018), it is not yet clear if the hemocytes proliferation could be a host reaction or a virus managed activity (Burioli *et al.,* 2018).

4.5 Introduction of parasites

Knowledge deepening of parasitic pathologies of bivalve molluscs is the key to the preservation of marine and estuarine environments and to the health management of shellfish farms distributed throughout the world (Calvi Zeidan *et al*., 2012; Robledo *et al*., 2014). Some species of protozoan parasites, such as *Bonamia* sp., *Martelia* spp., *Haplosporidium* and *Perkinsus* genera are a cause of economic losses and mortality in bivalve molluscs and, due to their pathogenicity, some species such as *Perkinsus olseni* are considered reportable diseases in the World Health Organization's list (Smolowitz, 2013).

The immune response against parasites in bivalves is characterized by cellular-mediated mechanisms, with the activation of two major paths, phagocytosis and encapsulation (Hine, 1999; Soudant *et al*., 2013; Lassudrie *et al*., 2015; Wang *et al*., 2018).

Both paths are accomplished by hemocytes that lead to parasite destruction by the release of enzymes and oxygen metabolites (Soudant *et al*., 2013). Hemocytes are mobile, capable of phagocytic activity and able to aggregate to each other (Hine, 1999; Canesi *et al*., 2002, Smolowitz, 2013; Soudant *et al*., 2013).

Phagocytosis is the main mechanism of the cell-mediated immune response in bivalve against the pathogenic microorganisms (Soudant *et al*., 2013). It is performed by granular hemocytes, able to internalize exogenous particles or pathogens and then carry out intracellular degradation (Soudant *et al*., 2013; Lassudrie *et al*., 2015; Wang *et al*., 2018).

Encapsulation is a mechanism activated when larger particles cannot be phagocytized by individual hemocyte (Fisher, 1986; Lassudrie *et al.,* 2015). It is characterized by multiple layers of granular hemocytes that allow the complete isolation of the pathogen from the host tissues by the development of a granuloma-like structure (Smolowitz, 2013; Wang *et al.,* 2018). Encapsulation is followed by extracellular degradation of the parasite.

Host response against Protozoa is widely described in bivalve molluscs and is characterized by a high variability depending on parasite species, infected organ and host capability to put in place defense mechanisms against parasites (Kroech, 2010; Smolowitz, 2013; Lassudrie *et al*., 2015).

Hemocytes are generally found localised in variable numbers in the connective tissue around digestive gland structures, in the mantle and in the gills (Kroech, 2010). Intracellular reproductive stages of protozoan parasites can be present inside hemocytes, as well as in epithelial cells of gills and digestive gland. Even in the presence of parasites and hemocytic infiltrate, damage to the gill epithelium is usually unnoticed, or characterized by mild lamellar hyperplasia (Smolowitz, 2013).

Only heavy protozoan infection elicits a severe inflammatory response that can lead to rupture of gill epithelium, gastric ulcers and erosion of glandular epithelium or the development of granuloma-like structures, such as reported in *Bonamia* sp., *Martelia* spp. and *Perkinsus* spp. infection (Kleeman *et al*., 2002; Kroech, 2010; Smolowitz, 2013; Carrasco *et al*., 2015)

Immune response against metazoan parasites in oysters is mainly characterized by infiltration of hemocytes and encapsulation of parasite or its attempt (Feng and Canzonier, 1970; Lassudrie *et al.,* 2015). The presence of trematodes in the digestive gland was associated with a more severe inflammation than what observed in other organs, characterized by a severe hemocytic infiltration and the partial destruction of connective tissue and nearby structures (Lassudrie *et al*., 2015).

4.6 Results

Histological examination of the samples revealed the presence of parasites in oysters from the four sampling sites. The lagoon of San Teodoro showed a greater variety of parasitic species than the other sites.

Parasites were observed in two anatomical locations, the gills and the digestive gland, whereas they were not detected in the mantle (Fig. 4.3).

The gills showed mainly protozoa probably belonging to the Phylum Haplosporidia or Endomyxa, and fewer metazoa, compatible with copepods. In digestive gland digenean cercariae or metacercariae were frequently observed, whereas protozoan parasites were only occasionally present.

Inflammatory reaction of the gills against protozoa was mostly localised in lamellae, and its degree of severity was mild to moderate. It was characterized by an increase in the number of hemocytes, frequently clustered in small groups in proximity to the parasites. Gills showed mild to moderate increase in number of mucous cells in association to infiltration sites, whereas mild lamellar hyperplasia was seldom observed.

Immune response associated with metazoan parasites in gills was mostly characterized by a local increase of hemocyte nearby the site of parasite attachment, and hyperplasia of epithelial mucous cells. Locally extensive erosion of the lamellar epithelium was observed in conjunction with a severe hemocytic infiltrate.

Parasites detected in the digestive gland were found located mainly in the glandular diverticula, in the intestinal area and in the connective tissue of the interstitial space.

Protozoan parasites were frequently found in variable numbers, from few to moderate, in the gastric lumen or, rarely, in the glandular diverticula. The associated inflammatory reaction was usually mild and restricted to the epithelium of the gastric mucosa, characterized by an

increase of hemocytes, which were also occasionally observed free in the gastric lumen intermingled with parasites. Mild hyperplasia of mucous epithelial cells was also observed.

Metazoan parasites were found mainly in the gastric lumen, intestinal lumen and less frequently in the connective tissue of the interstitial space and in the lumen of glandular diverticula. Affected samples revealed a low number of worms, ranging from one to few larvae (up to a maximum of five). The inflammatory reaction was generally close to the parasite but showed a variable intensity. In fact, in specimens where parasites seemed to be viable at the time of collection, inflammatory reaction was mild and characterized by a scarce infiltrate of hemocytes in the epithelium and mild mucous cell hyperplasia. In samples containing partially degenerated parasites in the luminal spaces of the digestive gland, a localised but moderate to high inflammatory reaction was observed. Hemocytes were arranged around the dead worms or their remains, free in the digestive cavities or grouped in the nearby glandular epithelium. A moderate epithelial mucous cell hyperplasia was also observed.

Rarely, metazoan parasites remnants were found in the connective tissue of the interstitial interglandular space, surrounded by a severe inflammatory infiltrate organised to form a granuloma-like structure. Multiple layers of hemocytes were arranged in a concentric fashion around degenerate worms, intermingled with a variable amount of basophilic granular necrotic material.

Fig. 4.3 Parasites in gill (A, B, C) and digestive gland (D, E, F). (A, B) Protozoan parasites in gill lamellar epithelium. (C) Metazoan parasite in gill filament associated with moderate hemocytes infiltration and eroded lamellar epithelium. (D) Protozoan parasites in the lumen of digestive gland. (E) Metazoan parasite in the lumen of digestive gland associated with moderate hemocytes infiltration. (F) Remnants of metazoan parasite surrounded by severe hemocytes infiltration in interstitial space of digestive gland. Bar A-B-C-D-E = 10 µm; Bar F = 50 µm.

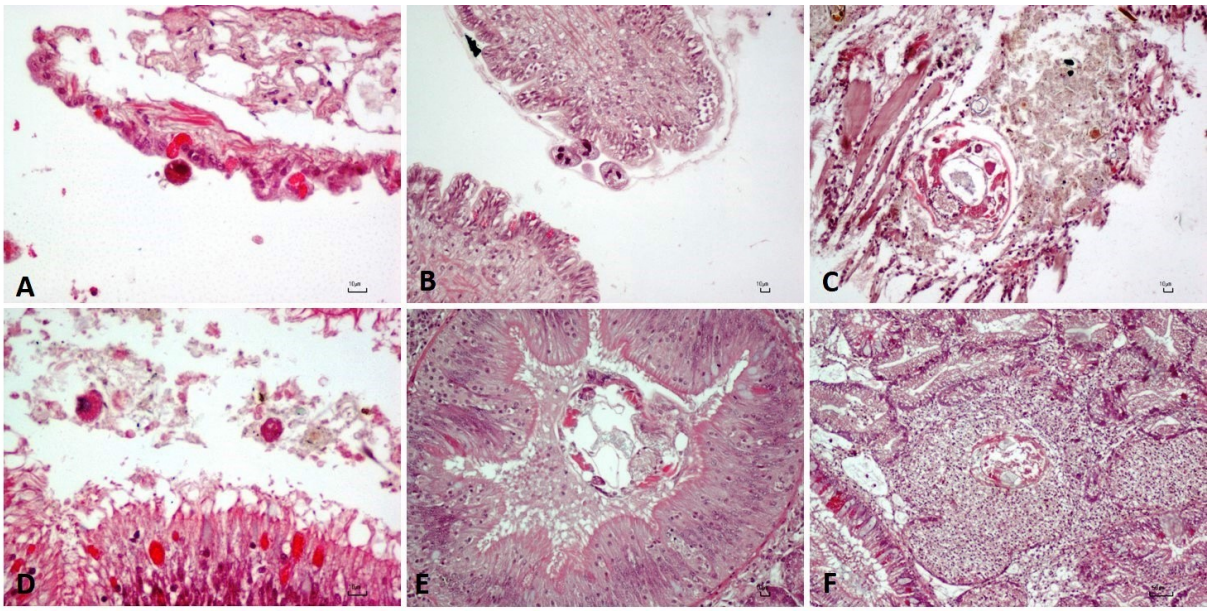

4.7 Discussion

Parasites found in oyster specimens belonged to both Protozoa and Metazoa. This is consistent with what reported by other authors that observed parasites from Ciliophora class and from Apicomplexa Phylum (Protozoa) and Trematoda and Cestoda worms belonging to the phylum Platyhelminthes (Metazoa) in *Crassostrea* species (Calvi Zeidan *et al*., 2012), other oyster species (Moore *et al.,* 2011) or other bivalve molluscs (Boehs *et al*., 2010).

Histopathological examination allowed to identify the presence of protozoan parasites in different anatomical districts, gills and digestive gland, as reported by other authors in several species of oysters infected with Cercozoan, Haplosporidian and *Perkinsus* spp. parasites (Kleeman *et al*., 2002; Kroech, 2010; Smolowitz, 2013; Soudant *et al*., 2013).

Hemocytic infiltration was usually associated with the presence of protozoan parasites and was localised in few lamellae with a mild degree of severity. These findings are consistent with what reported by Kroech (2010) and Smolowitz (2013) that found a scarce inflammatory response against *Bonamia* sp. and *Perkinsus* spp. respectively, mainly characterized by a moderate number of granular hemocytes in gills sinusoids and lamellar epithelium. Higher parasitic load was associated to mild damage to the filament epithelium in accordance with what reported in literature (Kleeman *et al*., 2002; Kroech, 2010).

Digestive gland showed a mild hemocytic infiltrate in the glandular epithelium and in the nearby connective tissue, in accordance with what reported by other authors (Kroech, 2010). Protozoa were found free in the glandular lumen and gastric cavity, intermingled with hemocytes and cell debris, but usually in low number, as observed by other authors in protozoan infection (Calvi Zeidan *et al*., 2012, Carrasco *et al.,* 2012; Carrasco *et al*., 2015).

The results of our study in specimens affected by metazoan parasites showed a higher inflammatory reaction in the digestive gland than in gills, consistently with what reported by other authors in oysters infested with bucephalid trematodes (Lassudrie *et al*., 2015). This fact could be explained with the greater ease for the hemocytes to reach the digestive gland and thus determine a more severe inflammatory reaction, as reported by other authors (Smolowitz, 2013). The presence of parasites inside the glandular lumina was associated, in addition to a moderate hemocyte infiltrate, also to an augmented cellular degeneration, sloughing of digestive epithelium and increase in mucus in glandular lumina. These features determined a more severe immune response than what observed with protozoa, in accordance with what reported by Lassudrie *et al*. (2015) in a study of oysters infected with different classes of protozoan and metazoan parasites. In addition, the inflammatory response was particularly severe when parasites were found in the periglandular connective tissue (Cheng and Burton, 1966; Calvi Zeidan *et al*., 2012).

4.8 References

- Arzul I., Renault T., Thébault A., Gérard A. (2002) Detection of oyster herpesvirus DNA and proteins in asymptomatic *Crassostrea gigas* adults. Virus Research 84, 151-160.
- Barbosa Solomieu V., Renault T., Travers M.A. (2015) Mass mortality in bivalves and the intricate case of the Pacific oyster, *Crassostrea gigas*. Journal of Invertebrate Pathology 131, 2–10.
- Boehs G., Villalba A., Oliveira Ceuta L., Rocha Luz J. (2010) Parasites of three commercially exploited bivalve mollusc species of the estuarine region of the Cachoeira river (Ilhéus, Bahia, Brazil). Journal of Invertebrate Pathology 103, 43-47.
- Bueno R., Perrott M., Dunowska M., Brosnahan C., Johnston C. (2016) *In situ* hybridization and histopathological observations during ostreid herpesvirus-1 associated mortalities in Pacific oysters *Crassostrea gigas*. Diseases of Aquatic Organisms 122, 43-55.
- Burge C.A., Griffin F.J., Friedman C.S. (2006) Mortality and herpesvirus infections of the Pacific oyster *Crassostrea gigas* in Tomales Bay, California, USA. Diseases of Aquatic Organisms 72, 31-43.
- Burioli E.A.V., Varello K., Lavazza A., Bozzetta E., Prearo M., Houssin M. (2018) A novel divergent group of Ostreid herpesvirus 1 μVar variants associated with a mortality event in Pacific oyster spat in Normandy (France) in 2016. Journal of Fish Diseases 00, 1–11.
- Calvi Zeidan G., dos Santos Aguiar Luz M., Boehs G. (2012) Parasites of economically important bivalves from the southern coast of Bahia State, Brazil. Revista Brasileira de Parasitologia Veterinária 21, 391-398.

- Canesi L, Gallo G., Gavioli M., Pruzzo C. (2002) Bacteria-hemocyte interactions and phagocytosis in marine bivalves. Microscopy Research and Technique 15, 469-476.
- Carrasco N., Villalba A., Andree K.B., Engelsma M.Y., Lacuesta B., Ramilo A., Gairín I., Furones M.D. (2012) *Bonamia exitiosa* (Haplosporidia) observed infecting the European flat oyster *Ostrea edulis* cultured on the Spanish Mediterranean coast. Journal of Invertebrate Pathology 110, 307–313.
- Carrasco N., Green T., Itoh N. (2015) *Marteilia* spp. parasites in bivalves: A revision of recent studies. Journal of Invertebrate Pathology 131, 43–57.
- Cheng T.C. and Burton R.W. (1966) Relationships between *Bucephalus* sp. and *Crassostrea virginica*: a histochemical study of some carbohydrates and carbohydrate complexes occurring in the host and parasite. Parasitology 56, 111-122.
- Davison A.J., Eberle R., Ehlers B., Hayward G.S., McGeoch D.J., Minson A.C., Pellett P.E., Roizman B., Studdert M.J. and Thiry E., (2009) The order Herpesvirales. Archives of Virology 154, 171-177.
- Davison A., Trus B., Cheng N., Steven A., Watson M., Cunningham C., Le Deuff R. and Renault T. (2005) A novel class of herpesvirus with bivalve hosts. Journal of General Virology 86, 41-53.
- EFSA (2015) Oyster mortality - EFSA Panel on Animal Health and Welfare (AHAW). EFSA Journal 2015; 13(6), 4122.
- Feng S.Y. and Canzonier W.J. (1970) Humoral responses in the American oyster (*Crassostrea virginica*) infected with *Bucephalus* sp. and *Minchinia nelsoni*. 5, 497-510. Conference paper: Special Publications. American Fisheries Society Conference Title: A symposium on diseases of fishes and shellfishes, SNIESZKO, S. F. editor.

- Fisher W.S. (1986) Structure and Functions of Oyster Hemocytes. In: Brehélin M. (eds) Immunity in Invertebrates. Proceedings in Life Sciences. Springer, Berlin, Heidelberg.
- Friedman CS, Estes RM, Stokes NA, Burge CA, Hargove JS, Barber B.J., Elston R.A., Burreson E.M., Reece K.S. (2005) Herpes virus in juvenile Pacific oysters *Crassostrea gigas* from Tomales Bay, California, coincides with summer mortality episodes. Diseases of Aquatic Organisms 63, 33–41.
- Hine P.M. (1999) The inter-relationships of bivalve haemocytes. Fish & Shellfish Immunology 9, 367-385.
- Kleeman S.N., Adlard R.D., Lester R.J.G. (2002) Detection of the initial infective stages of the protozoan parasite *Marteilia sydneyi* in *Saccostrea glomerata* and their development through to sporogenesis. International Journal for Parasitology 32, 767–784.
- Kroeck M.A. (2010) Gross signs and histopathology of *Ostrea puelchana* infected by a *Bonamia exitiosa*-like parasite (Haplosporidia). Diseases of Aquatic Organisms 89, 229–236.
- Lassudrie M., Wikfors G.H., Sunila I., Alix J., Dixon M.S. Combot D., Soudant P., FabiouxC., Hégaret H. (2015) Physiological and pathological changes in the eastern oyster *Crassostrea virginica* infested with the trematode *Bucephalus* sp. and exposed to the toxic dinoflagellate *Alexandrium fundyense*. Journal of Invertebrate Pathology 126, 51–63.
- Le Deuff R. and Renault T. (1999) Purification and partial genome characterization of a herpes-like virus infecting the Japanese oyster, *Crassostrea gigas*. Journal of General Virology 80, 1317-1322.

- Lopez-Sanmartin M., Power D.M., Herran-José F., Navas I., Batista F.M. (2016) Experimental infection of European flat oyster *Ostrea edulis* with Ostreid Herpesvirus 1 microvar: mortality, viral load and detection of viral transcripts by in situ hybridization. Virus Research 217, 55-62.
- Martenot C., Fourour S., Oden E., Jouaux A., Travaille E., Malas J.P. and Houssin M., (2012) Detection of the OsHV-1µVar in the Pacific oyster *Crassostrea gigas* before 2008 in France and description of two new microvariants of the Ostreid Herpesvirus 1 (OsHV-1). Aquaculture, 338, 293-296.
- Martenot C., Oden E., Travaillé E., Malas J-P. and Houssin M. (2011) Detection of different variants of Ostreid Herpesvirus 1 in the Pacific oyster, *Crassostrea gigas* between 2008 and 2010. Virus Research, 160, 25-31.
- Martenot C., Segarra A., Baillon L., Faury N., Houssin M., *et al*. (2016) In situ localization and tissue distribution of ostreid herpesvirus 1 proteins in infected Pacific oyster, *Crassostrea gigas*. Journal of Invertebrate Pathology 136, 124–135.
- Mazzi V. (1977) Tecniche Istologiche e Istochimiche. Piccin Editore.
- Moore J.D., Juhasz C.I., Robbins T.T. (2011) A histopathology survey of California oysters. California Fish and Game 97, 68-83.
- Moss J.A., Burreson E.M., Cordes J.F., Dungan C.F., Brown G.D., Wang A., Wu X., Reece K. S. (2007) Pathogens in *Crassostrea ariakensis* and other Asian oyster species: implications for non-native oyster introduction to Chesapeake Bay. Diseases of Aquatic Organisms 77, 207-223.
- Oden E., Martenot C., Berthaux M., Travaillé E., Malas J.P., Houssin M. (2011) Quantification of ostreid herpesvirus 1 (OsHV-1) in *Crassostrea gigas* by real-time PCR: Determination of a viral load threshold to prevent summer mortalities. Aquaculture 317, 27–31.

- Prado-Alvarez M., Darmody G., Hutton S., O'Reilly A., Lynchand S. A., Culloty S. C. (2016) Occurrence of OsHV-1 in *Crassostrea gigas* cultured in Ireland during an exceptionally warm summer. Selection of less susceptible oysters. Frontiers in Physiology 7, 492.
- Renault T. (2008) Shellfish viruses. Encyclopedia of virology 5, 560-567.
- Renault T., Arzul I. (2001) Herpes-like virus infections in hatchery-reared bivalve larvae in Europe: specific viral DNA detection by PCR. Journal of Fish Diseases 24, 161-167.
- Renault T., Bouquet A.L., Maurice J.T., Lupo C. and Blachier P. (2014) Ostreid herpesvirus 1 infection among Pacific Oyster (*Crassostrea gigas*) spat: relevance of water temperature to virus replication and circulation prior to the onset of mortality. Applied and Environmental Microbiology 80, 5419-5426.
- Renault T., Cochennec N., Le Deuff R.M., Chollet B. (1994) Herpes-like virus infecting Japanese oyster (*Crassostrea gigas*) spat. Bulletin of the European Association of Fish Pathologists 14, 64–66.
- Renault T., Le Deuff R. M., Chollet B., Cochennec N. and Gérard A. (2000) Concomitant herpes-like virus infections in hatchery-reared larvae and nursery-cultured spat *Crassostrea gigas* and *Ostrea edulis*. Diseases of Aquatic Organisms 42, 173-183.
- Robledo F.J.A, Vasta G.R., Record N.R. (2014) Protozoan Parasites of Bivalve Molluscs: Literature Follows Culture. PLoS ONE 9(6), e100872.
- Sauvage C., Pépin J.F., Lapègue S., Boudry P., Renault T. (2009) Ostreid herpes virus 1 infection in families of the Pacific oyster, *Crassostrea gigas*, during a summer mortality outbreak: differences in viral DNA detection and quantification using real-time PCR. Virus Research 142, 181–187.

- Schikorski D., Faury N., Pepin J.F., Saulnier D., Tourbiez D., Renault T. (2011) Experimental ostreid herpesvirus 1 infection of the Pacific oyster *Crassostrea gigas*: kinetics of virus DNA detection by q-PCR in seawater and in oyster samples. Virus Research 155, 28-34.
- Segarra A., Pépin J.F., Arzul I., Morga B., Faury N. and Renault T. (2010) Detection and description of a particular Ostreid herpesvirus 1 genotype associated with massive mortality outbreaks of Pacific oysters, *Crassostrea gigas*, in France in 2008. Virus Research 153, 92-99.
- Smolowitz R. (2013) A Review of Current State of Knowledge Concerning *Perkinsus marinus* Effects on *Crassostrea virginica* (Gmelin) (the Eastern Oyster). Veterinary Pathology 50, 404-411.
- Soudant P., Chu FL.E., Volety A. (2013) Host–parasite interactions: Marine bivalve molluscs and protozoan parasites, *Perkinsus* species. Journal of Invertebrate Pathology 114, 196–216.
- Vásquez-Yeomans R., García-Ortega M., Cáceres-Martínez J. (2010) Gill erosion and herpesvirus in *Crassostrea gigas* cultured in Baja California, Mexico. Diseases of Aquatic Organisms 89, 137-144.
- Wang L., Song X., Song L. (2018) The oyster immunity. Developmental and Comparative Immunology 80, 99-118.

Conclusions

Mortality episodes of Pacific oyster have been observed in France and several European countries since 2008. Since 2010, field and experimental studies were performed and OsHV-1 was identified as the causative agent of oyster's mortality observed in Europe. These studies showed also that mortalities episodes depended on the presence of other factors, in particular, water temperature. Genetic investigations showed numerous lineages of OsHV-1 isolated from mortality outbreaks, and OsHV-1 µVar was detected on a massive scale since 2008 (between 80-90%). Pacific oysters affected by OsHV-1 infections were mainly spat oysters and the susceptibility decreased with age.

However, since 2012 a marine bacterium belonging to the *Vibrio* genus has been detected during oyster mortality in France. From its characterization, two lineages were identified: *V. aestuarianus* subsp. *francensis* and *V. aestuarianus* subsp. *aestuarianus*.

However, data about *V. aestuarianus*/oysters interaction in the field are poorly reported in the literature, while most of data derives from experimental challenges.

In this work, we described the occurrence of *Vibrio* pathogens during a mortality outbreak of farmed oysters in Sardinia during winter season (December 2016 - March 2017) causing the loss of more than 80% of oysters.

A significant hemocytes infiltration affecting gills and mantle tissues of oysters were observed, associated with *V. aestuarianus* ($P < 0.05$). Moreover, no statistically significant results were recorded on the digestive gland.

Furthemore, the detection of a high number of protozoan and metazoan parasites observed only in the gills and in the digestive glands, identify the mantle as a valid target organ for the evaluation of tissue damages associated to pathogens like *V. aestuarianus* during mortality episodes of oysters.

Interestingly, highest *V. aestuarianus* loads were found in mantle tissues associated with moderate to severe hemocytes infiltration in sub-epithelial connective tissue. Therefore, we

postulate that *V. aestuarianus* alone could be associated to the severity of hemocyte infiltration in oyster mantle.

Indeed, as reported by EFSA (2015) and as observed in our work, a major susceptibility to *V. aestuarianus* infection has been recorded in adult oysters. Other factors are involved in oyster's mortality such as water temperature with mortality associated with both high and low temperatures. In particular, we observed high mortality episode(s) from December 2016 to March 2017 with water temperature ranging from 13°C to 16°C. This, according to other authors, reinforce hypothesis that interconnected factors (pathogenic bacteria and environmental factors) may act together in synergy inducing mortality episodes. However, the influence of temperature on *V. aestuarianus* and its ability to infect oysters still remains to be studied.

Further and more specific analyses, such as *in situ* hybridization or immunohistochemistry, are needed to establish the correlation between pathogens and tissue damages.

Remarkably, OsHV-1 and *Vibrio* infections are not included in listed diseases of the directive 2006/88/EC that established health requirements and prevention/control of diseases for aquaculture animals. However, a surveillance program is certainly needed in oyster farms to monitoring OsHV-1 and *Vibrio* infections in order to prevent mortality outbreak and to reduce economic losses.

Acknowledgements

I would like to express my sincere gratitude to my Tutor (Prof.ssa Elisabetta Antuofermo) and co-Tutor (Prof. Fulvio Salati) for being my guide and support during this work and for their suggestions and encouragements during these years.

I would like to thank Prof. Alberto Alberti for his help, suggestions and scientific support.

I am sincerely grateful to Dott. Giovanni Burrai and Dott.ssa Marta Polinas for their invaluable help and precious suggestions in writing the thesis.

I also would like to thank Dott.ssa Marina Sanna: she gives me an incomparable help teaching me technical procedures and helping me during all the PhD work; Dott.ssa Tiziana Cubeddu for her help and suggestions; Dott.ssa Rosanna Zobba for her technical support.

Thanks to all the Anatomical Pathology section for having kindly welcomed me in their laboratory and make me part of their group.

Thanks to Ylenia, for being more than a collegue, for her friendship, for her suggestions and support in bad and beautiful moments.

I would like to thank also Dott. Angelo Ruiu and all the components of Istituto Zooprofilattico Sperimentale della Sardegna, section of Oristano; thanks to Enrico Guiso for his help and patience.

I would also like to thank Alessandro Gorla for his precious contribution and his great willingness.

A special thanks goes to Marco and all my family for their unconditional love and for supporting and enduring me during this way.